

Characterisation of the N-terminal domain of human topoisomerase II α

by

Laurence Gardiner

A thesis submitted in fulfillment of the requirements for a degree of Doctor of
Philosophy at the University of Leicester.

Department of Biochemistry

University of Leicester

LEICESTER LE1 7RH

ENGLAND.

September 1998

UMI Number: U115923

All rights reserved

INFORMATION TO ALL USERS

The quality of this reproduction is dependent upon the quality of the copy submitted.

In the unlikely event that the author did not send a complete manuscript and there are missing pages, these will be noted. Also, if material had to be removed, a note will indicate the deletion.



UMI U115923

Published by ProQuest LLC 2013. Copyright in the Dissertation held by the Author.
Microform Edition © ProQuest LLC.

All rights reserved. This work is protected against
unauthorized copying under Title 17, United States Code.



ProQuest LLC
789 East Eisenhower Parkway
P.O. Box 1346
Ann Arbor, MI 48106-1346

To my family.

This work was carried out in the laboratory of Prof A. Maxwell in the Department of Biochemistry , University of Leicester.

I would like to thank Tony Maxwell for his excellent supervision throughout the long and winding course of the project. I am also deeply grateful to Tim Hammonds for the help, advise, money and shoes that he provided during the last three years.

I am also indebted to Ali Howells for all the material and help she provided. In addition I would like to thank all of the current members of the lab, Spencer Campbell, Symon Erskine, Jonathan Heddle, Lois Wentzell, Nicola Williams and former members Sotirios Kampranis and Clare Smith for providing help and making for a great atmosphere to work in.

Finally I would like to thank Shirley Burrow for her support during the last year of this project.

SPECIAL NOTE

**ITEM SCANNED AS SUPPLIED
PAGINATION IS AS SEEN**

Dedication	ii
Acknowledgements.....	iii
Abbreviations	iv
Abstract	v
Contents	vi
List of figures.....	xi

CHAPTER 1. INTRODUCTION 1

1.1 DNA topology	1
1.2 Topoisomerases	3
1.2.1 Type I topoisomerases	3
1.3 Type II topoisomerases	4
1.3.1 Evidence for the mechanism of DNA topoisomerase II	5
1.3.2 DNA topoisomerases as an ATP-operated clamp	7
1.3.3 The one-gate versus the two-gate model for type II topoisomerases.....	9
1.3.4 The structure of type II topoisomerases	10
1.3.5 Investigation of structure by electron microscopy	13
1.3.6 A detailed model of the action of type II topoisomerases	14
1.4 ATP utilisation by type II topoisomerases	15
1.4.1 The coupling of the hydrolysis of ATP to strand passage in type II topoisomerases	18
1.4.2 Examination of DNA-dependent ATP hydrolysis	19
1.4.3 Structural changes in the conformation of the enzyme on the binding of nucleotide	20
1.4.4 The effect of ATP hydrolysis on the breakage and re-union reaction	21
1.4.5 The effect of the binding of the T-segment in the cleavage reaction	22
1.4.6 The exit of the T-segment from the topoisomerase complex.....	22
1.4.7 Phosphorylation of eukaryotic type II topoisomerases	23

1.5 Human type II topoisomerases	24
1.6 Clinical importance of type II topoisomerases.....	25
1.6.1 Topoisomerase poisons	25
1.6.2 Topoisomerase II antagonists	27
1.7 Project aims	28
 CHAPTER 2. MATERIALS AND METHODS	31
Introduction	31
2.1.0 Bacteriology	31
2.1.1 Bacterial strains	31
2.1.2 Plasmids	32
2.1.3 Bacterial growth media	32
2.1.4 Antibiotics	33
2.1.5 Inoculation of overnight cultures	33
2.1.6 Preparation of competent <i>E. coli</i> cells	34
2.1.7 Transformation of competent <i>E. coli</i> cells	34
2.1.8 Trial induction of plasmid based gene expression	35
2.1.9 Full scale induction of recombinant protein	35
2.2 Protein purification	36
2.2.1 Preparation of crude extract from inclusion bodies	36
2.2.2 Re-folding techniques	37
2.2.3 Fast protein liquid chromatography techniques (FPLC)	37
2.2.4 Novobiocin affinity chromatography	38
2.2.5 Metal affinity chromatography	39
2.2.6 Gel purification of protein	40
2.3 Protein analysis	41
2.3.1 Estimating protein concentrations	41
2.3.2 SDS-polyacrylamide gel electrophoresis	41
2.3.3 Native polyacrylamide gel electrophoresis	42
2.3.4 Silver staining	42

2.3.5 Western blotting	43
2.3.6 Protein cross-linking	44
2.3.7 Phosphorylation of proteins	44
2.3.8 ATPase assays	45
2.3.9 Drug screening	46
2.4 DNA techniques	46
2.4.1 Small scale plasmid preparation	46
2.4.2 Agarose gel electrophoresis	46
2.4.3 Restriction analysis of DNA	47
2.4.4 Mutagenesis of plasmid DNA	47
2.4.5 Automated DNA sequencing	48
 CHAPTER 3. PRODUCTION AND PURIFICATION	50
Introduction	50
3.1 Analysis of clones	50
3.1.1 pET Expression system	51
3.2 Growth of cells	51
3.2.1 Problems with expression.....	52
3.2.2 Clarification of expression conditions	54
3.2.3 Attempts to increase solubility of recombinant protein	55
3.3 Purification of recombinant protein.....	55
3.3.1 Partial purification of protein from inclusion bodies	55
3.3.2 Establishing re-folding conditions	56
3.3.3 FPLC purification	57
3.3.4 Gel purification	57
3.3.5 Purification by metal affinity chromatography	58
3.3.6 Concentration of soluble protein	60
3.4 Identification of 52 kDa protein as a fragment of topo II α	61
3.5 Discussion	61

CHAPTER 4. CHARACTERISATION OF THE ATPase REACTION OF THE 52 kDa N-TERMINAL FRAGMENT OF HUMAN TOPO II α.	63
Introduction	63
4.1 Optimisation of reaction conditions	63
4.1.1 The effect of pH on ATPase activity	64
4.1.2 The effect of KCl concentration on the ATPase activity of the 52 kDa fragment	64
4.1.3 The effect of MgCl ₂ concentration on the ATPase activity of the 52 kDa fragment	64
4.1.4 Summary of optimised conditions	65
4.2 Intrinsic ATPase activity	66
4.2.1 ATP hydrolysis as a function of enzyme concentration	66
4.2.2 ATP hydrolysis as function of substrate concentration	67
4.2.3 The DNA dependence of ATPase activity	67
4.3 Characterisation of the DNA- dependent ATPase of the 52 kDa fragment	68
4.3.1 DNA-dependent ATPase activity as a function of enzyme concentration	68
4.3.2 DNA-dependent ATP hydrolysis as function of substrate concentration	69
4.3.3 Effect of Mg ²⁺ concentration on DNA-dependent ATP hydrolysis	69
4.3.4 Removal of DNA during the ATPase assay	69
4.3.5 Effect of KCl concentration on DNA-stimulated ATPase activity.	70
4.4 Studies to examine the 52 kDa fragment's interaction with DNA.	70
4.5 Dimersation studies on the 52 kDa fragment	71
4.6 The effect of drugs on the DNA-dependent ATPase activity of the 52 kDa fragment.	72
4.7 Phosphorylation studies on the 52 kDa fragment.	74
4.8 Discussion	75
CHAPTER 5. IDENTIFICATION OF THE ACTIVE SITE-RESIDUE OF THE 52 kDa N-TERMINAL FRAGMENT OF HUMAN TOPO IIα.	79

5.1 Introduction.	79
5.1.1 Quikchange™ site directed mutagenesis	80
5.1.2 Designing the mutagenic oligonucleotides	80
5.1.3 PCR conditions for the oligonucleotided extension	81
5.2 Analysis of the mutated plasmids	82
5.2.1 DNA sequencing	82
5.3 Preparation of the mutated protein.	83
5.3.1 Evidence identifying Glu 86 of the 52 kDa fragment as the catalytic base	84
5.3.2 Evidence that phosphorylation at Ser 29 has no direct effect on the rate of ATP hydrolysis of the 52 kDa fragment	85
5.4 Discussion	85
CHAPTER 6. DISCUSSION	88
6.1 Production and purification of the 52 kDa protein	88
6.2 Optimisation of conditions for ATPase activty	90
6.3 Analysis of the DNA -dependent ATPase activity of the 52 kDa fragment	91
6.4 Effects of drugs on the ATPase activity of the 52 kDa fragment	94
6.4 Effects of phosphorylation on the ATPase activity of the 52 kDa fragment	93
6.5 Mutational analysis of the 52 kDa protein	95
Conclusions	96
Future work	98
References	100

Figures

CHAPTER 1. INTRODUCTION	previous text
	page number
Figure 1.1a A schematic view of the topological states of DNA.	2
Figure 1.1b The formation of positive and negative domains of supercoiling during polymerase tracking.	2
Figure 1.2 A comparison of the polypeptide structure of type II topoisomerases.	5
Figure 1.3 The reactions catalysed by type II topoisomerases.	6
Figure 1.4 ATP-operated clamp.	7
Figure 1.5 One gate vs two gate model.	9
Figure 1.6 The crystal structure of the 43 kDa N-terminal domain of gyrase.	10
Figure 1.7 Mechanism of ATP hydrolysis by DNA gyrase.	10
Figure 1.8 Amino acid alignment of the region containing the active residues for the ATPase activity of several topo IIs.	10
Figure 1.9 The crystal structure of the 92 kDa fragment of yeast topo II.	11
Figure 1.10 Crystal structure of a 59 kDa fragment of gyrase.	12
Figure 1.11 Mechanism of strand passage in topo II.	14
 CHAPTER 2. MATERIALS AND METHODS.	
Figure 2.1 pET -21d(-)	32
 CHAPTER 3. PRODUCTION AND PURIFICATION.	
Figure 3.1 The pET expression system.	51
Figure 3.2 Partition of the recombinant protein into soluble and insoluble fractions.	55
Figure 3.3 Production of protein from SDS PAGE gels.	58
Figure 3.4 Purification of the his-tagged recombinant protein on a colbalt affinity column.	60
Figure 3.5 The production of soluble protein from denaturing conditions	

on a cobalt affinity matrix. 60

Figure 3.6 Identification of the 52 kDa protein as a fragment of topo II. 61

CHAPTER 4. CHARACTERISATION OF THE ATPase REACTION

OF THE 52 kDa N-TERMINAL FRAGMENT OF HUMAN TOPO II α .

Figure 4.1 ATPase activity of the 52 kDa protein vs pH. 65

Figure 4.2 52 kDa protein ATPase activity vs KCl concentration. 65

Figure 4.3 52 kDa ATPase rate vs MgCl₂ at 1.25 mM ATP. 66

Figure 4.4 A plot of ATP hydrolysis as a function of enzyme concentration. 67

Figure 4.5 A plot of ATP hydrolysis as a function of substrate concentration. 68

Figure 4.6 A plot of ATP hydrolysis of the 52 kDa fragment as function of
DNA concentration. 68

Figure 4.7 A plot of concentration of the 52 kDa protein vs DNA-dependent
ATPase activity. 69

Figure 4.8 A plot of DNA-dependent ATP hydrolysis as a function of substrate
concentration. 70

Figure 4.9 The effect of MgCl₂ on the DNA-dependent ATPase activity of the
52 kDa fragment. 70

Figure 4.10 Effect of DNase I on the DNA-dependent ATPase activity of the
52 kDa fragment. 71

Figure 4.11 ATPase rate of the 52 kDa protein vs KCl concentration. 71

Figure 4.12 Cross-linking studies on the 52 kDa fragment. 73

Figure 4.13 The effects of anti-topo II drugs on the ATPase of the 52 kDa
fragment. 74

Figure 4.14 Phosphorylation of the 52 kDa protein by PKC. 75

CHAPTER 5. IDENTIFICATION OF THE ACTIVE SITE-RESIDUE OF THE

52 kDa N-TERMINAL FRAGMENT OF HUMAN TOPO II α .

Figure 5.1 Sequence alignment. 80

Figure 5.2 Mutagenesis strategy. 81

Figure 5.3 Mutagenic primers.	82
Figure 5.4 Restriction analysis of plasmids containing a mutation at position 86.	83
Figure 5.5 Restriction analysis of plasmids mutated at position 29	83
Figure 5.6 Sequence of Glu 86 mutations	84
Figure 5.7 Sequence of Ser 29 mutations	84
Figure 5.8 Effect of point mutations at position Glu 86 on ATPase activity	85
Figure 5.9 Effect of point mutations at position Ser 29 on ATPase activity	86

CHAPTER 6. DISCUSSION.

Figure 6.1 Mechanism of strand passage in topo II	97
---	----

CHAPTER 1

INTRODUCTION

1.1 DNA TOPOLOGY.

Many of the activities involved with the processing of DNA, such as replication, transcription and recombination, will involve an alteration of the topological state of the DNA, for reference see Bates and Maxwell, 1993.

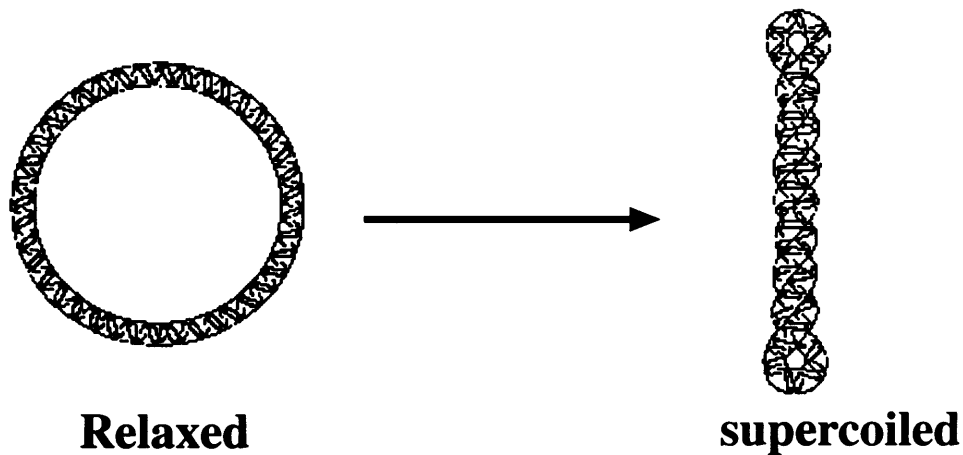
Since the discovery of the double helical structure of DNA (Watson and Crick, 1953) and its ability to replicate in a semiconservative fashion (Meselson and Stahl, 1958) there have been questions raised as to topological ramifications of this process. At first it appeared that the rotation of the free ends of the molecule of DNA as it replicated would be sufficient to release any accumulated torsional stress (Meselson, 1972). The discovery of the true length of natural intact DNA molecules (Kavenoff *et al*, 1974) coupled with the discovery of closed circular forms of DNA (Dulbecco and Vogt, 1963; Weil and Vinograd, 1963) rendered this theory untenable. It is immediately clear that for very long molecules of DNA containing tens of millions of base pairs constrained in loops, as they are in eukaryotic chromosomes, and for covalently closed circular forms, that the rotation of free ends cannot be responsible for the release of torsional stress accumulated through replication and cellular processing.

The parameter that is used to define the topological linkage in DNA molecules is linking number (Lk). If a closed ring of double stranded DNA is in its most stable state under standard conditions, 20°C-40°C at neutral pH, it is considered to be relaxed then

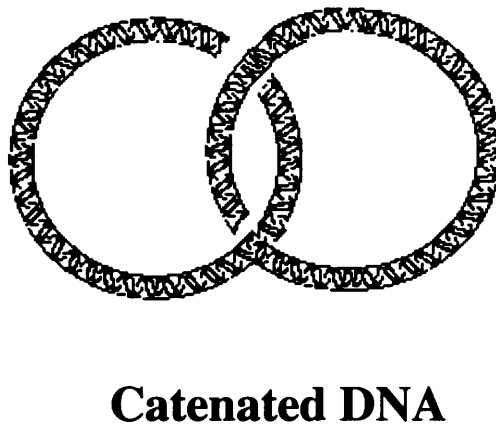
$Lk = Lk^{\circ}$. The relaxed linking number will approximate to $N/10.5$, where N is the size of DNA ring in base pairs and 10.5 is the helical periodicity of B form DNA (Wang, 1979). If a single or double stranded break is introduced into the ring and the DNA is rotated and the ends re-sealed then the DNA will be subjected to torsional stress and become distorted. Under these conditions the DNA can be considered to supercoiled. If $Lk < Lk^{\circ}$ then the DNA is negatively supercoiled, in effect the structure is underwound. If $Lk > Lk^{\circ}$ then the DNA is positively supercoiled and in effect the structure is overwound. In both cases the DNA is in an energetically unfavorable state.

Examples of the importance of resolving topological difficulties are 1) during the replication of chromosomes before cell division, newly replicated DNA molecules become catenated (topologically linked) the resulting mass of catenated DNA helices must be resolved before they can be successfully incorporated into a cell. Failure to resolve the individual helices will result in the DNA becoming fractured on cell division, this would be lethal to the cell. Figure 1.1a shows examples of catenated, relaxed and supercoiled DNA. 2) The process of tracking by polymerases along the DNA leads to the formation of domains of positive and negative supercoiling. As the DNA processing enzyme moves along the double helix it forces the strands apart, this leads to the DNA ahead of the polymerase becoming overwound and the DNA behind the polymerase becoming underwound. If this process goes unchecked it will lead to a point where the polymerase is unable to proceed against the overwound DNA. Figure 1.1b shows the effects of the procession of polymerases on DNA.

Figure 1a. A schematic view of the topological states of DNA.

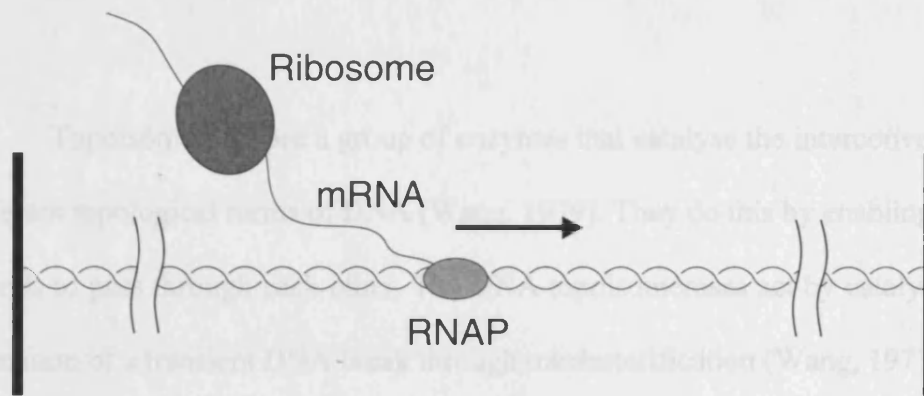


The above figure shows a schematic view of the effects of the introduction of supercoils into a relaxed closed circle of DNA. If the circle is cut, then twisted and resealed, the molecule will become distorted by the torsional stress. Under these conditions the molecule is said to be supercoiled.

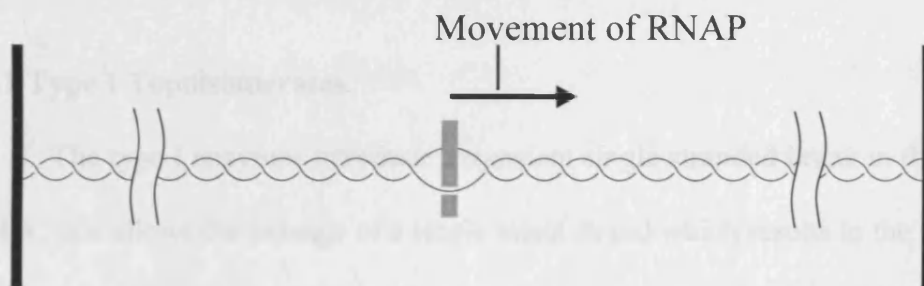


The above figure shows two double stranded rings of DNA that are interlinked. These strands can only be separated by the introduction of a double stranded break and the passing of a double stranded section of DNA through the break. Catenated DNA can arise during the latter stage of DNA replication.

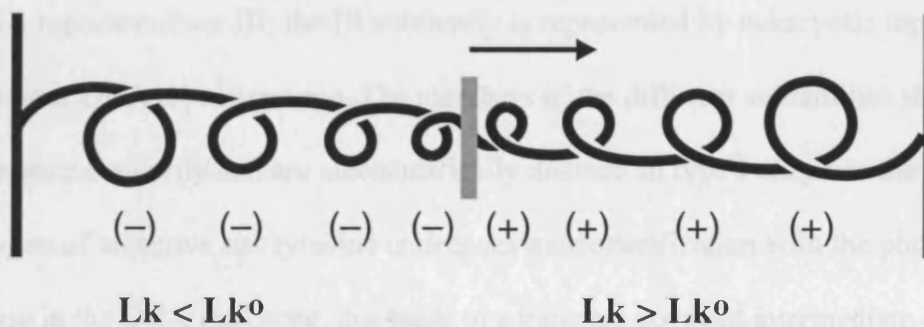
Figure 1.b The formation of positive and negative domains of supercoiling during polymerase tracking.



(a) Transcription elongation



(b) Schematic representation



(c) Formation of twin domains

The above figure shows a representation of how the tracking of polymerases along DNA can lead to build up of domains of positive and negative supercoiling. The movement of the polymerase forces the strands of DNA apart, this leads to overwinding of DNA in front of the polymerase and underwinding behind it, generating domains of positive and negative supercoiling. Unchecked this process will lead to a point where the polymerase is unable proceed against the overwound DNA.

1.2 TOPOISOMERASES.

Topoisomerases are a group of enzymes that catalyse the interconversion of different topological forms of DNA (Wang, 1979). They do this by enabling DNA strands to pass through each other. The DNA topoisomerases act by catalysing the formation of a transient DNA break through transesterification (Wang, 1971). The importance of these enzymes is reflected in the fact that they are ubiquitous. They can be divided into two groups, type I and type II.

1.2.1 Type I Topoisomerases.

The type I enzymes introduce a transient single stranded break in the DNA duplex, this allows the passage of a single intact strand which results in the release of torsional stress and the reduction of the linking number by one. Type I topoisomerases act as monomers and generally are ATP independent. The type I enzymes can be further divided into two sub families : IA represented by bacterial topo I and III and eukaryotic DNA topoisomerase III; the IB subfamily is represented by eukaryotic topo I and poxvirus DNA topoisomerase. The members of the different subfamilies show little sequence similarity and are mechanistically distinct. In type I enzymes the phenolic oxygen of an active site tyrosine undergoes transesterification with the phosphoryl group in the DNA backbone, this leads to a transient covalent intermediate containing a single stranded DNA break. For enzymes in the IA subfamily the tyrosyl residue becomes linked to the 5' phosphoryl group in the covalent intermediate and in the type IB subfamily the tyrosyl residue becomes linked to the 3' phosphoryl group in the covalent intermediate. An intact strand of DNA can then be passed through this

transient break. Following this strand passage event the DNA break is resealed. For a full review of type I enzymes see Wang, (1996).

1.3 TYPE II TOPOISOMERASES.

Type II topoisomerases generate a double stranded break in DNA and pass an intact duplex through this break resulting in a change of linking number by two. The type II enzymes until recently were thought to consist of just one subfamily but the discovery of a novel type II enzyme from archaeal hyperthermophiles (Bergerat *et al*, 1997) suggest that there are perhaps two subfamilies of type II enzymes. These subfamilies are type IIA and type IIB. The type IIB enzyme consist of the archaeal enzymes and the type IIA, all other type II enzymes. The type II enzymes act as dimers introducing a transient double stranded break by transesterification at a pair of active site tyrosyl groups, each becoming attached to the 5' phosphoryl in the DNA backbone. A double stranded segment of DNA is then passed through this break resulting in a change of linking number by two.

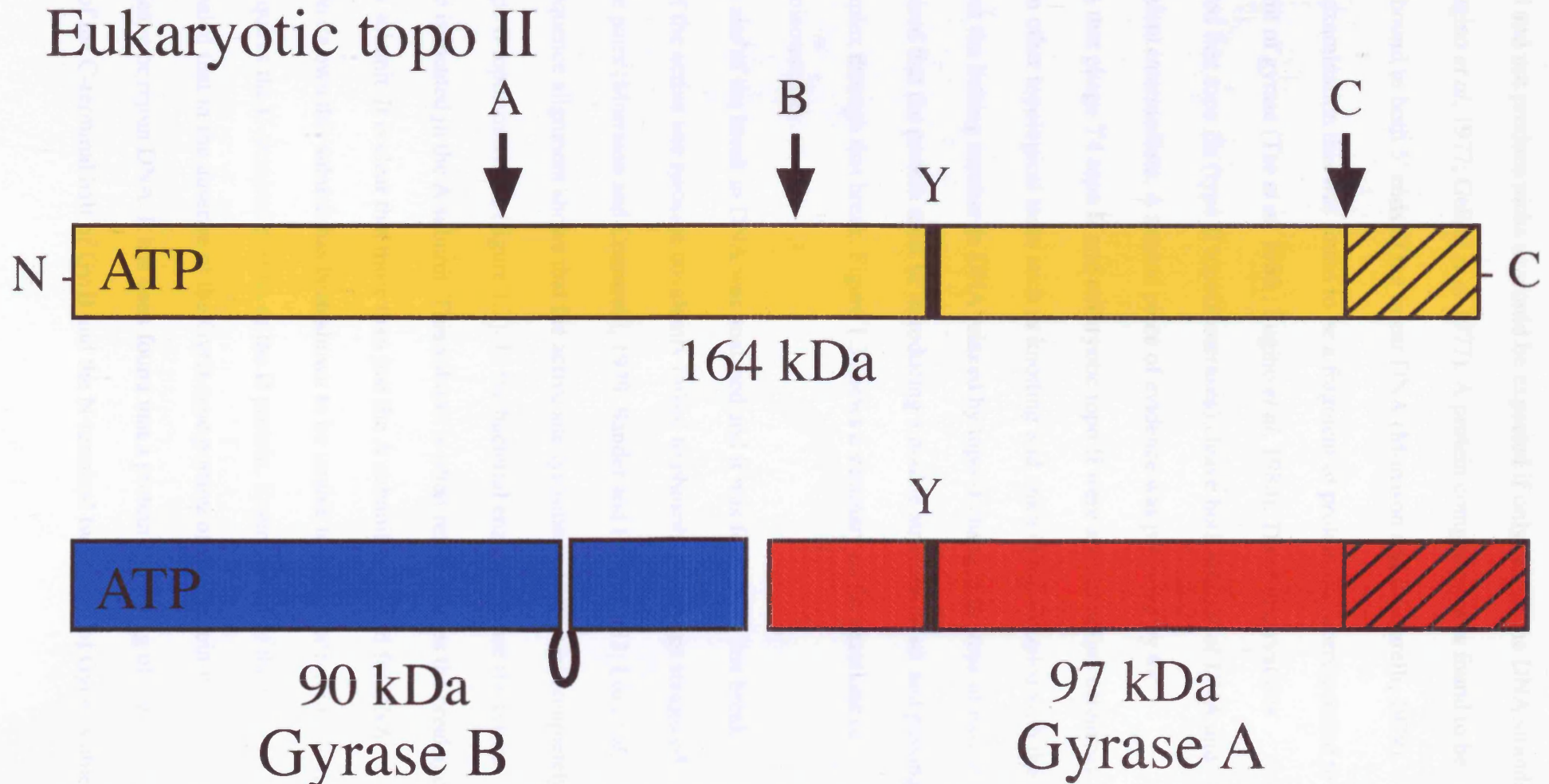
The type II enzymes are important in many cellular processes, their reactions include the ability to unlink catenanes which are linked circles of DNA (Fig 1.1a). They have been found to play a crucial role in the unlinking and resolution of entwined chromosomes at mitosis. In the absence of type II topoisomerases the cells will die. They are of clinical importance as they have been found to be the targets for many anti-tumour and antimicrobial agents, reviewed in (Froelich-Ammon and Osheroff, 1995). They are DNA-dependent ATPases and there has been considerable interest in the coupling of strand passage to the hydrolysis of ATP.

The first type II topoisomerase discovered was the bacterial enzyme gyrase (Gellert *et al*, 1976). The description of the phage T4 (Liu and Alberts, 1979) enzyme and the discovery of the eukaryotic topoisomerase II (Baldi *et al*, 1980, Hsieh and Brutlag, 1980; Miller *et al*, 1981) soon followed this discovery. These enzymes differ in important respects. The bacterial enzyme, gyrase, catalyses the introduction of negative supercoils into the DNA as well as decatenation (unlinking), catenation (linking) of closed circular DNA rings and relaxation of both positive and negative supercoils in DNA. Both the phage topoisomerase II and the eukaryotic enzyme are able to catalyse decatenation, catenation and can relax positive and negative supercoils, but the ability to introduce negative supercoils into DNA is unique to gyrase. The enzymes also differ in their subunit composition, the bacterial enzyme gyrase was found to consist of two subunits, GyrA and GyrB (Gellert *et al*, 1976) and to act as a A₂B₂ complex. The T4 topoisomerase has a three subunit composition (Liu and Alberts, 1979; Stetler *et al*, 1979) and the eukaryotic enzyme is a single subunit and acts as a homodimer (Miller *et al*, 1981, Sander and Hsieh, 1983; Goto and Wang 1984). A comparison between the yeast enzyme and gyrase is seen in figure 1.2. Sequence comparisons of the enzymes showed that all type II enzymes are closely related, the single polypeptide of the eukaryotic enzyme resembling a fusion of the GyrA and GyrB subunits of gyrase.

1.3.1 Evidence for the mechanism of DNA topoisomerase II.

It was initially thought that all type II topoisomerase must act by cutting only one strand of the DNA allowing the uncut strand to hold together the DNA molecule (Wang, 1971). Several lines of evidence undermined this view of events. First it was shown that a plasmid bound to gyrase in the presence of the drug, nalidixic acid (an antibiotic that targets DNA gyrase) when treated with a protein denaturant will linearise

Figure 1.2 A comparison of the polypeptide structure of type II topoisomerases.

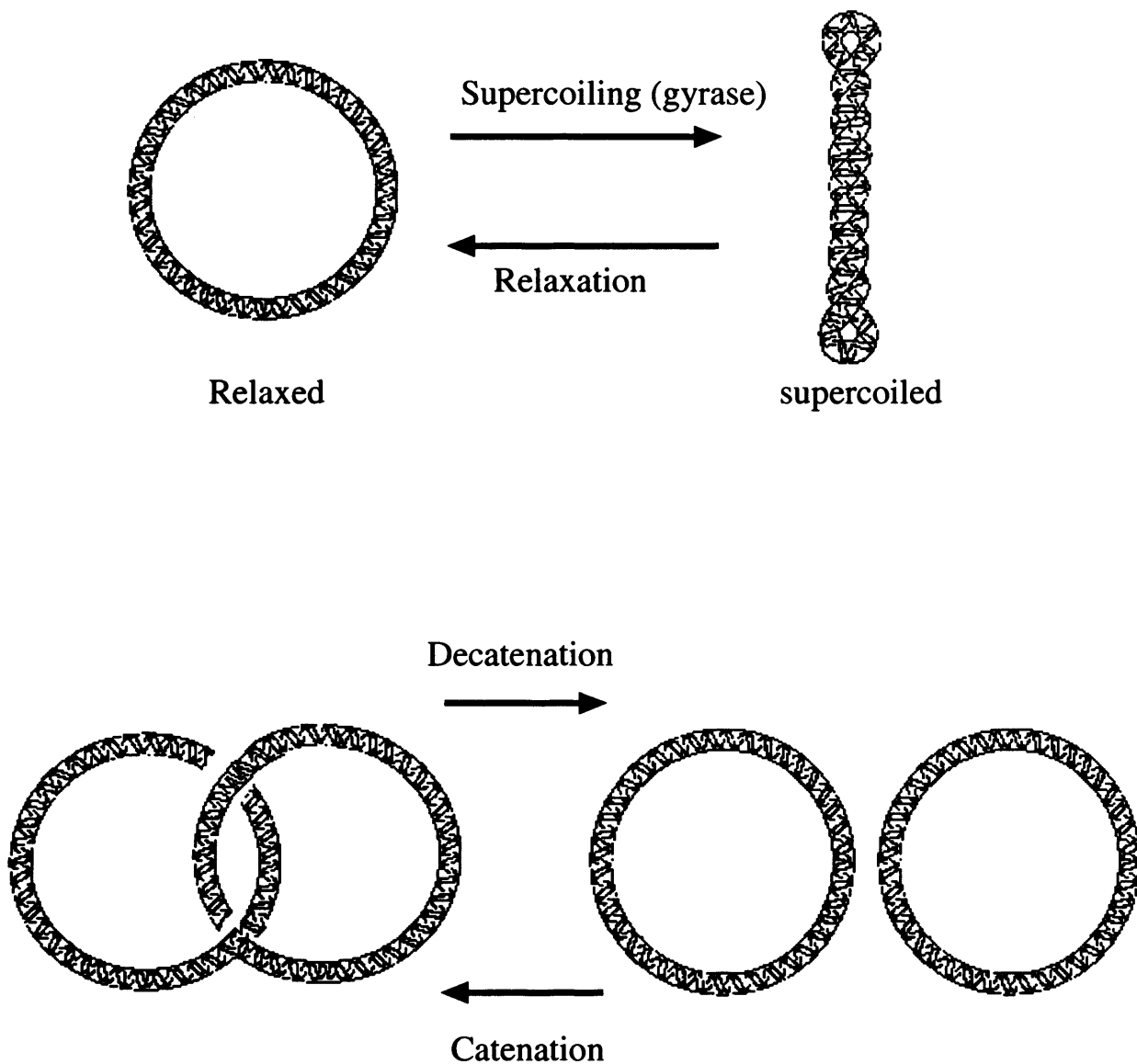


The above figure shows a comparison between the polypeptide structure of a yeast topo II and the bacterial *E.coli* enzyme gyrase. The eukaryotic enzyme can be considered to be the fusion of the GyrB and GyrA subunits seen in the bacterial enzyme. The site of the active site tyrosine is marked (Y). In the eukaryotic enzyme the letters A, B and C show the proteolysis sites seen with V8 endoprotease. Sites A and C are always present; site B is seen in the presence of nucleotide.

the plasmid and not produce nicks as would be expected if only one of the DNA strands was cut (Sugino *et al*, 1977; Gellert *et al* 1977). A protein component was found to be covalently bound to both 5' ends of the linear DNA (Morrison and Cozzarelli, 1979). On further examination this was found to be a fragment of protein that corresponded to the A subunit of gyrase (Tse *et al*, 1980 ; Sugino *et al*, 1980). These observations demonstrated that topo IIs (type II topoisomerases) cleave both strands of DNA and form a covalent intermediate. A second piece of evidence was provided by the observation that phage T4 topo II and eukaryotic topo II were able to unlink catenanes and perform other topological tasks such as knotting and unknotting. Coupled with the evidence that the linking number in DNA relaxed by topo II changed in steps of two, it was recognised that the protein must be introducing a double stranded break and passing an intact duplex through this break. Figure 1.3 shows a summary of the reactions of type II topoisomerases.

The site of the break in DNA was analysed and it was found that this break consisted of the active site tyrosine covalently linked to phosphoryl groups staggered by four base pairs (Morrison and Cozzarelli, 1979, Sander and Hsieh, 1983; Liu *et al*, 1983). A sequence alignment shows that the active site tyrosine is conserved completely amongst type II topoisomerases (figure 1.2). In the bacterial enzyme gyrase the active site tyrosine is located in the A subunit. This subunit is often referred to as the breakage and reunion subunit. It is clear that more than just the A subunit is needed for DNA cleavage. On its own this subunit has been shown to be unable to cleave or rejoin DNA, instead it requires the C-terminal portion of the B protein. Examination of the yeast topo II revealed that in the absence of the GyrB-type portion of the protein it was unable to cleave or rejoin DNA. It has been found that a protein consisting of the equivalent of the C-terminal half of GyrB and the N-terminal two thirds of GyrA is able

Figure 1.3 The reactions catalysed by type II topoisomerases.



The above figure shows the reactions of type II topoisomerases. The first panel shows supercoiling and relaxation of DNA, only the bacterial enzyme gyrase has been shown to supercoil DNA. The second panel shows the linking (catenation) and the unlinking (decatenation) of linked closed circular DNA molecules.

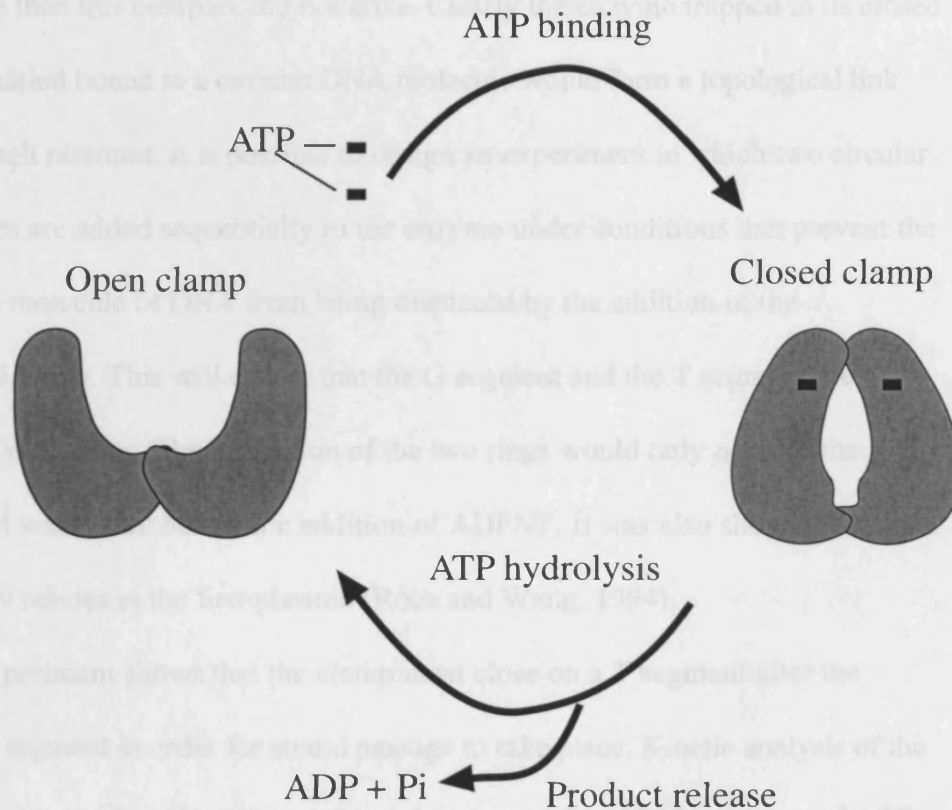
to perform breakage and reunion (Smith, 1998). This suggests that residues in both portions of the protein must be involved with the breakage and reunion reaction.

1.3.2 DNA topoisomerases as an ATP-operated clamp.

The above section outlines the basic mechanics of DNA topoisomerase II. In summary it can be said that the enzyme will bind to a section of DNA and create a double stranded DNA break, the DNA segment containing this break is termed the G or gate segment. The enzyme must then in some way bind a second piece of DNA and pass this segment through the double stranded break; this segment of DNA is termed the T or transfer segment. How can this manipulation be accomplished? Several studies to resolve this question have led to the development of a theory that the enzyme is acting as an ATP-modulated protein clamp (Roca and Wang, 1992). A diagrammatic representation is seen in figure 1.4.

The initial proposal of the clamp model suggested that the enzyme possesses a molecular clamp which would close on the binding of ATP and re-open upon ATP hydrolysis and product release. The evidence to support this model came initially from the studies of DNA binding by the yeast topo II in the presence and absence of a non-hydrolysable analogue of ATP, 5'-adenylyl- β , γ -imidodiphosphate (ADPNP). In these studies the enzyme was incubated in the absence of nucleotide with linear and closed circular DNA. It was found that the enzyme would bind to both forms of DNA. The experiment was repeated in the presence of ADPNP and it was found that protein would no longer bind to the closed circular molecules but could still bind the linear DNA. This observation was not explained by any specific interaction between the ends of the DNA molecules and the enzyme as the linear DNA bound to the enzyme could be joined by ligation. From this it was concluded that the presence of nucleotide had converted the

Figure 1.4 ATP-operated clamp.



The above figure shows a cartoon of the ATP-operated clamp. The clamp in the absence of nucleotide is in an open conformation. The binding of nucleotide leads to a conformational change resulting in the closure of the clamp. On the hydrolysis of ATP and the release of products the enzyme returns to an open clamp conformation.

enzyme into an annular form which allows linear DNA to thread onto the enzyme (Roca and Wang, 1992). This suggestion explains earlier observations that when complexed to circular DNA in the presence of ADPNP the *Drosophila* enzyme formed a stable complex that could not be dissociated with salt. If the enzyme was complexed to a linear DNA molecule then this complex did not arise. Clearly the enzyme trapped in its closed clamp conformation bound to a circular DNA molecule would form a topological link that would be salt resistant. It is possible to design an experiment in which two circular DNA molecules are added sequentially to the enzyme under conditions that prevent the enzyme-bound molecule of DNA from being displaced by the addition of the subsequent DNA ring. This will ensure that the G segment and the T segment are on different DNA molecules. The catenation of the two rings would only occur if the second plasmid was added before the addition of ADPNP. It was also shown that the G segment always resides in the first plasmid (Roca and Wang, 1994).

This experiment shows that the clamp must close on a T segment after the binding of a G segment in order for strand passage to take place. Kinetic analysis of the enzyme revealed that when this clamp is bound to a segment of DNA the rate of ATP hydrolysis is increased. For the yeast enzyme in the absence of DNA the Michaelis constant, K_M , was 0.3 mM and the turnover number k_{cat} was 0.4 per second per dimer.

In the presence of DNA cooperativity between the ATP binding sites was observed. At half-maximal velocity the $K_M = 0.13$ mM and the k_{cat} increased by about 20-fold (Lindsley and Wang 1993). Thus in the presence of DNA the rate of clamp opening and closing will be about 20- fold faster. To relate these observations to the manipulation of DNA the following model was proposed. An ATP-modulated DNA binding clamp in its open state binds a segment of DNA, the T segment. This binding is

possibly due to weak protein-DNA interactions. Upon the binding of ATP the clamp closes and the T segment is pushed through the G segment.

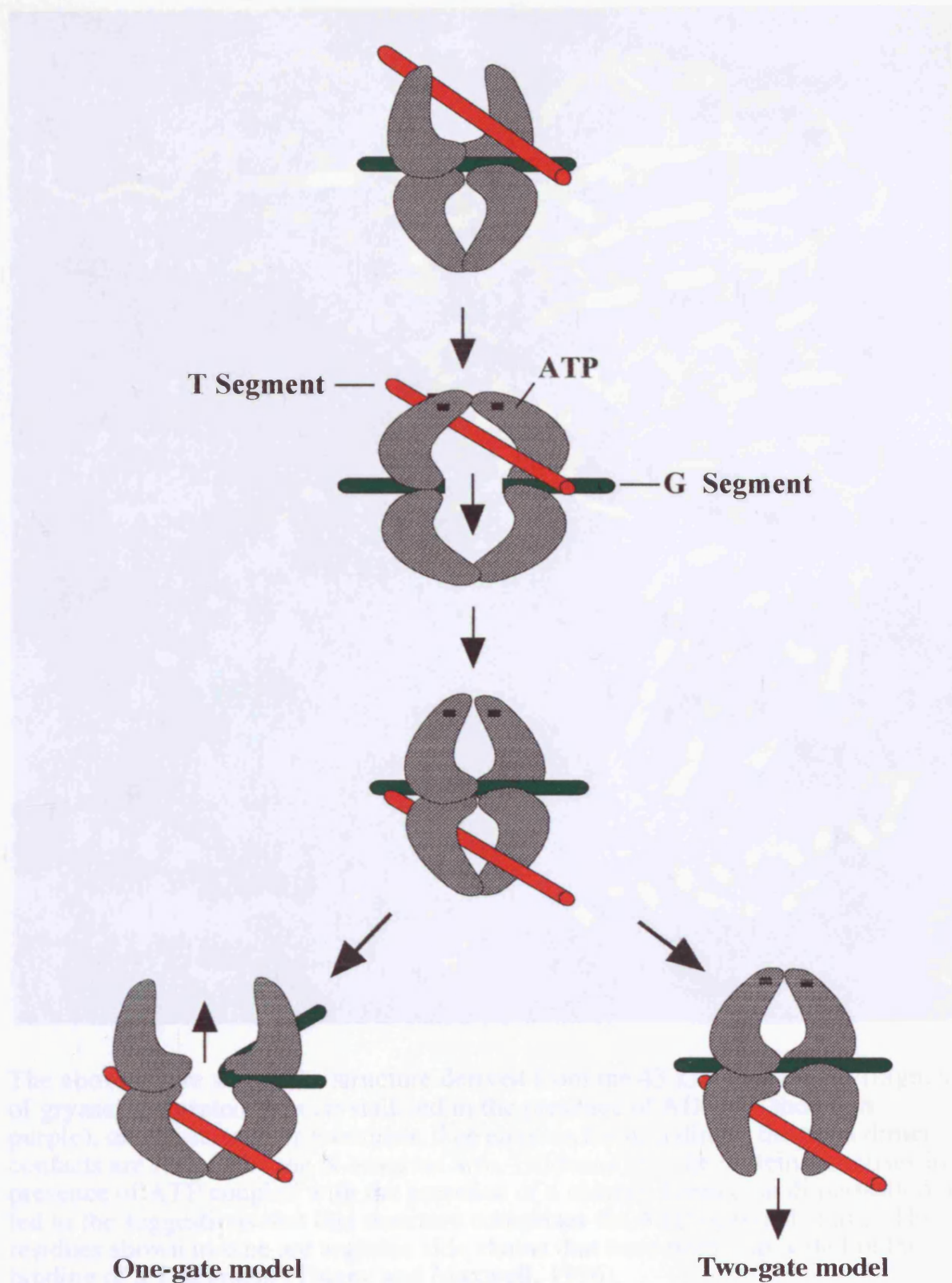
1.3.3 The one gate versus the two-gate model for type II topoisomerases.

Given the good evidence for the existence of a protein clamp in topo IIs there now remained the problem of how many gates for passage of the DNA the enzyme would possess. The two models are shown in figure 1.5. In the first solution the T segment passes through the G segment on the binding of ATP then the G segment partially dissociates from the enzyme. The ATP is hydrolysed, the clamp opens and the T segment dissociates through the now open clamp. This is referred to as the one gate model (Roca and Wang, 1994). In the second model the T segment enters the clamp, the binding of ATP closes the clamp and forces the T segment through the G segment and through a second protein gate in the enzyme. The ATP is then hydrolysed and the clamp re-opens. This is referred to as the two-gate model (Mizuuchi *et al*, 1980; Wang *et al*, 1980). In order to distinguish between these two models an experiment was devised in which two rings of DNA, linked at a single position, were treated with topo II. On the addition of ADPNP a single turnover event would take place. The one gate model would predicted that this would result in both DNA rings being trapped in the annular form of the enzyme stabilised by ADPNP, the clamp being permanently closed. The two-gate model would predict that a single turnover event would be sufficient to separate (decatenate) the rings and the one containing the T segment would be passed through the enzyme and released. What was found was that on the addition of ADPNP the plasmid was released from the complex, this evidence supported the two-gate model (Roca and Wang 1994).

1.3.4 The structure of type II topoisomerases.

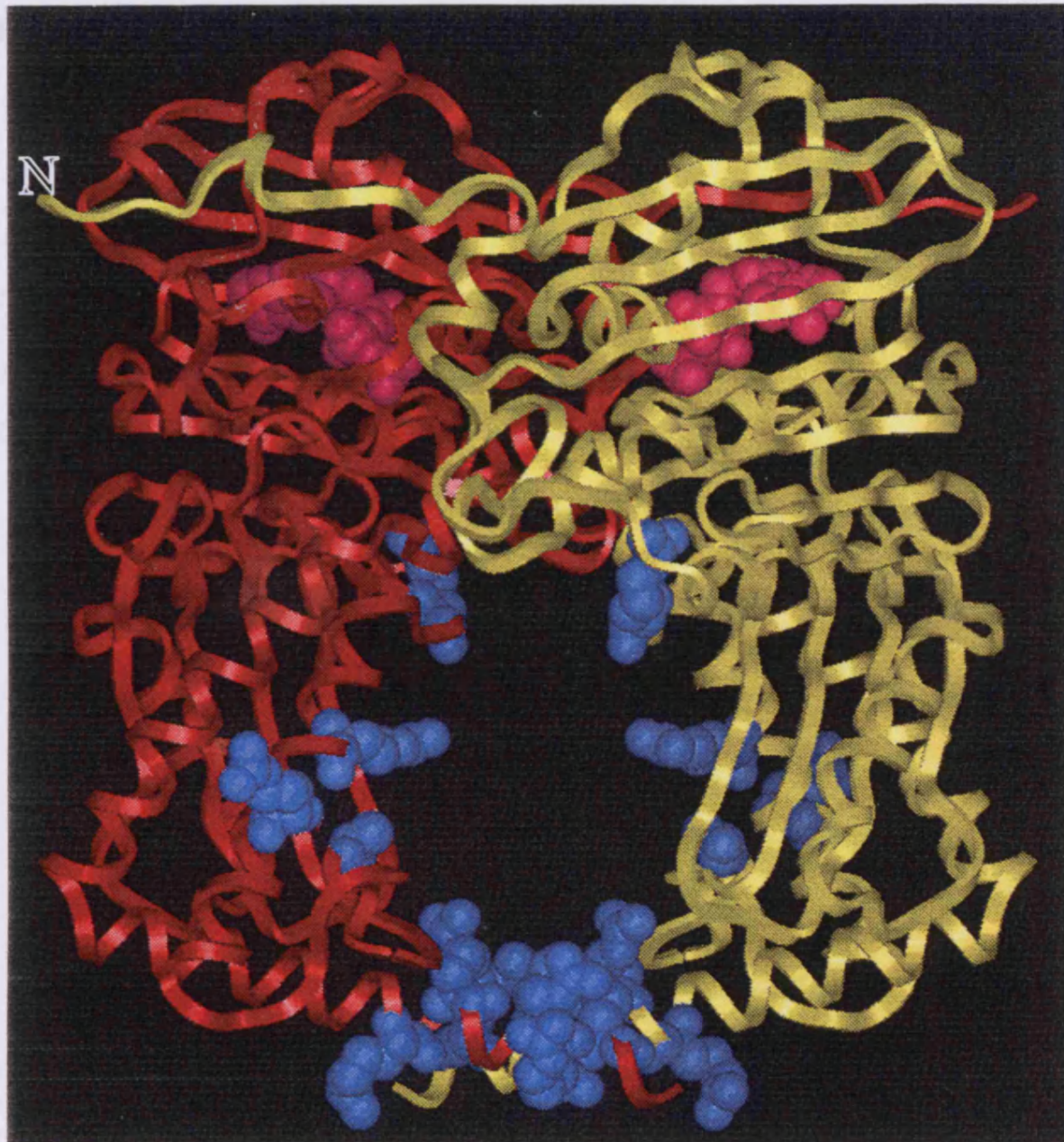
In figure 1.6 we see the crystal structure of the N-terminal domain of the bacterial enzyme gyrase (Wigley *et al*, 1991). This portion of the enzyme comprises amino acids 2 to 393 of the GyrB protein. This subunit has been shown to be responsible for the binding and hydrolysis of ATP in gyrase and the residues involved have been identified. From this structure a mechanism for the hydrolysis of ATP by the enzyme has been proposed and mutagenesis studies on this fragment have confirmed this proposal (Jackson and Maxwell, 1993). The mechanism for the hydrolysis of ATP is seen in figure 1.7. This mechanism involves His38 hydrogen bonding to Glu42, this interaction allows Glu42 to act as a general base that promotes a nucleophilic attack by a molecule of water on the γ -phosphate of ATP. A sequence comparison of this portion of this enzyme shows good homology to other type II enzymes (figure 1.8). The protein was crystallised in the presence of ADPNP and probably will represent the ATP-bound form of the enzyme. In the structure we see that an N-terminal arm comprising amino acids 2 to 15 extends out from one monomer to form dimer contacts with the second monomer. The C-terminal helix also appears to make dimer contacts, however these may represent a crystallographic contact rather than a native one. The structure shows the protein as a dimer with one molecule of ADPNP bound to each of the monomers. Studies performed on this 43 kDa fragment have shown that the protein is a monomer in solution but dimerises in the presence of ATP (Ali *et al*, 1995). Analysis of the turnover of ATP by this fragment has indicated that the binding of nucleotide to the binding pockets is not co-operative. However studies on the yeast enzyme (Lindsley and Wang, 1993) and binding studies using ADPNP with full-length gyrase (Tamura *et al*, 1992) have revealed co-operativity between the ATP binding sites. That this is not seen in the 43 kDa domain may be due to the observation that the

Figure 1.5 One gate vs two gate model.



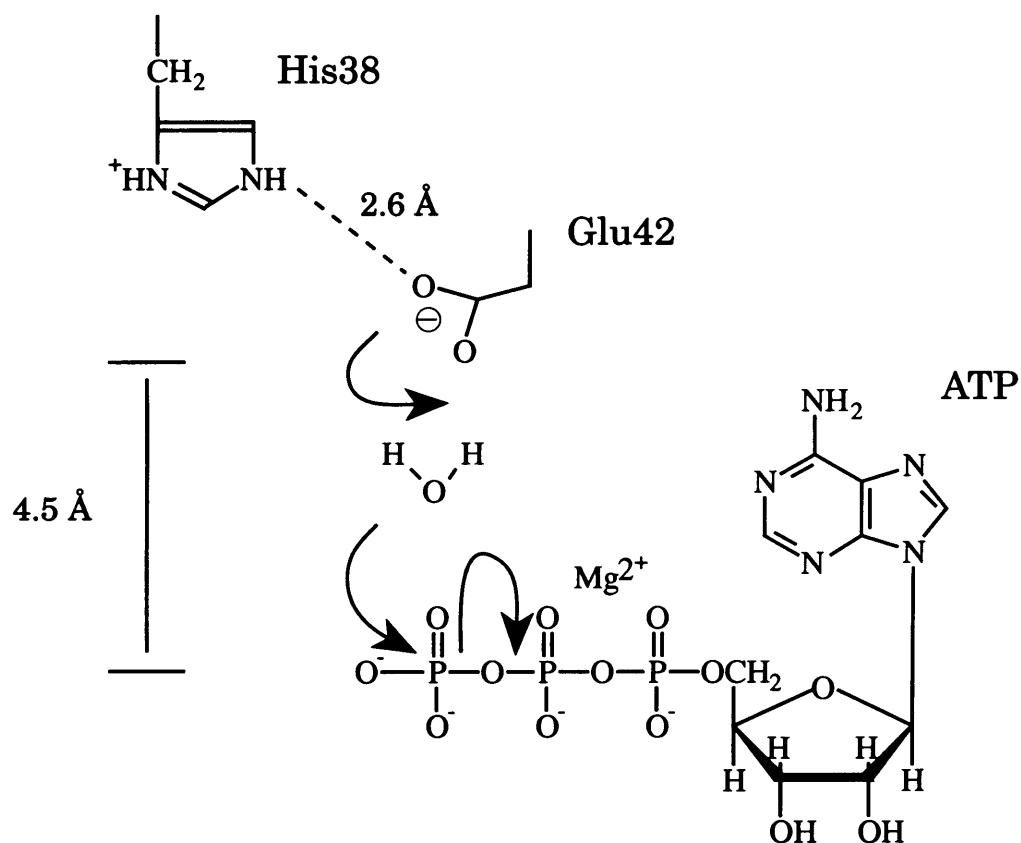
Following the passage of the T segment of DNA through the G segment there are two proposed models to explain the exit of the T segment from the enzyme-DNA complex. The one gate model allows the G segment to partially dissociate and the T segment to exit from same gate through which it entered the complex. The two gate model allows a second gate to open in the complex and the T segment to exit via this gate.

Figure 1.6 The crystal structure of the 43kDa N-terminal domain of gyrase



The above figure shows the structure derived from the 43 kDa N-terminal fragment of gyrase. The protein was crystallised in the presence of ADPNP (shown in purple), one molecule per monomer. The enzyme forms a dimer, the main dimer contacts are formed by the N-terminal arm. Evidence that the protein dimerises in the presence of ATP coupled with the presence of a channel formed on dimerisation has led to the suggestions that this structure comprises the ATP-operated clamp. The residues shown in blue are arginine side chains that have been implicated in the binding of a T-segment (Tingey and Maxwell, 1996).

Figure 1.7 Mechanism of ATP hydrolysis by DNA gyrase.



The above figure shows the proposed mechanism of ATP hydrolysis by the 43 kDa fragment of gyrase. The residue His 38 is hydrogen bonded to the Glu 42 residue, this interaction allows Glu 42 to act as a general base that promotes nucleophilic attack by a water molecule on the γ -phosphate of ATP.

Figure 1.8 Amino acid alignment of the region containing the active residues for the ATPase activity of several topoisomerase IIs.

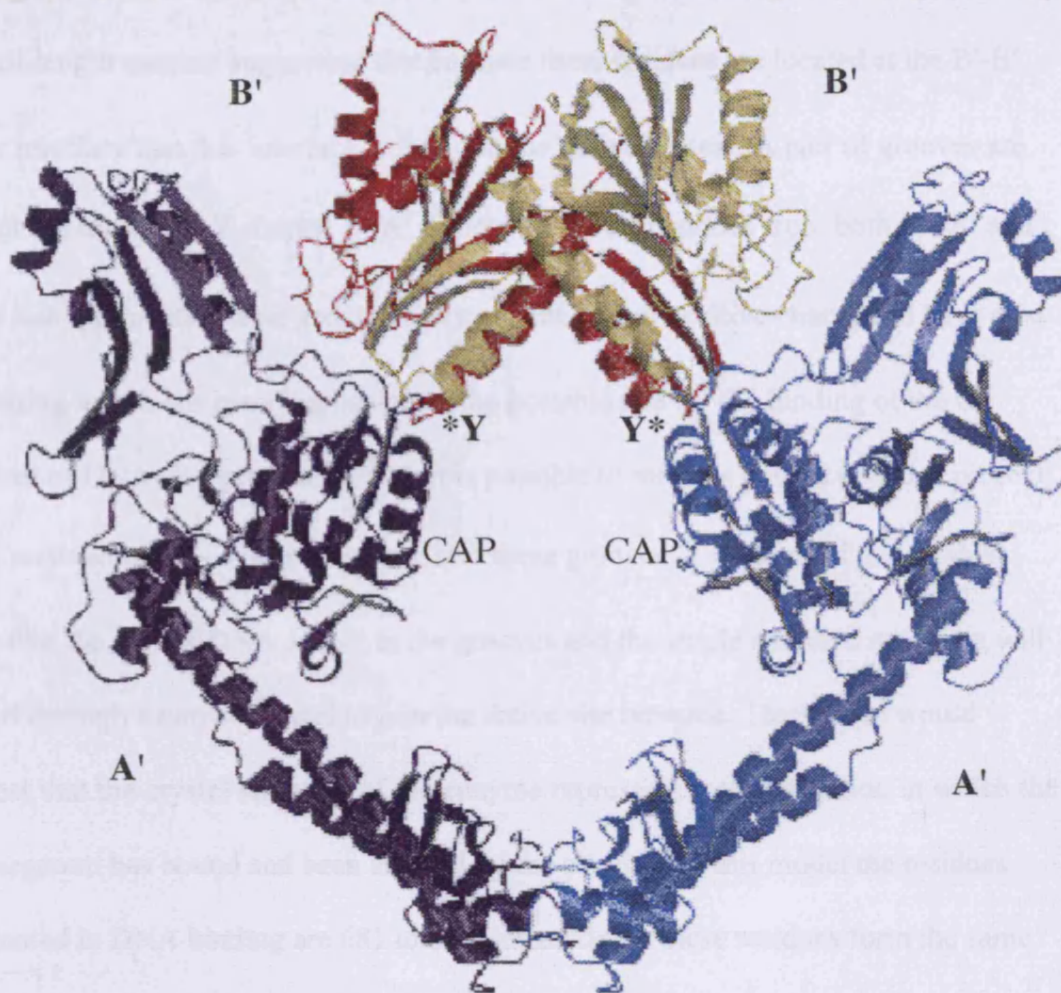
<i>E. coli</i> GyrB	G ₃₅	L	H	H	M	V	F	E	V	V	D	N	A	I	D ₄₉
<i>P. putida</i> GyrB	G ₃₇	L	H	H	M	V	F	E	V	V	D	N	S	I	D ₅₁
<i>N. gonorrhoeae</i> GyrB	G ₃₉	L	H	H	M	V	F	E	V	L	D	N	A	I	D ₅₃
<i>B. subtilis</i> GyrB	G ₃₆	L	H	H	L	V	W	E	I	V	D	N	S	I	D ₅₀
<i>Pr. mirabilis</i> GyrB	G ₃₅	L	H	H	M	V	F	E	V	V	D	N	A	I	D ₄₉
<i>S. aureus</i> GyrB	E ₄₂	L	H	I	S	V	.	E	I	V	D	N	S	I	D ₅₆
<i>Haloferax</i> GyrB	G ₃₆	L	H	H	L	V	Y	E	V	V	D	N	S	I	D ₅₀
<i>M. pneumoniae</i> GyrB	G ₃₉	L	H	H	M	I	W	E	I	I	D	N	S	I	D ₅₃
<i>E. coli</i> ParE	R ₃₁	P	N	H	L	G	Q	E	V	I	D	N	S	V	D ₄₅
bacteriophage T4 gp 39	G ₄₇	L	V	K	L	I	D	E	I	I	D	N	S	V	D ₆₁
bacteriophage T2 gp 39	G ₄₇	L	V	K	L	I	D	E	I	I	D	N	S	V	D ₆₁
<i>H. sapiens</i> Top II α	G ₇₉	L	Y	K	I	F	D	E	I	L	V	N	A	A	D ₉₃
<i>H. sapiens</i> Top II β	G ₇₉	L	Y	K	I	F	D	E	I	L	V	N	A	A	D ₉₃
<i>D. melanogaster</i> Top II α	G ₆₀	L	Y	K	I	F	D	E	I	L	V	N	A	A	D ₇₄
<i>Sa. cerevisiae</i> Top II α	G ₅₈	L	F	K	I	F	D	E	I	L	V	N	A	A	D ₇₂
<i>Sc. pombe</i> Top II α	G ₇₀	L	Y	K	I	F	D	E	I	I	V	N	A	A	D ₈₄
<i>T. brucei</i> Top II α	G ₅₃	L	L	K	I	V	D	E	I	L	L	N	A	S	D ₆₇
<i>C. fasciculata</i> Top II α	G ₅₃	L	L	K	I	V	D	E	I	L	L	N	A	A	D ₆₇

The above figure shows the sequence alignment of several type II topoisomerases. As can be clearly seen there is a considerable degree of homology between them in this region. Experiments on the 43 kDa fragment of *E. coli* GyrB have provided good evidence that Glu42 acts as the catalytic base during the ATPase reaction of that enzyme. This evidence suggests that Glu86 would fulfil a similar role in human topoisomerase II α . There is evidence that His38 in *E. coli* GyrB is important; it has been suggested that a hydrogen bond formed by this residue to Glu42 allows Glu 42 to act as a general base. A similarly charged amino acid (Lys 82) is found in the human sequence.

enzyme cannot dimerise until both monomers have independently bound nucleotide. These results provided evidence that the binding of nucleotide promotes dimerisation and that ATP cannot be hydrolysed until the dimer is formed. The dimerisation of the 43 kDa in the presence of nucleotide has supported the view that the ATPase domain is the site of the ATP-modulated clamp in type II enzymes. This clamp is denoted as the N-gate as in the single polypeptide chain eukaryotic enzymes this domain is the N-terminal portion of the enzyme.

Figure 1.9 shows the crystal structure of the 92-kDa fragment of the yeast type II topoisomerase representing amino acids 409 to 660. This structure lacks the ATPase domain and 227 amino acids comprising the C-terminus. The protein is capable of forming covalent adducts with double stranded DNA. This fragment can be sub divided into two portions. The B' fragment represents the C-terminal end of the GyrB subunit and the A' fragment represents the N-terminal portion of the GyrA subunit, but is lacking the 227 residue C-terminal portion. It has been demonstrated that in the yeast enzyme the C-terminal portion is not necessary for the catalysis of DNA transport (Shiozaki and Yanagida, 1991). Taken along with the 43 kDa structure of the N-terminal portion of gyrase these structures can be used to provide a framework, albeit incomplete, on which can be modelled the action of type II topoisomerases. In detail the yeast structure reveals that the two B' fragments contact each other forming an arch over the V shaped A'-A' dimer. This encloses a cavity some 55 Å in width at its base. The major dimer interface is formed by the contacts between the A' subunits at the C-terminal end. This interface buries 1000 Å². The contacts formed by the B'-B' contacts would appear to be less extensive but are of importance (Berger *et al*, 1996). Studies have shown that lysine side chains near residues 550 and 600 are less reactive in the full

Figure 1.9 The crystal structure of the 92 kDa fragment of yeast topo II.



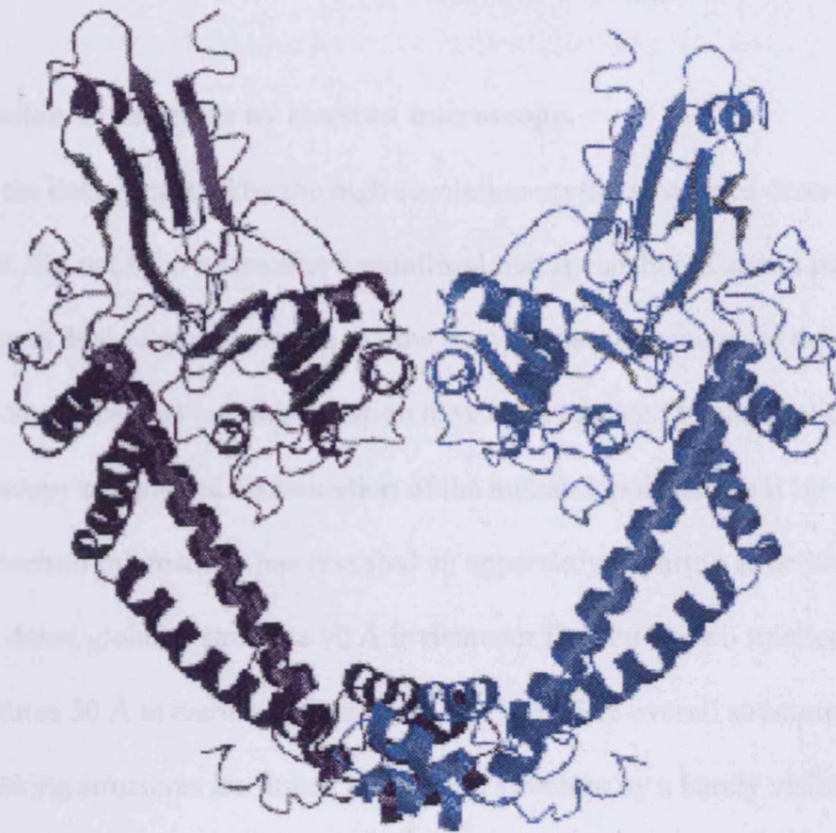
Primary dimer interface, C-gate.

The above figure shows the crystal structure derived from a 92-kDa fragment of the yeast enzyme, the structure represents amino acids 410 to 1202. This structure can be divided into sub fragments A' and B'. The fragment cannot perform strand passage but can cleave DNA. The active site tyrosines are shown (Y). The primary interface has been implicated to be the site of the C-gate. The CAP sites marked are the position of domains that contain the same fold as the DNA binding region in the *E. coli* catabolite activator protein (Berger *et al*, 1996)

length enzyme than in just the N-terminal fragment. This may indicate they are buried in the full-length enzyme suggesting that because these residues are located at the B'-B' dimer interface that this interface is found in the native protein. A pair of grooves are seen at the top of the V shaped A'-A' dimer formed by residues from both the A' and the B' sub fragments. These grooves carry a great deal of positive charge and have a 20 Å opening which has been implicated as the possible site for the binding of the G segment of DNA (Berger *et al*, 1996). It is possible to model a double stranded piece of DNA containing a 5'- 4 base overhang into these grooves. The result of this models show that the duplex DNA can sit in the grooves and the single stranded overhang will extend through a narrow tunnel to join the active site tyrosine. This model would suggest that the crystal structure of the enzyme represents a conformation in which the gate segment has bound and been cleaved by the enzyme. In this model the residues implicated in DNA binding are 681 to 819, interestingly these residues form the same fold as the DNA-binding region in the *E. coli* catabolite activator protein (CAP). The same fold is also present in histone H5, this region has been termed the CAP-domain. Evidence to support this interpretation of the model has recently been provided by lysine footprinting data (Li and Wang, 1997).

Figure 1.10 shows the crystal structure derived from a 59-kDa fragment of the *E. coli* GyrA protein (Morais Cabral *et al*, 1997). This fragment represents residues 2-523 of GyrA protein. A sequence alignment of this fragment shows that it is analogous to the A' subfragment of the yeast enzyme. As can be seen, the general structural architecture of the protein is broadly similar to the yeast enzyme although the comprising elements show a different conformation, it has been suggested that this structure may represent a further conformation in the catalytic cycle. The conformation

Figure 1.10 Crystal structure of a 59 kDa fragment of gyrase.



GyrA59

The above figure shows the a crystal structure of the 59 kDa fragment of gyrase; this fragment represents residues 2-523 of the Gyr A protein. A sequence analysis of this fragment shows good homolgy to the A' fragment of the yeast enzyme seen in figure 1.9. A comparison of the two structures show very similar architecture. The sub-domains within the two enzymes are arranged differently, this may reflect different conformation within the enzymes.

that has been suggested is that in which the G segment of the DNA has bound but is not yet cleaved.

1.3.5 Investigation of structure by electron microscopy.

For all the data generated by the high-resolution crystal structures described above there has still not been a structure crystallised that is capable of strand passage. This leaves a great deal of speculation as to how the various subdomains of the enzyme are connected. Some insights into this question have been revealed by the application of electron microscopy techniques. Examination of the human topoisomerase II by transmission electron microscopy has revealed an apparently tripartite structure consisting of a dense globular structure 90 Å in diameter flanked by two smaller spherical structures 50 Å in diameter (Schultz *et al*, 1996). The overall structure is V shaped, the flanking structures are linked to a central structure by a barely visible linker regions 30-40 Å in length. The angle of separation between the flanking structures and the central domain varied widely between 40° and 180°. Images of the yeast enzyme revealed a similar tripartite structure (Benedetti *et al*, 1997). However deletion of the N-terminal 409 residues representing the GyrB type ATPase domain showed a significant reduction in the density of the two flanking domains. This suggested that the flanking structures are the N-terminal GyrB like domains. Interestingly pre-incubation of either the yeast or the human enzyme with ADPNP alters the structure, the two flanking domains appearing to move together to come into contact with each other. Drawing on data from both the x-ray crystallography and the observations made using electron microscopy the following general conclusions can be drawn. The eukaryotic enzyme can be broadly subdivided into two modules that correspond approximately to the GyrA and GyrB subunits in the bacterial gyrase. The A units appear to form permanent

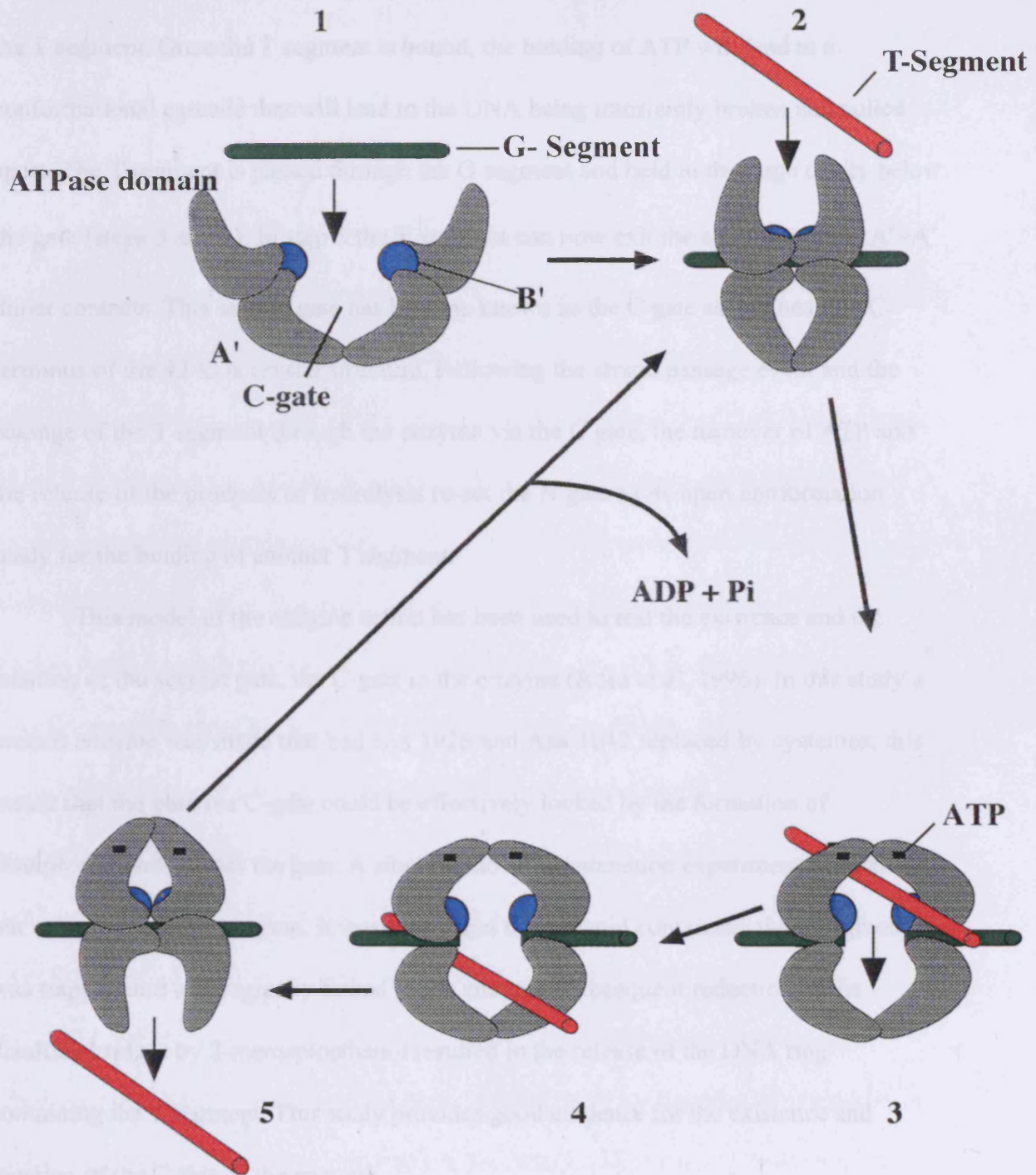
contacts in the presence or absence of nucleotide. The B units appear to undergo dimerisation in the presence of nucleotide. This observation may be related to the presence of a nucleotide operated clamp located in the GyrB like module of the eukaryotic enzyme.

It can be noted from these studies that there appear to be very few links between the A and the B units seen. The observation is backed up in a footprinting study of the lysyl residues to see whether residues in either the GyrA like subunit or the GyrB like subunit are protected by the presence of the other polypeptide (Li and Wang, 1997). This study shows that lysyl residues present in this region are not protected in the presence of the other protein.

1.3.6 A detailed model of the action of type II topoisomerases.

The relative wealth of recent data on the structure and function of the type II topoisomerase allows the construction of a detailed model relating this structure to the enzyme's action. This is summarised as a cartoon in figure 1.11. In the first step the protein is seen in an open state. In this state the core of this figure represents the 92-kDa crystal structure, the ATPase domains are depicted on top of the main structure. In the absence of bound nucleotide the ATPase domains are apart, the N-gate is in an open conformation. The B' subdomains are also apart in this conformation the overall dimer structure is maintained by the A'A' contacts at the bottom of the structure. The open structure now binds a segment of DNA that will make up the G gate. This will trigger a conformational change in the enzyme in which the two halves of the dimer move closer together, it has been estimated by as much as 35-40 Å (Berger *et al*, 1996). This brings catalytic site tyrosines in each half of the enzyme near to the G segment phosphate groups for nucleophilic attack and the introduction of a double stranded break. In step 2

Figure 1.11 Mechanism of strand passage in topo II.



The above figure shows the proposed mechanism for strand passage by type II topoisomerases. See text for detailed discussion.

the open N-gate at the top of the model is ready to bind a duplex of DNA that will form the T segment. Once the T segment is bound, the binding of ATP will lead to a conformational cascade that will lead to the DNA being transiently broken and pulled apart. The T segment is passed through the G segment and held in the large cavity below the gate (steps 3 and 4). In step 5 the T segment can now exit the enzyme via the A'-A' dimer contacts. This second gate has become known as the C gate as it is near the C-terminus of the 92-kDa crystal structure. Following the strand passage event and the passage of the T segment through the enzyme via the C gate, the turnover of ATP and the release of the products of hydrolysis re-set the N gate to its open conformation ready for the binding of another T segment.

This model of the enzyme action has been used to test the existence and the location of the second gate, the C-gate in the enzyme (Roca et al, 1996). In this study a mutant enzyme was made that had Lys 1026 and Asn 1042 replaced by cysteines; this meant that the putative C-gate could be effectively locked by the formation of disulphide bonds across the gate. A single turnover decatenation experiment was carried out using the mutant enzyme. It was found that the plasmid containing the T segment was trapped and topologically linked to the enzyme. Subsequent reduction of the disulfide bridges by 2-mercaptoethanol resulted in the release of the DNA ring containing the T segment. This study provides good evidence for the existence and location of the C gate in the enzyme.

1.4 ATP UTILISATION BY TYPE II TOPOISOMERASES.

A question which has been of fundamental interest in the study of the type II topoisomerases, has been how they couple the binding and hydrolysis of ATP to the

movement of DNA. It must also be noted that the removal of supercoils from DNA is not a process that would appear to require the need to use a high-energy co-factor such as ATP. As it is possible to have one round of strand passage from the binding of a non-hydrolysable analogue of ATP, ADPNP, it is generally thought that it is the binding of ATP that promotes strand passage and the hydrolysis and the release of products are involved in enzyme turnover (Sugino *et al*, 1978; Peebles *et al*, 1979). The process may well be more complex than this. In a study on a bacterial GTPase involved in the translocation of ribosomes along the messenger RNA (Rodnina *et al*, 1997), it has been found that although the binding of a non-hydrolysable GTP analogue is sufficient to promote one round of translocation, GTP itself is rapidly hydrolysed prior to translocation. This gives rise to the possibility that the hydrolysis of the GTP is responsible for rapid translocation. This may provide a model for the role of ATP in the type II topoisomerases, the binding of nucleotide being sufficient to initiate a conformational cascade resulting in a strand passage event whereas the hydrolysis of nucleotide will drive the strand passage and the conformational changes needed to turnover the enzyme. Investigations using pre-steady state kinetics of the intimate turnover details of ATP on enzyme have shown that the enzyme as expected hydrolysed two ATP molecules per turnover event but that they are hydrolysed sequentially (Harkins and Lindsley, 1998; Harkins *et al*, 1998). One of the bound ATP molecules is hydrolysed and the products of the reaction are released before the hydrolysis of the second ATP. How this sequential hydrolysis is coupled to the function of the enzyme is still matter for speculation.

Theoretically the binding of one ATP molecule could be sufficient to promote a strand passage event. Studies on a yeast enzyme heterodimer consisting of one wild-type monomer and one monomer containing a mutation in the ATPase active site

(Lindsley and Wang, 1993b) suggest that the binding of one ATP is sufficient to lead to the dimerisation of the N-gate. Several studies have looked at the efficiency of coupling between ATP hydrolysis and strand-passage. In a study using the yeast enzyme and the non-hydrolysable analogue ADPNP to initiate one round of relaxation from a moderately supercoiled plasmid, it was shown that 90% of all enzymes bound to the DNA were able to perform strand passage in the presence of excess ADPNP (Roca and Wang, 1996). This estimate does not account for the likelihood of some of the enzyme being inactive. Taking this into account it can be said that the efficiency with moderately supercoiled DNA approaches the theoretical limit. In studies using ATP and the yeast enzyme (Lindsley and Wang, 1993) it was found that at saturating ATP concentrations the enzyme hydrolysed 7.4 ± 1 ATP molecules per strand passage event. When the experiment was repeated using lower ATP concentrations it was seen that the enzyme hydrolysed 1.95 ± 0.5 ATP molecules per strand passage event. This result can be interpreted in the following way. At high concentrations of ATP the enzyme rapidly binds ATP closing the clamp without trapping a T segment. Effectively the enzyme is closing the clamp and hydrolysing ATP at a rate that is greater than the rate at which the T segment can be trapped. At lower ATP concentrations the rate at which the enzyme binds ATP and closes the clamp is slower than the rate at which the T segment can move into the clamp. So the enzyme will on average have bound a T segment of DNA prior to the binding of nucleotide and the closing of the N-gate. At very low concentrations of ATP the binding of a single molecule to the dimer could in theory be sufficient to promote strand passage. At higher concentrations the effect of cooperativity between ATP-binding sites would cause the binding of one molecule of ATP to lead to the closure of the N-gate and lead very rapidly to the binding of a second

ATP molecule. This would lead to the hydrolysis of two ATP molecules per turnover event at high ATP concentrations.

1.4.1 The coupling of the hydrolysis of ATP to strand passage in type II topoisomerases.

The above described observations lead to an understanding of how the enzyme utilises the binding and hydrolysis of ATP to pass the T segment from the N-gate through the double stranded break in the G gate and through the C gate to complete a round of strand passage. Experimental evidence demonstrates that if a T segment is present within the N gate on the binding of nucleotide a strand passage event will occur. Evidence for this view is provided by the decatenation of singly linked rings of DNA by the binding of ADPNP (Roca and Wang, 1994). Given this observation it can be assumed that the actual efficiency of strand passage will be determined by the probability of finding a T segment in the N-gate. This probability will differ according to the topology of the DNA. For topo IIs the evidence of experiments using ADPNP and a supercoiled DNA substrate suggests that the probability of binding a T-segment is very high therefore the coupling of the binding of nucleotide with strand passage is good. For the same experiment using a relaxed DNA substrate only 25% of nucleotide binding events will lead to strand passage (Roca and Wang, 1994). The probability of binding a T-segment from a relaxed substrate is considerably lower than a supercoiled substrate.

In general it can be said that the high degree of coupling between ATP usage and strand passage is reliant on two reactions. The binding of two molecules of ATP will almost always lead to the closure of the N-gate and that if a T segment is present in the N-gate it will be passed through the enzyme. To achieve a high degree of coupling it is clear that the dimerisation must occur before the hydrolysis of ATP. This is achieved by

ensuring that residues on both monomers are needed for ATP hydrolysis to occur. The catalytic pocket that is required to hydrolyse ATP could only be formed when the N-gate is closed.

1.4.2 Examination of DNA-dependent ATP hydrolysis.

In the yeast enzyme in the presence of DNA the rate of ATP hydrolysis is 20-fold higher than in its absence (Lindsley and Wang 1993). This DNA-stimulated ATPase activity is thought to be largely the product of the enzyme binding the G-segment of DNA. This theory arises from the observation that the structural data indicate that the binding of the G-segment will involve both the GyrA and GyrB like regions of the enzyme and that this might lead to the conformational changes that will help facilitate the dimerisation of the N-gate. The role of the T segment is still a matter of debate. DNA stimulates the ATPase activity of the N-terminal fragment of the yeast enzyme by 20% (Wang, 1998).

Experiments on the bacterial gyrase have shown that DNA stimulation is dependent on the length of the DNA (Maxwell and Gellet, 1984). At less than 70 bp, a high concentration of DNA is necessary to stimulate ATP turnover (a four fold excess over enzyme dimer, by molar weight). This result can be interpreted as the need to bind DNA at two sites in the enzyme for maximum stimulation. A recent study using the human enzyme also suggested that enzyme required binding of DNA at two sites for maximum stimulation (Hammonds and Maxwell, 1997). A study on the structure of the ATPase domain the 43 kDa N-terminal fragment of the bacterial enzyme gyrase led to the construction of a mutation involving an arginine residue. This residue, Arg-286, is situated within the channel formed by the closure of the clamp and it has been postulated that it could play a role in the binding of the T segment. The arginine residue

was replaced with a glutamine and it was found that the mutant enzyme retained its intrinsic ATPase activity but no longer had any DNA-stimulated ATPase activity (Tingey and Maxwell, 1996). These studies tend to suggest a role for the binding of the T segment in the DNA-dependent stimulation of the enzyme. It would seem advantageous to ensure that ATP hydrolysis could not occur until the T segment was present in the clamp. As the enzyme can bind ATP in the absence of a T segment and this will lead to closure of the clamp, this would effectively leave the enzyme stranded in a closed clamp conformation. ATP will now only be turned over at a non DNA-dependent rate

1.4.3 Structural change in the conformation of the enzyme on the binding of nucleotide.

On the binding of nucleotide to the N-gate, the enzyme would undergo a series of conformational changes that would lead to a strand passage event in the presence of a bound G and T segment. The structural changes that takes place have been examined by performing proteolysis on the enzyme (Lindsley and Wang, 1991). In the yeast enzyme, using V8 endoprotease a major conformational change has been detected on the binding of ADPNP (see fig 1.2). In the absence of ADPNP the two protease sites in the enzyme are at Glu409 (site A) and around residue 1200 (site C), in the presence of ADPNP the first site is shifted to after Glu679 (site B) whilst the second site remains unchanged.

Changes in the conformation of the 43 kDa N-terminal domain of gyrase have been investigated by limited tryptic digest. Under conditions of limited proteolysis in the presence of ADPNP the protein is cleaved after Lys307 and produces a 33 kDa protease resistant fragment, this protease resistance is not seen in the absence of ADPNP (Ali *et al*, 1995). Additional evidence for the conformational change on the

binding of nucleotides comes from studies involving the citraconylation of lysyl residues. Three sites in the yeast enzyme Lys 11/14, 98/102, and 135/136 have been shown to show a change in susceptibility to citraconylation on the binding of ADPNP. These sites have been mapped onto the existing crystal structure of the ATPase domain of gyrase, based on sequence alignments and have shown that the sites at 98/102, and 135/136 are probably directly contacting the bound ADPNP. The 11/14 site is probably affected because it appears to lie at the N-gate dimerisation interface (Li and Wang, 1997).

1.4.4 The effect of ATP hydrolysis on the breakage and re-union reaction.

There are two conflicting lines of evidence for the effect of ATP hydrolysis on the breakage and reunion reaction at the G-segment. It has been shown that the formation of covalent adducts of protein on DNA are often enhanced in the presence of nucleotide (Sugino *et al*, 1978; Peebles *et al*, 1978; Fisher *et al*, 1981; Sander and Hsieh, 1983; Kreuzer and Alberts, 1984; Osheroff and Zechiedrich 1986). It has also been seen that in a mutant yeast topoisomerase with the active site tyrosine responsible for cleavage replaced with phenylalanine, making DNA cleavage impossible, the DNA-dependent ATPase rate was largely abolished (Wang, 1998). Both of these observations would suggest that ATP hydrolysis affects the cleavage of DNA. However it has been observed on many occasions (Jackson and Maxwell, 1993; Lindsley and Wang 1993; Berger *et al* 1996; Tingey and Maxwell, 1996) that truncated forms of the enzyme lacking the ATPase domain can cleave DNA as can full-length enzyme in the absence of ATP. Enzymes that have point mutations within the ATPase site have also been shown to cleave the DNA. These data would suggest that ATP has no effect on cleavage. These conflicting observations remain a matter for further investigation.

1.4.5 The effect of the binding of the T-segment on the cleavage reaction.

Studies using the *Drosophila* enzyme and a 40-bp DNA duplex have shown that the rate of cleavage of this DNA has a sigmoidal dependence on DNA concentration. This would suggest that the enzyme is binding two duplexes of DNA and that the T-segment is possibly required for promotion of cleavage in the G-segment (Corbett *et al*, 1992). In studies on the yeast enzyme in the presence of ADPNP, which effectively converts the enzyme into an annular form, linear DNA was allowed to thread through the closed enzyme-ADPNP complex. With the clamp closed it is impossible for the T-segment to become trapped. In this study treatment of the enzyme-DNA complex with etoposide, a drug that stabilises the cleavage of DNA, and SDS as denaturant, cleavage of the G-segment was found to be extensive (Roca and Wang, 1992). This study therefore provides good evidence that binding of the T segment is not required for the cleavage of the G-segment to take place.

Once a T-segment has been bound it must be moved through the break in the G segment, to do this the G segment must be pulled apart. This suggests that although the binding of a T-segment is not coupled to the breakage of the G segment it must be strongly coupled to the mechanism which results in the G segment being pulled apart. Studies on the crystal structure of the N-terminal 43 kDa fragment of the bacterial gyrase have shown that the channel formed by the dimerisation of the two halves of the gate is not large enough to accommodate a duplex of DNA (Tingey and Maxwell, 1996). This has lead to the suggestion that the steric repulsion associated with the trapping of the T-

segment could lead directly to the opening of the G-segment. Once the T-segment has been passed through the G-segment it will enter the large cavity seen in Figure 1.9. The positive charges that line the cavity will help with the movement of the T segment.

1.4.6 The exit of the T-segment from the topoisomerase complex.

Once the T-segment has been passed through the break in the G-segment it would now appear to be in a large cavity lined with positive charge. This raises the question of how the T-segment can now be driven from this favourable environment to exit at the C-gate. The mechanism is still a matter of speculation. If the gate-open conformation is not energetically stable once the T-segment has passed then the enzyme could rapidly return to a more stable conformation with the DNA gate shut. The movement of the subunits accompanying this change could narrow the cavity holding the T-segment and lead to its exit from the complex (Berger *et al*, 1996).

1.4.7 Phosphorylation of eukaryotic type II topoisomerases.

Eukaryotic topoisomerases are known to be phosphorylated at multiple sites and there is evidence to suggest that phosphorylation may modulate the catalytic activity of the enzyme (Watt and Hickson, 1994). Phosphorylation of *Drosophila* topo II by casein kinase II or protein kinase C results in an increase in relaxation activity (DeVore *et al*, 1992) and ATPase activity (Corbett *et al*, 1992; Corbett *et al*, 1993). The major site of phosphorylation is the C-terminal domain. In the yeast enzyme, *S. cerevisiae*, multiple sites of phosphorylation have been mapped to the C-terminal domain and phosphorylation has been proposed to have a regulatory effect on the enzyme (Cardenas *et al*, 1992; Alghisi *et al*, 1994). The human topo II α has been shown to be the target of three kinases, casein kinase II, protein kinase C and p34cdc2 (Wells *et*

al, 1994; Wells and Hickson, 1995; Wells *et al*, 1995). The major site of phosphorylation by protein kinase C in the human enzyme is again the C-terminal domain. Although one site at Ser 29, in the N-terminal domain, has been found to be phosphorylated *in vivo* and *in vitro* (Wells *et al*, 1995) the effect of phosphorylation at this site on the ATPase activity of the enzyme is unknown.

1.5 HUMAN TYPE II TOPOISOMERASES.

In contrast to lower eukaryotic cells, which are thought to express only a single type II topoisomerase, e.g., *S. cerevisiae*, mammalian cells express two genetically different but closely related isoforms. Studies in human cell lines have revealed the presence of a 170-kDa isoform (topo II α) and a 180-kDa isoform (topo II β) (Jenkins and Hickson, 1992; Drake *et al*, 1989). These isoforms are the products of different genes (Tsai-Pflugfelder *et al*, 1988; Tan *et al*, 1992; Jenkins and Hickson, 1992) and while the enzymatic significance of the two forms is not clear, there is evidence to suggest they are differentially expressed and regulated during the cell cycle (Drake *et al*, 1989). The α form has been shown to be highly expressed in rapidly cycling cells but only expressed at low levels in quiescent cells. In contrast it has been shown that the β form is preferentially expressed in plateau phase cells (Drake *et al*, 1989). The two forms of the enzyme are highly homologous showing 90% sequence similarity, a sequence alignment showing they diverge only in the C-terminal portion. This C-terminal portion is known to be the major site of phosphorylation in the enzymes. There is additional evidence to suggest that the phosphorylation state of the two enzymes differ throughout the cell cycle (Burden and Sullivan, 1994; Wells *et al*, 1995; Wells and Hickson, 1995) and that subcellular localisation of the two isoforms may

differ (Nergi *et al*, 1993) . This evidence has led to the suggestion that the two classes have differing roles in the cell cycle. It has been suggested that the α isoform of the enzyme plays a major role in the untangling of replicated chromosomes at mitosis, whilst the β isoform performs a “house-keeping” function managing the torsional stresses arising from the cellular processing of DNA.

1.6 CLINICAL IMPORTANCE OF TYPE II TOPOISOMERASES.

Since the classification of type II topoisomerases as necessary cellular enzymes for the processing of DNA, they have also been recognised as the targets of many of the clinically important antitumour agents (Froelich-Ammon and Osherooff, 1995; Chen and Liu, 1994; Isaacs *et al*, 1995). This has led to studies into the actions of these compounds to gain insights into how their interaction with topoisomerases can lead to cellular death. As a result of these studies, the anti-topo II compounds can be broadly classified by their modes of action : topoisomerase poisons and topoisomerase antagonists. Studies on the two isoforms of human topoisomerase have suggested that the β form is less sensitive to anti-topoisomerase agents than the α -form. This observation may result from the greater abundancy of the α form in the cell (Drake *et al*, 1989).

1.6.1 Topoisomerase poisons

Ellipticine, m-AMSA, doxorubicin and etoposide (VP-16) all act by interfering with the breakage and reunion step of the topo II cycle leading to protein-associated

double stranded breaks in DNA. This interaction creates structures that convert topo II into a cellular poison. These structures are referred to as cleavable complexes. They consist of a topo II protomer bound covalently to the 5' end of the DNA break via a protein tyrosyl residue. There is evidence to suggest that brief heating of the complex to 80°C will result in reversal of the cleaved complex (Gellert *et al*, 1977), possibly suggesting that the mechanism for cell killing is a consequence of the drug-protein-DNA complex acting as a block to cellular processing of DNA. Evidence for this is provided by the quinolone drugs, a class of antibacterial drugs targeting the *E. coli* enzyme gyrase. These drugs form a cleavable complex with gyrase and DNA. It has been shown that this complex can block the passage of RNA polymerase thus interfering with transcription (Willmott *et al*, 1994). Other consequences of this model can lead to cell death. The interaction between the processing enzymes such as helicase can lead to the stabilised transient covalent breaks becoming permanent double stranded fractures in the DNA, this could lead to cell death (Howard *et al*, 1994).

Different classes of these drugs appear to stabilise the cleavable complex in different ways, etoposide is thought to interfere with the re-ligation step of the cleavage reaction (Corbett and Osheroff, 1993; Sorensen *et al*, 1992; Osheroff *et al*, 1989; Robinson and Osheroff, 1989); it has been suggested that ellipticine enhances the forward rate of cleavage (Corbett and Osheroff, 1993; Robinson *et al*, 1991; Froelich-Ammon *et al*, 1995). Treatment of the cleavable complex by denaturation with SDS and digestion with proteinase K allows the resulting DNA fragments to be released. Studying the resulting DNA fragments has allowed some insight in to the possible interactions of these drugs with the enzyme-DNA complex. Studies on bacteriophage T4 topo II have shown bases that flank the cleavage site tend to be similar regardless of

drug used and the bases immediately 5' or 3' to the cleavage site are specific to the drug used (Freudenreich and Kreuzer, 1993). These features suggest that the two protomers of the enzyme homodimer interact in the same way with the drugs and that the drugs must bind very close to the breakage reunion site. A model has been suggested that involves the drugs stacking in the DNA at the site of cleavage. Evidence for this model is the apparent ability to get a photo-reactive derivative of m-AMSA to cross link to a residue 5' of the cleaved ends (Freudenreich and Kreuzer, 1994). It has been shown that there is no direct correlation between the levels of intercalation and potency of drug action. Etoposide and amsacrine are both potent inhibitors of topo II yet etoposide is strongly intercalative (Wilson *et al*, 1981; Nelson *et al*, 1984) whereas amsacrine is apparently non-intercalative (Robinson *et al*, 1991).

1.6.2 Topoisomerase II antagonists.

There are number of topo II targeting drugs that do not act as topoisomerase poisons but are specific inhibitors of the topo II reaction (topo II antagonists). These compounds have been shown to antagonise the formation of cleavable complexes in the presence of topoisomerase poisons (Chen and Beck, 1995; Corbett *et al*, 1993;). Drugs in this category include bisdioxopiperazines, ICRF-193, fostriecin, merbarone, aclarubicin and novobiocin. Until recently there was little information on the mechanism by which these drugs inhibit topoisomerase activity. Drugs in this class do not appear to have one site of action, they are characterised by their ability to inhibit the enzyme activity. Novobocin has been shown to block the binding of ATP to gyrase and so inhibit the enzyme activity (Ali *et al*, 1995). It has been reported that novobiocin can inhibit the ATPase activity of *Drosophila* topo II (Robinson *et al*, 1993), however

recent work has demonstrated that novobiocin does not inhibit the ATPase activity of full-length human topoisomerase II α (Hammonds and Maxwell, 1997).

Recent work has gone some way to suggesting a mechanism for the action of the bisdioxopiperazine drug ICRF-193. It has been shown that upon the binding of ATP by topoisomerase the enzyme is converted into the form of a closed protein clamp (Roca *et al*, 1994). Upon hydrolysis of ATP it is proposed that the protein returns to the open clamp form. This has been taken as a possible way in which the passage strand may be trapped prior to strand passage in the reaction cycle (Roca *et al*, 1994). Work on yeast topo II showed that ICRF-193 failed to bind to the open clamp form of the enzyme but bound to this closed clamp form irreversibly so that even upon the removal of ATP the closed protein clamp was maintained. The stabilisation of this closed clamp form will inhibit enzyme turnover. This also suggests a mechanism for circumventing the formation of cleavable complex in the presence of cleavable complex -forming drugs, as the trapped protein clamp is unable to bind to DNA and so unable to give rise to covalent DNA-topoisomerase complex (Roca *et al*, 1994).

In addition to the above mechanisms of topo II inhibition there may be various other compounds that can inhibit the affects of topo IIs. Intercalative agents may physically prevent the enzyme from binding to DNA or UV damage of DNA may inhibit strand passage (Corbett *et al*, 1991).

1.7 PROJECT AIMS

A previous project in this lab had involved the cloning and expression of the N-terminal domain of the B subunit of the *E.coli* enzyme gyrase (Ali *et al*, 1993). This project had provided direct evidence that this domain contained the site for the

binding and hydrolysis of ATP. Kinetic analysis of the ATPase reaction of this domain coupled with chemical crosslinking data showed that the enzyme existed as a monomer in solution dimerising in the presence of nucleotide. The 43 kDa fragment was shown to contain the binding site for the coumain drugs, eg novobiocin. This domain has provided a high resolution crystal structure, seen in figure 1.6. From this structure the mechanism of ATP hydrolysis was deduced, figure 1.7. This work has provided great insights into the mechanisms of the prokaryotic enzyme.

In this project we wished to study the equivalent domain in the human enzyme, topo II α . The choice of the human enzyme was made as it provided scope for research into areas of clinical importance. To help effect these ends, we were given by Dave Roper of York University a series of N-terminal constructs of the human topoisomerase II α gene. These were made as part of a proposed study of the structure of this domain using X-ray crystallography. It was hoped that this project would generate useful biochemical data in parallel with the ongoing attempts at structural analysis. The size of the constructs ranged from 264 to 435 amino acids. The largest recombinant fragment cloned resembled a proteolytic fragment of the yeast topoisomerase II (Lindsley and Wang, 1991). This suggested that this fragment would most closely resemble a putative domain of the human topo II α protein, which would aid the recombinant fragment in folding to resemble the domain present in the full length enzyme and so retain its biochemical function. This construct is analogous to the N-terminal portion of gyrase and contains regions that are highly conserved including the putative regions responsible for ATP binding and hydrolysis.

The priority of this project was to study the ability of this protein to bind and hydrolyse ATP. Based on the previous observations on the 43 kDa gyrase fragment,

which had been shown to dimerise in the presence of ATP, we hoped this study would lead to observations of the monomer-dimer equilibrium of the recombinant fragment of the human enzyme. Assuming we could detect an intrinsic rate of ATP hydrolysis, we would look at the effect of DNA on the rate of hydrolysis as this would provided an insight into the role of the T segment in ATP hydrolysis. Given the importance of the human enzyme as a drug target we would then examine the effects of known topo II targeted drugs. On a related subject there is still some confusion over the reported inhibition of eukaryotic type II enzyme by novobiocin, so the interaction of this drug with the N-terminal domain would be examined. Studies have shown that topo II contains multiple sites of phosphorylation the majority of which are found in the extreme C-terminal portion. There is however one possible site located in the N-terminal domain at Ser 29 (Wells *et al*, 1995). It was hoped that this project could proceed to a point where we could examine the effects of phosphorylation on this site in the context of the ATPase rate of the domain. Overall it was hoped that these studies would provided useful insights into the how the eukaryotic enzyme utilizes ATP and possibly look at the role of DNA binding by the N-terminal clamp and how this effects the rate ATP hydrolysis.

CHAPTER 2

MATERIALS AND METHODS

INTRODUCTION.

All reagents used in the course of this project were of analytical or molecular biological grade. Sigma was the major supplier of reagents, other suppliers are listed where they were the sole suppliers of that product. Many of the methods and reagent recipes below have been adapted from Sambrook *et al*, (1989).

2.1.0 BACTERIOLOGY.

2.1.1 Bacterial strains.

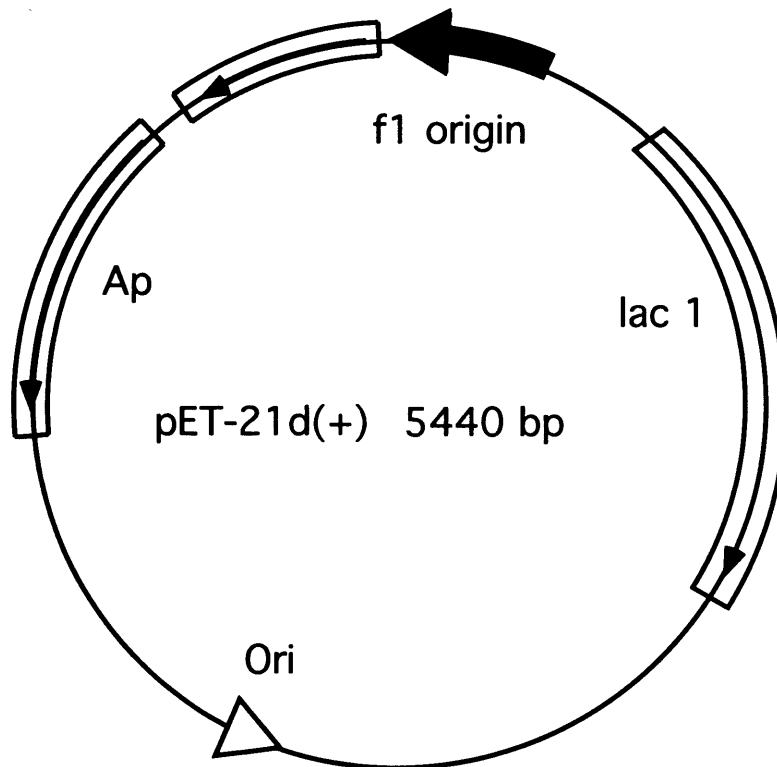
Table 2.1 Bacterial strains.

STRAINS	SUPPLIER	GENOTYPE
B834(DE3)pLysS	Novogen	<i>F'ompT hsdS_B (r_B·m_B⁻)gal dcm met</i> (DE3) pLysS (Cm ^R).
BL21(DE3)pLyS	Novogen	<i>F'ompT hsdS_B (r_B·m_B⁻)gal dcm</i> (DE3) pLysS (Cm ^R).
XL1-Blue	Stratagene	<i>recA1 endA1 gyrA96 thi-1 hsdR17 supE44 Rel A1 lac</i> [F' <i>proAB lacI^q ZΔM15 Tn 10</i> (Tet ^r)] ^c

The above table shows the strains of *E.coli* used throughout this project.

B834(DE3)pLysS and BL21(DE3)pLyS were the main strains used for the expression of recombinant protein, these expression strains contain a chromosomal copy of the T7

Figure 2.1 pET-21 d(+), the main expression vector used throughout this project.



The above figure shows a representation of the main expression vector used throughout this project.

RNA polymerase gene under *lacUV5* control and are used in conjunction with a plasmid in which the target genes are cloned under the control of a bacteriophage T7 promoter. XL1-Blue was used for cloning mutated plasmids during site directed mutagenesis studies.

2.1.2 Plasmids.

The plasmid pLysS (Novogen) produces T7 lysozyme in a constitutive fashion within the expression strain, this binds to T7 RNA polymerase and prevents the production of recombinant protein prior to induction. This allows tight control of expression of the recombinant protein (Moffatt and Studier, 1987).

pET-21d(+) (Novogen) was the main expression vector used throughout this project it contains an ampicillin resistance gene for selection: Target genes are cloned under the control of a bacteriophage T7 promoter, see figure 2.1.

pBR322 was used as a substrate to be used in the DNA-dependent ATPase assays on recombinant protein.

2.1.3 Bacterial growth media.

Media used for growing bacterial cultures were prepared and sterilised by autoclaving for 15 minutes at 15 lb/sq.in. For culturing on agar plates, 15 g/L of agar (Oxoid) was added to each recipe and the mixture was autoclaved, as above, and allowed to cool. 25 ml of broth/agar was aseptically poured into each sterile plastic petri dish (Bibby Sterilin Ltd) and allowed to set at room temperature. The agar plates were dried at 50°C for 10 minute then stored at 4°C until they were to be used.

Table 2.2 Broth composition.

BROTH	COMPOSITION	AMOUNT
Luria-Bertani (LB) medium	Tryptone (Oxoid) Yeast Extract (Oxoid) NaCl Water	10.0 g 5.0 g 10.0 g to 1 liter
Nutrient Broth (NB)	Nutrient broth powder (Oxoid)	13 g/liter
“Old Gits” Broth (OGB)	Tryptone (Oxoid) Yeast Extract (Oxoid) NaCl Water	10.0 g 5.0 g 15.0 g to 1 liter

The above table shows the composition of the broths used in the growth of bacterial strains for the expression of recombinant protein.

2.1.4 Antibiotics.

Ampicillin was made up at a stock concentration of 50 mg/ml in water, aliquotted into 0.5 ml samples and stored at -20°C. Ampicillin was added to broth-medium and broth-agar plates to a final concentration of 50 µg/ml immediately prior to use.

2.1.5 Inoculation of overnight cultures.

A 5 ml aliquot of broth medium was dispensed aseptically into a 30 ml Sterilin™ tube (Bibby Sterilin Ltd). Antibiotics were added to the correct concentration, as necessary. The culture was inoculated with a single colony from a stock agar plate, transferred aseptically with a wire loop. The culture was incubated overnight at 37°C with agitation, 200 revolutions per minute(rpm) in a Innova™ 4300 shaker, New Brunswick Scientific.

2.1.6 Preparation of competent *E. coli* strains.

1 ml of an overnight culture (section 2.1.5) was added to 9 ml of sterile broth in a 30 ml Sterilin™ tube and incubated with agitation, 200 rpm, at 37°C for 1 hour. The cells were then centrifuged at 2100 rpm at 4°C for 10 minutes (MSE Mistral 2000, Sanyo). The supernatant was removed and the pellet re-suspended in 1 ml of sterile ice cold 100 mM CaCl₂. The suspension was then transferred to 1.5 ml tubes and centrifuged at 13000 rpm for 30 seconds at 4°C in a bench top centrifuge (Biofuge, Heraeus instruments). The supernatant was then removed and the pellet re-suspended in a further aliquot of 400 µl of sterile ice cold 100 mM CaCl₂. Competent cells prepared by this method can be stored at 4°C for up to 12 hours prior to use.

2.1.7 Transformation of competent *E. coli* strains.

1 µl of plasmid DNA (0.5µg) was added to 200 µl of re-suspended competent cells prepared by the calcium chloride method (sec 2.1.6). After gentle mixing the samples were placed on ice for 30 mins. The samples were then subjected to heat shock by transferring the tubes to a water bath at 42°C for 90 seconds then replaced on ice for a further 2 minutes. 800 µl of sterile broth was then aliquoted into a 1.5 ml tube then the samples were transferred to the 1.5 ml tube which was incubated, with agitation at 200 rpm, at 37°C for 1 hour to allow for the expression of the antibiotic markers. The cells were then plated onto agar plates containing the appropriate antibiotic for selection. Typically aliquots of 10 µl, 50 µl, and 200 µl were plated out on agar plates to give a range of amounts of cells.

2.1.8 Trial induction of plasmid based gene expression.

10 ml of sterile broth was transferred to a 30 ml Sterilin™ and the appropriate antibiotic was added to the required concentration. 200 µl of an overnight culture (section 2.1.5) was used to inoculate the broth. The sample was then transferred to a shaking incubator at 37°C and grown with agitation, 200 rpm.. Optical density readings at $\lambda = 560$ nm (OD_{560}) were taken (Unicam SP1800 Ultraviolet Spectrophotometer) until OD_{560} reached approximately 0.5 . The culture was then split into two 5 ml fractions. In one fraction protein expression was induced by the addition of 50 µM IPTG (isopropyl- β -D-thiogalactopyranoside) stock the other fraction was not induced. Both cultures were then grown for 3 hours at 37°C with agitation at 200 rpm. The cultures were then centrifuged at 2100 rpm for 10 minutes at 4°C, the supernatant was discarded and the pellet re-suspended in 200 µl of Tris/sucrose (50 mM Tris.HCl (pH 7.5), 10% w/v sucrose). This suspension was then flash frozen in liquid nitrogen and stored at -70°C prior to analysis.

2.1.9 Full scale induction of recombinant protein.

Typically, six liters of broth were prepared, 1 liter in each of six 2 liter flasks. The addition of stainless steel metal springs to each flask allowed full aeration of the broth during incubation. Broth was sterilised in flask by autoclaving, and allowed to cool before the addition of the appropriate antibiotic. 5 ml of a prepared overnight culture (section 2.1.5), inoculated from a freshly transformed plate (section 2.1.7), was used to inoculate the broth. The culture was then transferred to a shaking incubator and grown

with agitation, 200 rpm, at 37°C. Optical density readings were taken until OD₅₆₀ was approximately 0.5. The culture was then induced by the addition of IPTG to a final concentration of 50 µM, and grown with agitation at 37°C, 200 rpm, for a further 4 hours. The culture was then removed and decanted into 500 ml centrifuge pots (Beckman) and centrifuged at 10,000 rpm for 10 minutes in a JA-10 rotor (Beckman JT-21 centrifuge). The supernatant was removed and the resulting pellets were then re-suspended in 5 ml Tris/sucrose buffer (50 mM Tris.HCl 10% sucrose, pH 7.5) and flash frozen in liquid nitrogen and stored at -70°C prior to protein purification.

2.2 PROTEIN PURIFICATION.

2.2.1 Preparation of crude extract from inclusion bodies.

Cellular material in Tris/sucrose buffer (paste) was removed from the -70°C freezer and thawed on ice. The cells were then lysed by sonication for 90 seconds at 10µ amplitude (Soniprep 150, MSE). The sonicated material was transferred to a 30 ml centrifuge tube (Sorvall, Dupont) and the insoluble material was then pelleted by centrifugation at 34,000 rpm, 4°C for 30 minutes (OTD65B Sorvall Ultracentrifuge, Dupont in a TFT.50.38 rotor) and the soluble material removed. The pellet was then resuspended in Tris buffered (50 mM Tris.HCl, pH 8) 1% Triton X-100 followed by sonication for 90 seconds at 10µ amplitude. The insoluble material was then re-pelleted by centrifugation at 34,000 rpm for 30 minutes as before. Triton X-100 was removed by washing the pellet thoroughly in distilled water. The pellet was then resuspended in sonication buffer (50 mM Tris.HCl (pH 8), 100 mM NaCl, 8 M Urea) and solubilised by sonication for 90 seconds. Insoluble material was then removed by centrifugation at

34,000 rpm for 30 minutes as before. This technique resulted in a crude protein extract solubilised in urea that can be re-folded prior to further purification or purified directly.

2.2.2 Re-folding techniques.

The solubilised protein extract was re-folded for additional purification by dialysis overnight into a Re-folding Buffer (Tris.HCl (pH 8.8), 100 mM KCl, 1 mM EDTA (ethylenediaminetetraacetic acid), 1 mM DTT,(Dithiothreitol), 10% glycerol). The extract was placed into dialysis tubing which was sealed and placed in at least 1,000-fold excess of re-fold buffer and gently stirred overnight at 4°C. Following dialysis insoluble material in the extract was removed by centrifugation at 4°C in a benchtop centrifuge at 13,000 rpm for 20 minutes.

2.2.3 Fast protein liquid chromatography techniques (FPLC).

Two methods of purification were employed in an attempt to find an optimal purification protocol.

1) Cation exchange chromatography: Re-folded protein, 500µl volume, was applied to a Hi Trap SP affinity column (Pharmacia) in 50 mM sodium phosphate buffer (pH 7.2), 100 mM KCl (load buffer). Sodium phosphate buffers of increasing ionic strength were then prepared containing, 200 mM, 400 mM and 700 mM KCl. The 500 µl sample was loaded, using a loop at 1ml / minute, in 50 mM sodium phosphate buffer (pH 7.2). The column, volume 1ml, was washed with 3 column volumes of load buffer at 1ml / minute. Elution was performed with a step gradient in steps of 200, 400, and 700 mM KCl in a 50 mM sodium phosphate buffer (pH 7.2). Each buffer was loaded onto the column at 1ml / minute and 5 column volumes flowed through the column. Fractions of 1ml were

collected and were made up to 10% glycerol then flash frozen in liquid nitrogen to be stored at -70°C prior to analyses.

2) Metal affinity chromatography: A Hi Trap Chelating column (Pharmacia), was prepared by loading 3 column volumes (column volume 1ml) of nickel sulfate to ensure the matrix was equilibrated with Ni^{2+} . The column was then washed with 10 column volumes of load buffer, 50 mM sodium phosphate buffer (pH 7.4). Sodium phosphate buffers were then prepared containing, 10 mM, 50 mM, 100 mM and 500 mM imidazole. The sample, 500 μl , was loaded using a loop at 1ml / minute in 50 mM sodium phosphate buffer (pH 7.4). The column was washed with 3 column volumes load buffer at 1ml / minute. Elution was performed with a step gradient in steps of 10 mM, 50 mM, 100 mM and 500 mM imidazole in 50 mM sodium phosphate buffer (pH 7.4). 4 column volumes of each buffer was loaded onto the column at 1ml / minute and flowed through the column. Fractions of 1ml were collected and made up to 10% glycerol then flash frozen in liquid nitrogen to be stored at -70°C prior to analyses.

2.2.4 Novobiocin affinity column.

Refolded protein was applied to a novobiocin-sepharose matrix in Enzyme Buffer (50 mM Tris.HCl (pH 7.5), 100 mM KCl, 0.5 mM DTT, 1 mM EDTA, 10% glycerol). Enzyme Buffers containing 1 M NaCl, 2 M urea, 4 M urea, 6 M urea and 8 M urea were prepared. The novobiocin column was prepared by placing 1ml of previously prepared novobiocin-sepharose (a gift from Alison Howles) into a 10 ml disposable column (Bio Rad). The matrix was equilibrated by adding 10 column volumes of EB to the matrix, column was run by gravity flow. The sample was loaded by pipetting 500 μl of refolded protein in Enzyme Buffer onto the top of the matrix and allowing it to flow

through the matrix by gravity. The column was then washed by loading 5 column volumes of Enzyme Buffer and allowing it to flow through the column. Elution was performed in a step wise fashion by the sequential addition of 5 column volumes of Enzyme Buffer containing 1 M NaCl, 2 M urea, 4 M urea, 6 M urea and 8 M urea. Fractions of 1ml were collected flash frozen in liquid nitrogen to be stored at -70°C prior to analyses

2.2.5 Metal affinity chromatography.

This method was employed for the purification of six-His C-terminally tagged protein. Initial purification strategies were based on the nickel-binding matrix sepharose 6B fast flow (Pharmacia). This column was prepared by charging the matrix with 50 mM NiCl₂. The material was loaded in Loading Buffer (25 mM sodium phosphate buffer (pH 8.0), 800 mM NaCl, 8 M urea) and the column was then washed with loading buffer containing 10, 50 and 100 mM imidazole. The protein can then be eluted with loading buffer containing 500 mM imidazole. A second metal affinity matrix was later used for the purification of the six-His tagged protein: Talon, a cobalt affinity resin (Clontech). The protein, typically in a denatured state in 8 M urea, was purified in the following way. The resin was washed with a wash buffer (50 mM Tris.HCl (pH 8.0), 100 mM NaCl) to remove the 20% ethanol storage buffer. The resin was then mixed with the protein solution in 8 M urea typically a ratio of 1:20 resin to protein solution then incubated with gentle agitation for 1 hour. Then the resin was pelleted in a 10 ml Sterilin and the pellet is suspended in 20 volumes of wash buffer and left for 10 minutes. The resin was then re-pelleted and the pellet was re-suspended in a further 20 volumes of wash buffer for a 10 minutes. This suspension was decanted into a 10 ml disposable column and the resin was allowed to settle. Bound protein was eluted from the column

by the addition of an elution buffer (50 mM Tris.HCl (pH 8.0), 100 mM NaCl, 50 mM imidazole).

2.2.6 Gel purification of protein.

This protocol was based on method of Hager and Burgess (1980). Protein samples were run on a 12% SDS-polyacrylamide gel (section 2.3.2). A vertical gel slice was removed and stained with Coomassie stain (30% (v/v) methanol, 0.01% (w/v) Coomassie Brilliant Blue, 12% (w/v) TCA, 10% (w/v) sulphosalicylic acid) to reveal the protein bands present. The vertical slice was used as a reference to show the horizontal position of the protein of interest and a scalpel blade was used to carefully cut out a horizontal section of the gel that contained the protein of interest. The gel slice was then transferred to a tube (14 ml Falcon, Becton and Dickinson) crushed and 1 ml of Elution Solution [(50 mM Tris.HCl, 100 μ M EDTA, 5 mM DTT, 150 mM NaCl, 1% SDS (sodium dodecyl sulfate))] was added to the gel matrix. The gel matrix was left overnight in the Elution Solution to allow the protein to diffuse into solution. The slurry of gel matrix and Elution Solution was loaded in a 10 ml disposable column (Bio Rad) and this was in turn placed into a 10 ml Sterilin™ tube (Bibby Sterilin Ltd) and centrifuged for 1 minute at 2100 rpm. The protein was then precipitated from the Elution Solution by the addition of an equal volume of acetone at -20°C, this mixture was then kept at -20°C for one hour. The protein was pelleted by centrifuging at 13,000 rpm in a bench top centrifuge for 30 minutes. The resulting pellet was then re-suspended in an appropriate buffer e.g. (Tris.HCl (pH 8.8), 100 mM KCl, 8 M urea) for subsequent refolding.

2.3 PROTEIN ANALYSIS.

2.3.1 Estimating protein concentrations.

Protein concentrations were estimated by the method of Bradford (1976). This method involves the binding of Coomassie Brilliant Blue dye to protein which causes a shift in absorbance of the dye from 465 nm to 595 nm. The Bradford reagent was obtained commercially from Bio-Rad. The increase in absorbance at 595 nm was observed by spectrophotometric means (Unicam SP1800 Ultraviolet Spectrophotometer). Protein concentration was estimated by reference to a standard curve. BSA (bovine serum albumin) was used to generate a standard curve.

2.3.2 SDS-polyacrylamide electrophoresis.

This was conducted in a discontinuous gel system with a 5% stacking gel and either an 8% separating gel, for cross-linking experiments, or a 12.5% separating gel for general protein analysis. Composition of the gels is shown in the table 2.3. The thickness of the gels varied from 0.75 to 1.5 mm, depending upon the volume of sample to be loaded and the application. Typically, 15 µl of sample would be added to 15 µl of Sample Application Buffer, SAB (125 mM Tris.HCl (pH 6.8), 4% (w/v) SDS, 20% (w/v) glycerol, 10% (v/v) β-mercaptoethanol, 0.002% (w/v) bromophenol blue). The tubes containing samples were then placed in a water bath at 100°C for 3 minutes before loading an aliquot (typically 20 µl) onto the gel. Gels were cast and run using a Bio-Rad Mini Protean II electrophoresis system electrophoresis at 200 V for 45 minutes.

Proteins were stained in Coomassie stain (30% (v/v) methanol, 0.01% (w/v) Coomassie Brilliant Blue, 12% (w/v) TCA, 10% (w/v) sulphosalicylic acid) and destained in 10% IMS(Industrial Mentholated Spirit) 15% Acetic Acid in water to visualise the protein bands. Where the bands were faint silver staining was performed using a Bio Rad silver staining kit (section 2.3.4)

Table 2.3 Polyacrylamide gel composition.

	8% separating gel	12% separating gel	4%stacking gel
30% acrylamide*	2.67 ml	4.0 ml	1.3 ml
1 M Tris.HCl (pH 8.8)	3.75 ml	3.75 ml	-
1 M Tris.HCl (pH 6.8)	-	-	1.25 ml
10% SDS	100 µl	100 µl	100 µl
Water	3.43 ml	2.1 ml	7.35 ml
10% APS	100 µl	100 µl	100 µl
TEMED	10 µl	10 µl	10 µl

[* 30% acrylamide is commercially as ultra pure from National Diagnostics]

2.3.3 Native polyacrylamide gel electrophoresis.

Native gels were used for the analysis of ATP binding to the protein and protein DNA interactions. A 5% acrylamide gel in TBM buffer (90 mM Tris.HCl pH 7.5, 90 mM boric acid, 5 mM $MgCl_2$). DNA was visualised by staining with ethidium bromide for 5 minutes in 5µg/ml ethidium bromide and destained in TBM. Protein is visualised by staining with Coomassie stain or by silver staining(section 2.3.4).

2.3.4 Silver staining.

Silver staining was carried out using a Bio-Rad silver stain kit following the provided protocol. This kit is based on the protocol of Gottlieb and Chavko (1987). Staining takes place by the deposition of silver ions onto nucleation sites, this allows the

protein bands on a polyacrylamide gel to be visualized. Silver staining is 10 times more sensitive than Coomassie staining and was used to detect faint bands such as protein-protein cross links.

2.3.5 Western blotting.

Western blotting was used to detect low quantities of protein, 1-5 ng. Proteins were transferred from SDS /PAGE gels to Hybond-C Extra nitrocellulose (Amersham) by electrotransfer. Blotting was accomplished using a Bio-Rad transfer apparatus filled with Transfer Buffer (12.5 mM Tris base (pH 8.2), 200 mM glycine, 10% (v/v) methanol). The gel was “blotted” for 1 hour at 200 mA. To ensure adequate protein transfer had taken place the nitrocellulose membrane (the blot) was stained with Ponceau S, and the position of any markers permanently marked. The blots were then washed in TBS (25 mM Tris.HCl (pH 7.5), 154 mM NaCl) to remove any traces of Ponceau S and incubated in Block Buffer (TBS containing 5% dried skimmed milk (Marvel™ and 0.1% Tween-20) overnight at 4°C to block excess protein binding sites. The blot was incubated with the primary antibody (a polyclonal antibody against the 52 kDa fragment of human topo II α raised in rabbit, a gift from John Jenkins CMHT Leicester) for one hour in block buffer at a 1:5000 dilution. The membrane was then washed for five minutes with 4x 20 mls of TBS. The secondary antibody was a goat anti-rabbit antibody conjugated to horseradish peroxidase diluted 1:1000 from a stock solution(Dako) into TBS and was incubated with the membrane for 1 hour at room temperature and the membrane was washed as before. To prepare the membrane for chemiluminescent detection excess moisture was first removed by carefully blotting between two sheets of Whatman 3MM paper. 1 ml of each chemiluminescent reagent (ECL detection kit, Amersham) was then added to the blot and allowed to mix for 1

minute. Excess reagents were then removed from the blot with Whatman 3MM paper. The blot was carefully wrapped in Saran wrap and exposed to Fuji X-ray film (100 NIF) for a range of times from 10 seconds to 1 minute depending on the strength of the chemiluminescent signal. Films were developed using a Cronex CX-100, automated development system (Du pont).

2.3.6 Protein cross-linking.

Before cross-linking the protein was dialysed for at least four hours into a cross-linking buffer (4 mM DTT, 4 mM MgCl₂, 50 mM Hepes (pH 8.5), 100 mM KCl). The samples of protein and nucleotides ADPNP (5'-adenylyl β,γ -imidodiphosphate) ATP (Adenosine triphosphate) and ADP (Adenosine diphosphate) were incubated for one hour prior to cross linking. The Cross-Linking reagent DMS (dimethyl suberimidate) was added to a concentration of 0.4 mg/ml and the samples incubated at 25°C for two hours. Due to the short half-life of the cross-linking reagent, a second batch of cross linker was added after two hours and the protein incubated for a further two hours. Cross-linked species were resolved by subsequent running of the protein on an 8% SDS-polyacrylamide gel. Silver staining or western blotting were used to reveal the cross linked species.

2.3.7 Phosphorylation of proteins.

Two protein kinases were used: casein kinase II (CK II, human recombinant, Boehringer Mannheim) and protein kinase C (PKC, rat brain , mixture of the A and B isoforms, Boehringer Mannheim). The two kinase were used in two different buffers: CKII Buffer (50 mM Tris.HCl (pH 7.4), 150 mM KCl, 10 mM MgCl₂, 100 μ M

EDTA) and PKC Buffer (20 mM Hepes.NaOH (pH 7.4), 10 mM MgCl₂, 0.5 mM CaCl₂, 5 µg/ml dicalcein). Each reaction mix also contained 10 µCi of [γ -³²P] ATP (adenosine 5' triphosphate, Amersham) in 100 µM ATP. The reactions were performed in total volume of 20 µl at 30°C for 15 minutes. Experiment was stopped by quenching with SAB. Samples were then run on a 12% SDS-polyacrylamide gel (section 2.3.2) which was then dried in a vacuum dryer, 2 hours at 70°C and the gels were then exposed to Fuji X-ray film (100 NIF) for 1 hour and overnight.

2.3.8 ATPase assays.

ATPase assays were carried out using an ADP-linked enzyme assay (Tamura and Gellert, 1990). In this assay system, as ADP is produced by the hydrolysis of ATP it is phosphorylated back to ATP by pyruvate kinase using phosphoenol pyruvate as the phosphorylating agent. During this process phosphoenol pyruvate is converted to pyruvate which is then reduced to lactate by lactate dehydrogenase. This results in the oxidation of NADH to NAD⁺ i.e. the hydrolysis of ATP can therefore be followed by the reduction in absorbance of NADH at 340 nm. A typical ATPase assay was carried out in a volume of 200 µl under the following conditions: 50 mM Tris.HCl (pH 7.5), 80 mM KCl, 2 mM ATP, 2 mM MgCl₂, PEP 400 µM, NADH 250 µM, 5 µl PK/LDH mix (in 50% w/v glycerol, 100 mM KCl, 10 mM Hepes (pH 7.0), 0.1 mM EDTA; obtained commercially from Sigma). The initial ATP concentration was 2 mM. Assay is typically run at 37°C for one hour and monitored spectrophotometrically (Perkin Elmer Lambda 5 or Bio-Tek EL340 microplate reader) and the rate of change at OD₃₄₀ was related to the ATPase rate by using $A_{340} \text{ 1M} = 6220 \text{ cm}^{-1}$ in the Spectrophotometer and $A_{340} \text{ 1M} =$

4140 (0.7)cm⁻¹ (absorbance of 1M NADH equals 6220 per cm in the spectrophotometer and 4140 per 0.7 of a cm in the microplate reader). The microplate reader was driven by Delta soft™ software, in these assays the sample were overlaid with mineral oil to eliminate the possibility of evaporation affecting the reading. The microplate reader had the advantage that a large number of experiments and controls could be performed in a single plate. Typically each experiment and control was repeated in triplicate error between duplicates approximated to 10%. A large number of controls allowed an accurate assessment of background variation allowing low rates to be measured with confidence.

2.3.9 Drug screening.

Drug sensitivities of the refolded protein were analysed by the addition of the compounds of interest to an ATPase assay performed in a microplate reader (section 2.3.8). Compounds used were: Merbarone, m-AMSA (National Cancer Institute), ICRF-159 (a gift from Ian Hickson, Imperial Cancer Research Fund, Oxford) and Novobiocin (Sigma). Merbarone, m-AMSA and ICRF-159 were dissolved in dimethyl sulfoxide (DMS), and Novobiocin was dissolved in water and stored at -20°C. All of the compounds were added to the ATPase assay to give a final concentration of 20µg/ml.

2.4 DNA TECHNIQUES.

2.4.1 Small scale plasmid preparation.

All plasmid preparation was carried using a QIAprep™ Plasmid kit (Qiagen) following the provided protocol. This kit is based on alkaline lysis of bacterial cells

following the absorption of DNA to silica in the presence a of high concentration of a chaotrophic salt.

2.4.2 Agarose gel electrophoresis.

Agarose gel electrophoresis was used to examine the quality and quantity of plasmid DNA and also to separate and size fragments of DNA following restriction analysis. 1% agarose gels were made and electrophoresed in 1x TAE (40 mM Tris.acetate (pH 7.6), 1 mM EDTA) at 5 V/cm. Gels were stained in ethidium bromide solution (2 µg/ml in TAE) for 15 minutes and destained in TAE for 5 minutes, the DNA was then visualised by UV fluorescence. Photographs were taken using a gel doc system (UVP) or using Kodak Tmax 100 film.

2.4.3 Restriction analysis of DNA.

Restriction enzymes were obtained commercially from NEB. Restriction analysis of DNA is performed in order to size whole plasmids or their fragments and this can be used as an indication of whether a plasmid is correct or contains the correct insert. Plasmid pET-21 d was sized by linearisation using 10 units (1 unit = total cleavage of 1 µg DNA in one hour at 37°C) of *Xba* I incubated at 37°C for one hour in Nebuffer 2. The cloned fragment was excised from the plasmid by a double digest using restriction enzymes *Xba* I and *Sac* I. A general reaction mix for a restriction analysis of plasmid DNA is seen below.

DNA	x µl
10 x Reaction buffer	1 µl
Enzyme	y µl (often 10 units/µg DNA)
Water	to 10 µl total

The reaction was stopped by the addition of STEB (40% sucrose (w/v), 100 mM Tris.HCl (pH 7.5), 100 mM EDTA, 0.5 mg/ml bromophenol blue) then loaded onto a 1% agarose gel for examination.

2.4.4 Mutagenesis of plasmid DNA.

Site-directed mutagenesis was performed using a Quick Change™ site directed mutagenesis kit (Stratagene). The method associated with this kit is outlined below. Two complementary mutagenic primers were designed which were then synthesised by the staff of the university Protein and Nucleic Acid Chemistry Laboratory(PNACL). They were purified by the method of Sawadago and van Dyke (1991). A 100 µl aliquot of the synthesis was vortexed briefly with 1 ml of dry butanol and centrifuged for 1 minute, 13000 rpm in a benchtop centrifuge. The supernatant was aspirated and the pellet dried under vacuum, resuspended in TE buffer (pH 7.5) and the yield and purity assessed from OD readings at 260 nm and 280 nm. These oligonucleotide primers were extended in a PCR reaction using *Pfu* DNA polymerase (Stratagene) a high fidelity polymerase. This resulted in the synthesis of a mutated copy of the plasmid that would contain two staggered nicks. Following the PCR (polymerase chain reaction) the template DNA was removed by digestion with *Dpn* I endonuclease, an enzyme specific for methylated and hemimethylated DNA. The nicked mutated vector was then transformed into *E. coli* (XL 1 blue) where the nicks are repaired. A typical PCR strategy for the creation of a mutant plasmid is outlined below.

Table 2.4 A typical strategy for PCR.

Segment	Cycles	Temperature	Time
1	1	95°C	30 seconds
2	12-18	95°C	30 seconds
		55°C	1 minute
		68°C	2 minutes/kb of plasmid length

2.4.5 Automated sequencing.

Samples for DNA sequencing were prepared in the following way. An aliquot of 32 µl of plasmid DNA was PEG (polyethylene glycol) precipitated by addition to 8 µl of 4 M NaCl and 40 µl sterile 13% (w/v) PEG₈₀₀₀. The sample was stored on ice and then centrifuged at 13,000 rpm at 4°C in a benchtop centrifuge. The pellet was then washed with 70% ethanol, dried under vacuum and resuspended in 20 µl water.

PRISM™ Ready reaction DyeDeoxy™ terminator cycle sequencing kit was used to prepare the samples for automated sequencing. The sequencing reaction was set up using 5 µl aliquots of the purified plasmid DNA with 9.5 µl of terminator premix and 3.2 pmol of sequencing oligo in a total volume of 20 µl. The reaction was then put through 25 of the following PCR cycles :

96°C	30 seconds.
50°C	15 seconds.
72°C	4 minutes.

Samples were then collected and analysed on an ABI automated sequencer by PNACL who also provided the terminator premix. Data acquisition was performed by PNACL staff and the raw data returned on computer disk for analysis. Data was analysed using Seqed™ (Applied Biosystems).

CHAPTER 3

PRODUCTION AND PURIFICATION.

INTRODUCTION.

The aim of this section of the project was initially to select from the available clones of the N-terminal portion of topo II α the one most likely to produce active protein. Once this clone had been selected we would produce a reliable protocol for the production and purification of recombinant protein to be used in further studies.

3.1 ANALYSIS OF CLONES

We received from Dave Roper of York University four *E. coli* clones of the N-terminal domain of human topoisomerase II α . The fragments were cloned into a pET21d expression vector for use with the pET expression system. After some initial studies we received a fifth clone (table 3.1) based on the pTOPSTOP clone that included four further C-terminal amino acids of topo II, plus eleven codons introduced during cloning and the six histidine tag. Each of the clones would produce a different sized protein fragment as shown on table 3.1.

Table 3.1 Clones

PLASMIDS	SIZE OF PROTEIN ENCODED BY PLASMID IN AMINO ACIDS	SIZE OF PRODUCT kDa
pTOPO264	264	28.5
PTOPO399	399	45.8
PTOPO419	419	47.9
pTOPSTOP	435	49.8
PTOPSTOP/HIS	456	52.05

It had been reported that the best protein expression, albeit in an insoluble form, was from the largest clone i.e. pTOPSTOP (Roper. D personal communication). As this clone represented a fragment terminating near a natural proteolysis point (lys 425, Lindsley and Wang, 1991) in the full-length enzyme, it was thought that protein produced from this clone would most likely represent a whole domain and was therefore more likely to produce functional protein. Initial expression studies showed a good level of production of protein from this clone so initial expression and purification studies were performed using the clone pTOPSTOP.

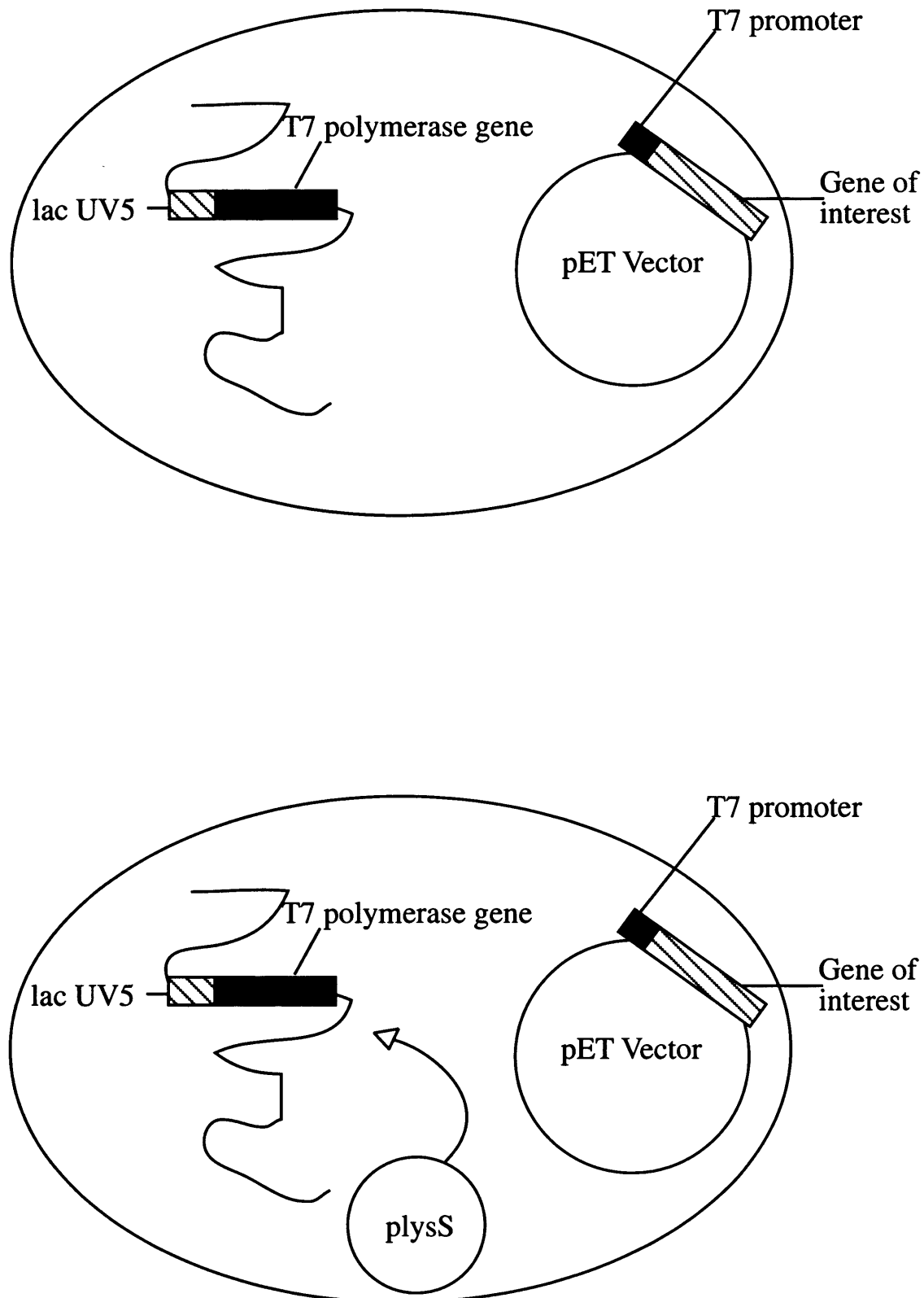
3.1.1 pET Expression system

The pET expression system used throughout this project works in the following way. Target genes are cloned into a plasmid, under the control of a bacteriophage T7 promoter. Expression of the target genes is induced on the provision of T7 RNA polymerase. The expression strain contains a chromosomal copy of the T7 RNA polymerase gene under *lacUV5* control. When the plasmid is transformed into the expression strain and IPTG added this allows the production of T7 RNA polymerase which in turn controls the expression of the gene of interest on the plasmid (figure 3.1).

3.2 GROWTH OF CELLS.

The plasmid, pTOPSTOP, was transformed in to a suitable expression strain of *E. coli*, BL21(DE3) and transformants were selected using ampicillin. Typically an overnight culture was grown from a single colony and this culture used to inoculate the broth for a trial induction. The cells had a doubling time of approximately 30 minutes at

Figure 3.1 The pET expression system.



The above figure outlines the pET expression system. This system was used throughout this project for the expression of N-terminal domain of human topo II α . The expression strain contains an integrated T7 polymerase gene under the control of a lac UV5 promoter. The gene of interest is cloned under a T7 promoter on a pET vector. plyS constitutively expresses T7 lysozyme which will bind to and inactivate any T7 polymerase produced prior to induction.

37°C with agitation. Once the culture had reached $OD_{560} = 0.5$ the cells were induced by the addition of IPTG.

3.2.1 Problems with expression

Expression of the 50 kDa fragment of topo II in *E. coli* proved to be problematic. After some initial success all expression was lost and a series of strategies for regaining expression were attempted.

Fresh transformants were plated out from glycerol stocks. Following the initial loss of protein expression it was suspected that the current stock of clones had simply become “fatigued” characterized by gradual loss of expression with time, so a new set were plated out from a fresh glycerol stock. This failed to restore expression. Fresh transformants were prepared from stocks of plasmid. When expressing recombinant protein in *E. coli* it is always desirable to have freshly transformed clones so we returned to the original stocks of plasmid and made fresh transformants. Trial inductions with these transformants failed to generate any recombinant protein. A new expression strain B834(DE3) was purchased and transformed. It had been suggested (Roper.D personal communication) that B834(DE3) was a better expression strain but the resulting expression studies failed to demonstrate any improvement in the yield of recombinant protein.

Stocks of the plasmid pTOPSTOP, produced from several mini DNA preps, were checked by restriction digestion. The plasmid was linearised to estimate its size and a double digest was performed to release the cloned fragment. The plasmids proved to be the correct size and fragments produced by the double digest showed no anomalies. This was to rule out the possibility that the plasmid had lost or altered the insert during storage. The stability of the plasmid in the expression strain was then

checked over the time course of the trial induction and the plasmid was found to be stable. This eliminated the possibility that the plasmids was unstable and was being lost during the course of the trial induction. A fresh supply of the expression strain BL21(DE3) was purchased and transformed. It was possible that our stocks of the original expression strain had deteriorate during storage as a glycerol stock at -70°C. In order to eliminate this possibility, the strain was re-purchased and transformed but once again no expression of protein was seen. It was suggested (Roper.D personal communcation) that we use a variant of the expression strains that contained a pLysS plasmid that allows tighter control of expression. The pLysS plasmid constitutively produces a small amount of T7 lysozyme which will bind to any T7 polymerase produced before the addition of IPTG and so prevent the production of recombinant protein that may be toxic to the cell prior to induced expression. Cells that carry the pLysS plasmid have an additional advantage in that the presence of lysozyme makes them easier to lyse when producing the recombinant protein. In addition we were also provided with a plasmid containing a re-cloned fragment based on TOPSTOP that had four further C-terminal amino acids of topo II, plus eleven extra codons and a six histidine tag for ease of purification. The protein produced from this clone, the TOPSTOP/HIS clone, is referred to as the 52 kDa protein (Table 3.1). Unfortunately neither the strain containing the pLysS plasmid nor the new clone showed any improvement in expression.

An attempt to grow large scale cultures from single colonies was performed, i.e. avoiding a starter culture. It was thought that the growth of the cells overnight prior to trial induction could be affecting the production of the recombinant protein. To examine this possibility the trial induction was set up directly from a single

colony from a freshly produced plate. This approach failed to improve the production of recombinant protein.

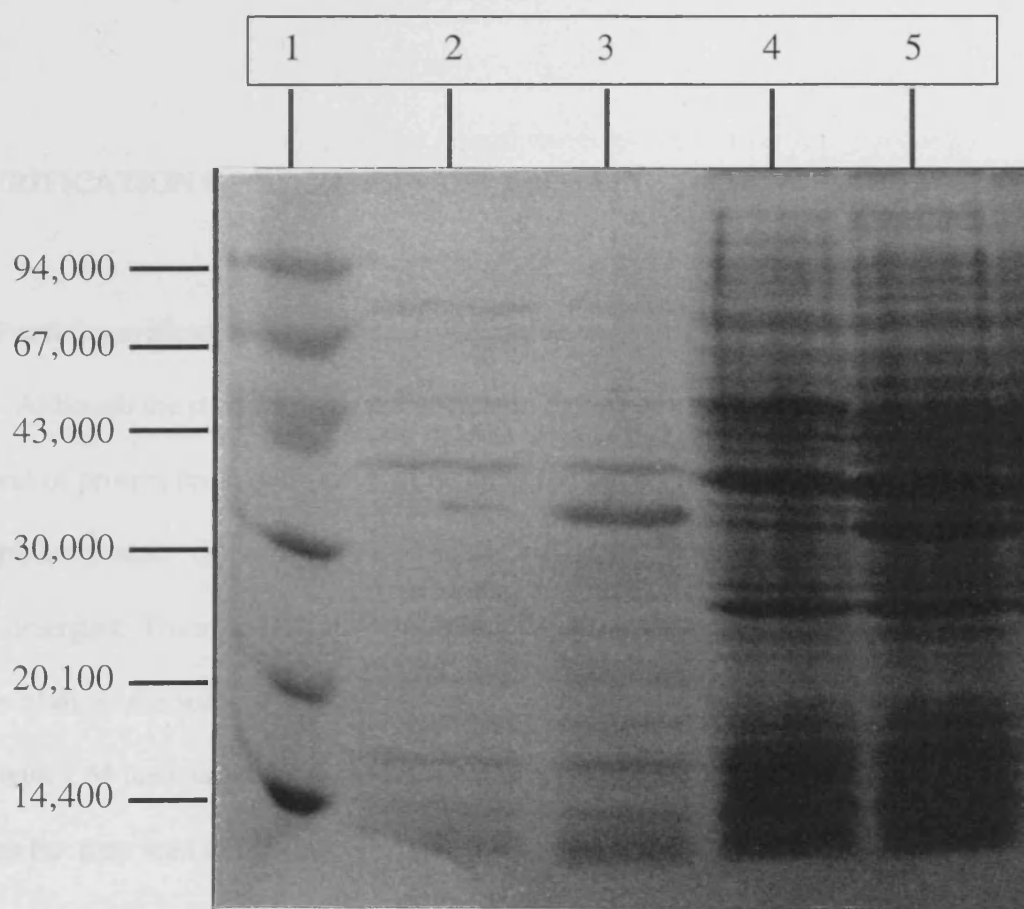
3.2.2 Clarification of expression conditions

The assumption from the previous section was that the broth composition was the major factor in determining satisfactory protein expression, specifically the supplier of the broth components. In an attempt to clarify the difficulties encountered in expressing this protein a series of experiments to examine the expression of the 50 kDa fragment in different broth compositions with ingredients from different suppliers was performed. This study failed to provide consistent evidence to explain the loss of protein expression. However as a result of these experiments it can be said that the protein is reliably expressed in Oxoid Nutrient Broth. All future protein preparations were carried out from cultures grown in Oxoid NB.

3.2.3 Attempts to increase solubility of recombinant protein

Both the 50 kDa protein made from the pTOPSTOP clone and His-tagged 52 kDa protein made from the pTOPSTOP/HIS clone were produced almost entirely as insoluble material associated with inclusion bodies. Figure 3.2 shows the partition of the recombinant protein in a typical cell preparation. It was obvious that insoluble protein would require additional work in order to re-solubilise and purify the material. It was considered to be a good strategy to attempt to produce a greater proportion of the recombinant protein in the soluble fraction. In order to try to produce soluble protein the following strategies were adopted. The cells were grown at 25°C instead of 37°C; it was hoped that as the cells were growing more slowly this would help a larger proportion of the recombinant protein to be produced in a soluble form. A second

Figure 3.2 Partition of the recombinant protein into soluble and insoluble fractions.



This figure shows the partition of the protein into soluble and insoluble fractions in a typical trial induction; lane 1 markers, lane 2 soluble fraction of protein from an induced sample, lane 3 soluble fraction of protein from an uninduced sample, lane 4 insoluble fraction of protein from an induced sample and lane 5 insoluble fraction of protein from an uninduced sample.

strategy involved growing the cells at the normal temperature i.e., 37°C, but using 0.1mM IPTG, i.e. ten-fold less than would be normally used for induction; it was hoped that this would reduce any stress the cell might suffer upon the production of recombinant protein and thus aid solubility. Neither of these approaches gave any significant increase in the amount of recombinant protein in the soluble fraction. Given these results it was decided to develop a strategy of re-folding the protein from inclusion bodies.

3.3 PURIFICATION OF RECOMBINANT PROTEIN

3.3.1 Partial purification of protein from inclusion bodies

Although the production of the protein in *E. coli* in inclusion bodies is not ideal, this form of protein production does allow an initial partial purification of the recombinant protein. Once the soluble fraction has been removed, treating the pellet with a detergent, Triton X 100, and sonicating disperses the membranes and removes a portion of more the soluble proteins contained within the pellet. Further washing of the pellet with 2 M urea assists with the removal of a greater portion of contaminating proteins but may lead to the loss of some target protein. This process will result in partially purified protein which can then be solubilised into Tris-buffered 8 M urea, 50 mM Tris.HCl (pH 8).

3.3.2 Establishing re-folding conditions

Working initially with non-His-tagged 50 kDa protein produced as inclusion bodies, the first step was to re-fold the protein from inclusion bodies into a soluble form. In order to establish the best conditions for producing soluble protein for

additional purification steps the inclusion bodies were solubilised, following partial purification after cell lysis, by sonication into Tris-buffered 8 M urea 50 mM Tris.HCl (pH 8). Refold Buffer (Tris.HCl, 100 mM KCl, 1 mM EDTA, 1 mM DTT, 10% glycerol) was made up and buffered across a pH range from 6.5 to 9.5. 200 µl aliquots of the protein solution in 8 M urea were dialysed overnight at 4°C into the prepared range of buffers. Following dialysis the protein solution was centrifuged at 13,000 rpm for 30 minutes to pellet any insoluble material and the soluble fractions were applied to an SDS polyacrylamide gel. The fraction that produced the most soluble 50 kDa protein after dialysis was the aliquot that had been dialysed into re-fold buffer at pH 8.8. In this fraction it was noted that a large portion of the protein remained insoluble. This experiment was repeated using Refold Buffer that varied in KCl concentration from 0 to 200 mM. The result of this experiment was to show that soluble protein was best produced at 100 mM KCl in the Refold Buffer. These experiments allowed the production of Refold Buffer that would optimise the production of soluble re-folded 50 kDa protein for further purification steps : Refold Buffer (Tris.HCl (pH 8.8), 100 mM KCl, 1 mM EDTA, 1 mM DTT, 10% glycerol).

3.3.3 FPLC purification

Initially we attempted to purify the re-folded protein by ion exchange chromatography on a Mono SP column using a FPLC system. Mono SP is strong cation exchanger. This choice was based on the predicted pI of the recombinant protein which was 9.3. The soluble 50 kDa protein was dialysed into 50 mM sodium phosphate buffer (pH 7.2), 100 mM KCl and applied to the column. Sodium phosphate buffers of

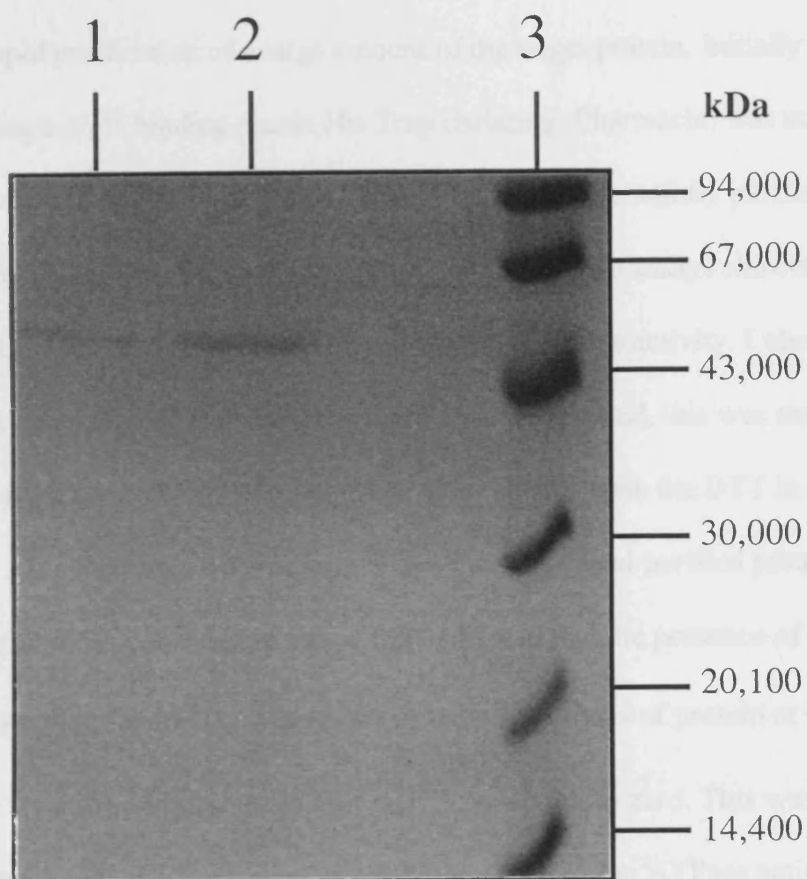
increasing ionic strength were then prepared containing, 200 mM, 400 mM and 700 mM KCl. These were then used in batches to elute the protein from the column.

These attempts resulted in the loss of the re-folded 50 kDa protein. The protein could not be removed by increasing ionic strength in the buffers and could only be detected following the cleaning of the column. The protein was apparently binding to the column in such a way that that it could not be eluted under any normal conditions. After several attempts with the same result this approach was abandoned.

3.3.4 Gel purification

It was considered that a sample of purified protein was needed to evaluate the merits of continuing the project. Based upon the problems we had encountered with the protein on the FPLC system it was thought that an expeditious method of evaluation might be provided by the direct purification of the protein sample from a SDS polyacrylamide gel. Protein was extracted from the gel as previously described in Chapter Two and assayed for ATPase activity by linked enzyme assay. This protein proved to have ATPase activity and this was sufficiently encouraging to warrant a continued pursuit of this project. The method of gel purification was not a practical option for the production of large quantities of protein and the nature of the method caused the protein to be treated harshly, consequently the method was judged to be unreliable. Figure 3.3 shows protein resulting from SDS PAGE gels, although the protein shown is the 52 kDa His tagged protein this figure indicates the purity and quantity of protein produced by this method. Using this method we compared the ATPase activity of the 52 kDa His tagged protein with the non-His tagged 50 kDa protein, the 50 kDa protein at 0.6 μ M gave a rate of 2.9 nM s⁻¹ and the 52 kDa protein at 0.6 μ M gave a rate of 3.0 nM s⁻¹.

Figure 3.3 Production of protein from SDS PAGE gels.



The above figure shows typical 52 kDa protein preparation by gel purification. Lanes 1 and 2 show gel purified 52 kDa protein, lane 3 shows the markers.

3.3.5 Purification by metal affinity chromatography

As the non-His-tagged 50 kDa fragment had proved to be very difficult to purify in any usable quantity a decision was taken to take advantage of the C-terminal His tag cloned into the 52 kDa protein produced by the pTOPSTOP/HIS clone. This would allow rapid purification of a large amount of the target protein. Initially a column containing a Ni^{2+} binding matrix His Trap chelating (Pharmacia) was utilised using the method described in Chapter Two. The protein was successfully purified in good quantities. However, following refolding, the subsequent assays showed no activity; in contrast gel purified 52 kDa protein did have an ATPase activity. I observed that on dialysis into a Refold Buffer a brown precipitate appeared, this was result of the Ni^{2+} eluting from the column with the protein and reacting with the DTT in the Refold Buffer. An experiment was performed in which active gel purified protein had Ni^{2+} added to it during an ATPase assay, this indicated that the presence of Ni^{2+} would inactivate the protein. The initial rate of ATP hydrolysis of protein at $0.4\mu\text{M}$ was 3.6 nM sec^{-1} , on the addition of 50 mM Ni^{2+} the rate fell to zero. This was further supported by an observation of in this laboratory that the ATPase activity of full length human Topo II was also compromised by the presence of Ni^{2+} in the assay buffers (Hammonds. T personal communication). Four attempts were made to overcome these problems. Vigorous pre-washing of the Ni^{2+} bound matrix was attempted to remove any excess Ni^{2+} from the column. Following elution from the matrix, the protein was precipitated with acetone in an attempt to remove bound Ni^{2+} from the protein. Following elution the fraction containing the 52 kDa protein was reapplied to a blank column e.g. one that had not been charged with Ni^{2+} , in the hope that eluted Ni^{2+} would removed from solution by binding to the matrix. The solution of protein was also

dialysed against a buffer containing a high concentration of EDTA in the hope that this would remove the eluted Ni^{2+} . All approaches were limited in their success and it was obvious that more reliable method of purification was needed to generate a good quantity of active 52 kDa protein for characterisation.

The ease of use and rapid purification achieved by using the Ni^{2+} binding matrix suggested this was still potentially the best approach to the purification of the 52 kDa fragment. It was decided to continue to use this approach but to use a different metal affinity matrix. Talon, a cobalt-affinity resin (Clontech), whilst having a greater binding capacity for the protein and less affinity for non-His- tagged protein also had the further advantage that the metal ions were fixed to the matrix making the chances of metal leaching less likely. Talon affinity matrix was utilised using the protocol describe in Chapter Two. This resulted in the production of a good yield of purified 52 kDa protein prior to refolding overnight. Upon refolding it was noted that the majority of 52 kDa protein failed to re-fold successfully and precipitated out of solution, this resulted in a typically low concentration of protein in solution following re-folding. The typical concentration of protein in solution was approximately 0.15 mg/ml. This protein was assayed for ATPase activity and found to be active. The range of activities of protein at $0.4\mu\text{M}$ were 0.2 nMs^{-1} to 0.8 nMs^{-1} . The cobalt affinity matrix proved to be the most reliable method for large-scale purification of the 52 kDa protein. Figure 3.4 shows the purification of 52 kDa protein using a cobalt affinity matrix. Figure 3.5 shows refolded protein following purification on a cobalt affinity column.

3.3.6 Concentration of soluble protein

Although the protein produced from the cobalt column was active the majority did not solubilise upon refolding. Conditions for refolding the protein had already been

Figure 3.4 shows a typical purification of the 52 kDa protein under denaturing conditions on a Cobalt column.

Lane 1 Markers.

Lane 2 Flow through.

Lanes 3, 4 and 5 wash buffer(50 mM Tris.HCl (pH 8.0), 100 mM NaCl).

Lanes 6, 7, 8, 9, and 10, elution with 50mM imidazole in 8M urea (50 mM Tris.HCl (pH 8.0), 100 mM NaCl).

Figure 3.4 Purification of the his tagged recombinant protein on a colbalt affinity column.

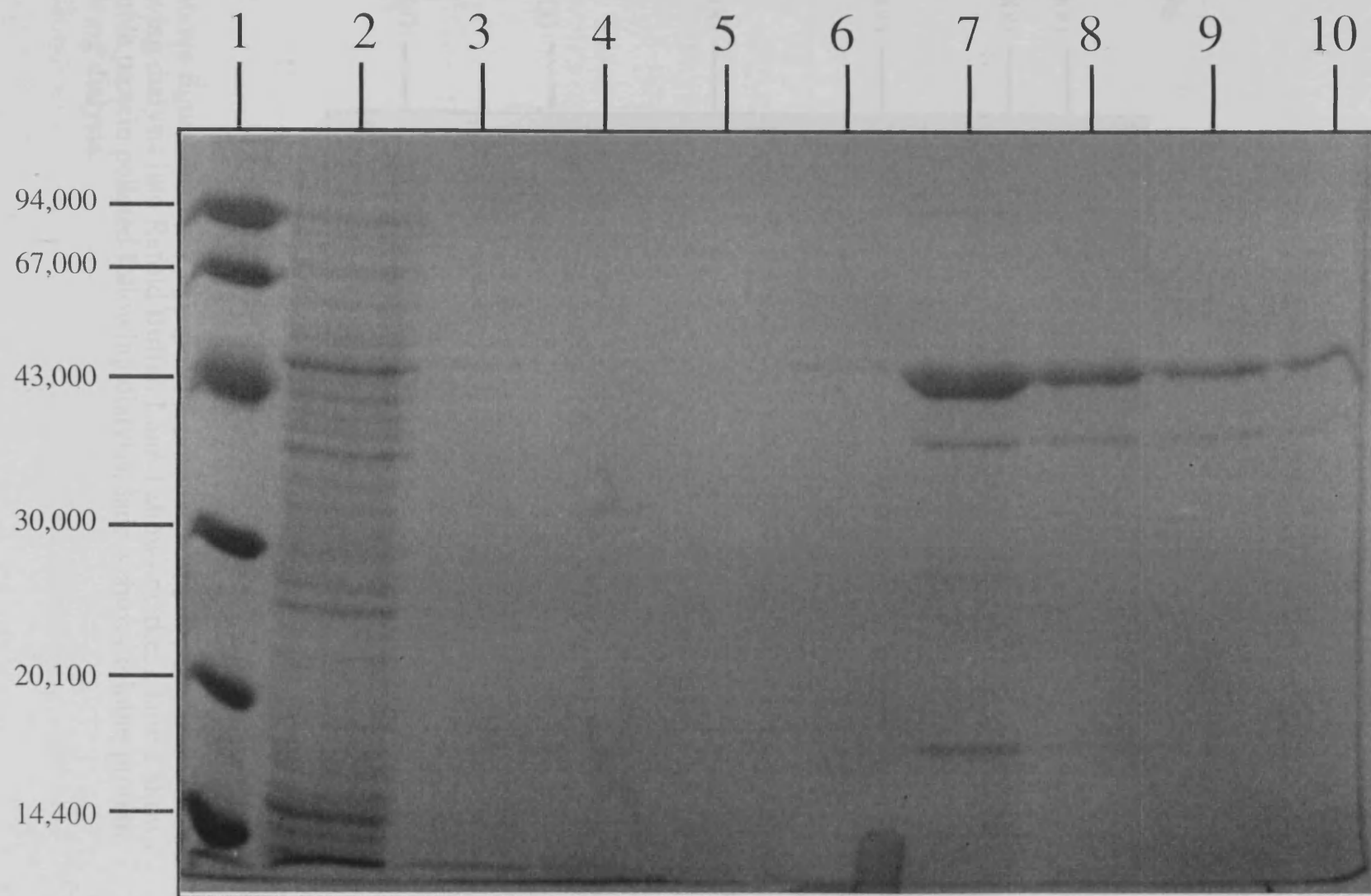
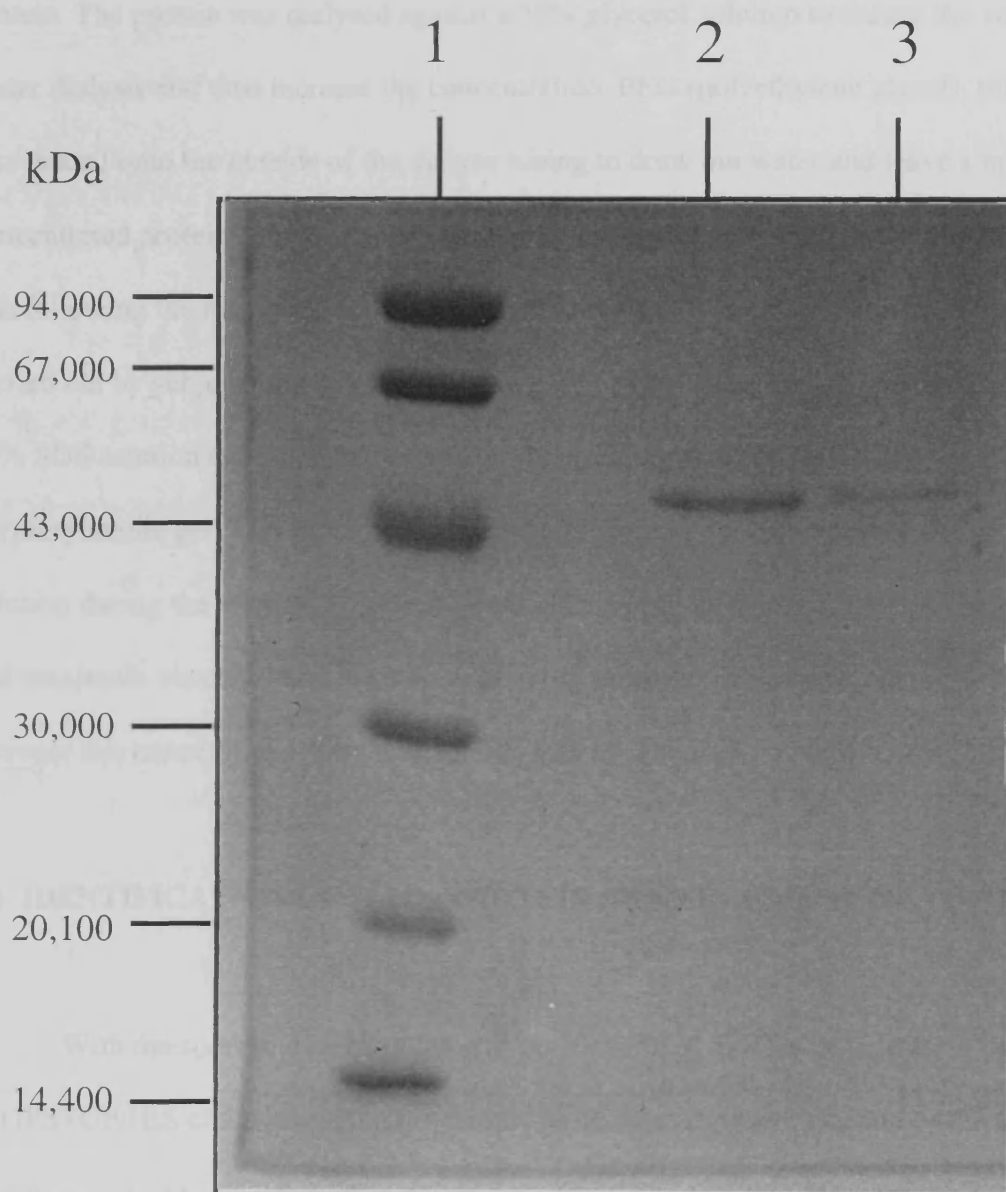


Figure 3.5 The production of soluble protein from denaturing conditions on a cobalt affinity matrix.



The above figure shows 52 kDa protein produced on a cobalt affinity matrix following dialysis into Refold Buffer. Lane 1 shows markers, lane 2 shows insoluble protein pelleted following dialysis, lane 3 shows soluble protein following dialysis.

optimised and so we attempted to concentrate the protein following the re-folding step. A variety of methods were employed to try and increase the concentration of 52 kDa protein in solution. Amicon spin units were used to try and concentrate the soluble protein. The protein was dialysed against a 50% glycerol solution to reduce the volume under dialysis and thus increase the concentration. PEG (polyethylene glycol), powder was dusted onto the outside of the dialyse tubing to draw out water and leave a more concentrated protein solution. In all of these cases the concentration of the protein was less following the attempted concentration. An investigation of this observation was carried out by subjecting either the dialysis tubing or the concentration unit to a wash of 10% SDS solution and running a sample of the resulting solution on a SDS polyacrylamide gel. This revealed that the soluble protein had precipitated out of solution during the attempt to concentrate it. This observation indicated that the protein had maximum concentration in solution of approximately 0.15 mg/ml, any attempt to increase this concentration would result in a loss of protein.

3.4 IDENTIFICATION OF 52 kDa PROTEIN AS A FRAGMENT OF TOPO II.

With the successful production and purification of 52 kDa protein from the pTOPSTOP/HIS clone it was then necessary to confirm the identification of the protein as a fragment of human Topo II α . This was achieved by Western blotting. The protein was challenged with a primary antibody raised against human topoisomerase II α . This antibody successfully revealed the recombinant protein. In addition in conjunction with John Jenkins CMHT Leicester , polyclonal antibodies were raised against the 52 kDa protein. Subsequent Western blots using these antibodies demonstrated their ability to

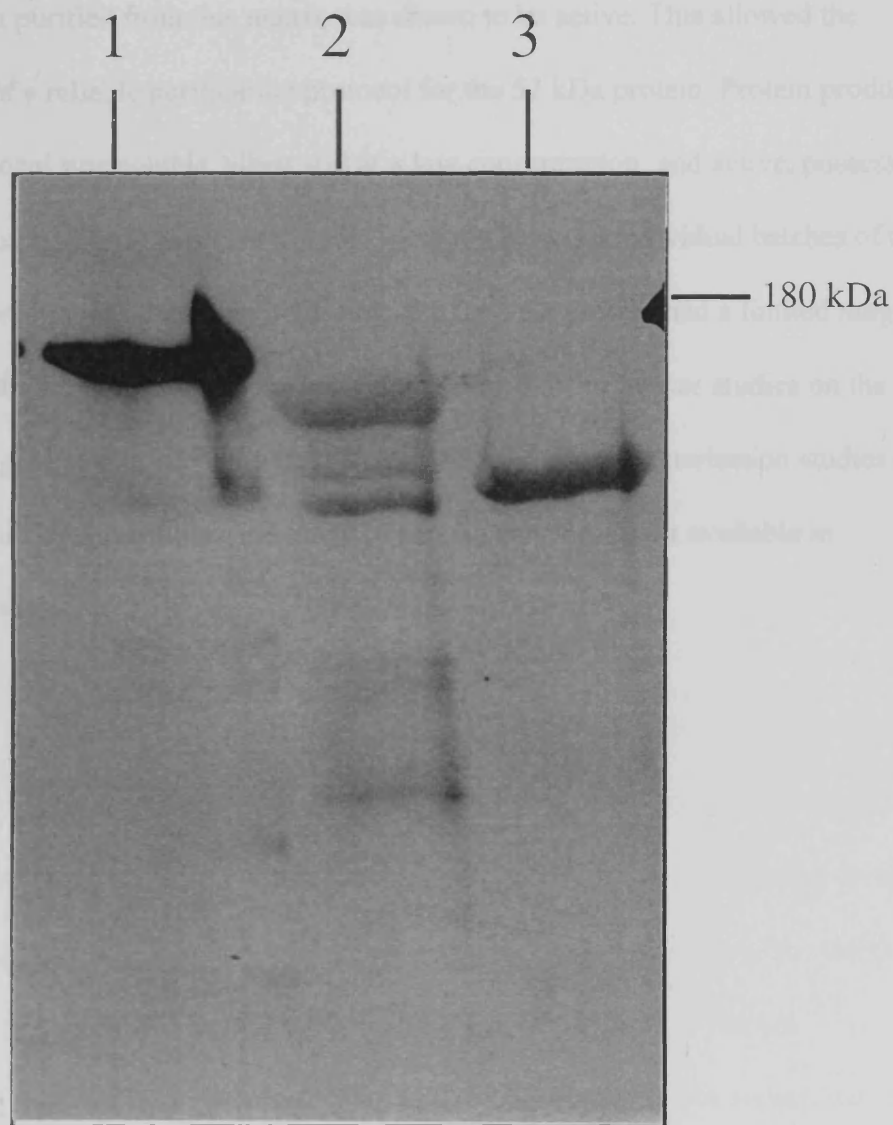
recognise the full-length human α enzyme the yeast enzyme and truncated yeast enzyme lacking the C-terminal region (figure 3.6). From this evidence I was able to conclude that the 52 kDa protein produced from the pTOPSTOP/HIS clone was a fragment of human topoisomerase II α .

3.5 DISCUSSION

The object of this first section of the project was to produce and purify protein representing the N-terminal domain of human topo II α . It was initially found that the protein produced from our chosen clone was found in the insoluble fraction of the cell prep. All attempts to produce soluble protein directly from a cellular prep failed. We were therefore forced to address the problems associated with developing a reliable protocol for re-folding the protein from inclusion bodies prior to purification.

Following the development of a successful re-fold protocol we attempted to purify the protein on a Mono SP column, the predicted pI of the protein suggested it would carry a significant positive charge so a strong cation exchanger was chosen : these attempts failed. The reason for this failure was probably due to limited solubility of the protein. As the protein bound to the column the local concentration rose to beyond that which could remain in solution resulting in the protein precipitating out of solution. This explanation matches our observation of apparently irreversible binding to the Mono SP column often followed by a increase in back pressure, typical of the column becoming blocked. This explanation is also supported by our attempts to concentrate the protein in solution which also resulted in a loss of protein, apparently due to precipitation.

Figure 3.6 Identification of the 52 kDa protein as a fragment of topo II



The above figure shows a blot using polyclonal antibodies raised against the 52 kDa fragment. Lane 1 shows full length human topo II α , lane 2 shows full length yeast topo II and lane 3 shows C- terminal deletion of yeast topo II.

The use of protein that incorporated a His tag allowed the purification of the protein under denaturing conditions. The protein could then be re-folded following purification to generate soluble protein. It is likely that the loss of activity due to Ni^{2+} leeching from the column may be a result of competition for a Mg^{2+} binding site on the enzyme. Given the problems associated with the Ni^{2+} column we switched to a cobalt matrix. Protein purified from this matrix was shown to be active. This allowed the development of a reliable purification protocol for the 52 kDa protein. Protein produced using this protocol was soluble, albeit still at a low concentration, and active, possessing an ATPase activity. There was considerable variation between individual batches of the purified protein, perhaps due to the refolding step, and the protein had a limited range of solubility. Both of these observations had implications for the further studies on the enzyme : a single batch of protein would have to be used for characterisation studies and the limited solubility would limit the range of protein concentrations available in subsequent assays.

CHAPTER 4

CHARACTERISATION OF THE ATPase REACTION OF THE 52 kDa N-TERMINAL FRAGMENT OF HUMAN TOPO II α .

INTRODUCTION

Following the development of successful production and purification protocols resulting in active recombinant protein, the next step was to conduct a series of experiments to examine and optimise the reaction conditions for the hydrolysis of ATP by this protein. The relevant conditions for optimisation were pH, KCl concentration and Mg^{2+} concentration. Initial conditions for the ATPase assay were 50 mM Tris.HCl (pH 8.8), 10 mM $MgCl_2$, 1.25 mM ATP and 100 mM KCl. These conditions represent a combination of the conditions used in the ATPase assays for the 43 kDa domain of gyrase (Ali et al, 1993) with conditions in the buffer used for refolding the recombinant 52 kDa protein. In addition to optimising the assay, it was hoped these experiments would provide some insight into the ATPase activity of the protein. Following these experiments the next stage involved an examination of the basic kinetics of the reaction, involving the effects of varying the protein and ATP concentrations. Further experiments included looking for the effects of phosphorylation, DNA stimulation and the effect of a range of anti-topo II agents.

4.1 OPTIMISATION OF REACTION CONDITIONS

4.1.1 The effect of pH on ATPase activity.

ATPase assays were conducted in the above conditions using a series of Tris.HCl buffers at a concentration of 50 mM, across a range of pH from 7 to 9. This range was selected as it was thought to include the most likely conditions for optimal activity based on evidence from the full-length enzyme (Hammonds and Maxwell, 1997). The resulting rates were then plotted (figure 4.1). As can be seen in this figure the optimal pH for this ATPase reaction is ~7.5, the rates rapidly decreasing at higher values of pH. Based on these data all future assays would be conducted at a pH of 7.5.

4.1.2 The effect of KCl concentration on the ATPase activity of the 52 kDa fragment.

The next series of experiments were on the effects of KCl concentration on the ATPase activity. The relatively low activity of this protein meant that a large volume of the protein in solution had to be assayed in order to observe reliable activity, typically 40 µl of protein solution in a total assay volume of 200 µl. As this protein had been refolded into a buffer containing 100 mM KCl this imposed a restriction on the lowest KCl concentration possible. The concentration in the experiment ranged from 80 mM KCl to 225 mM. The results of this experiment were then plotted (figure 4.2). As can be seen from this figure, the rate of ATP hydrolysis was highest at the lowest KCl concentration. In further assays the KCl concentration was maintained at 100 mM, although this concentration is not necessarily optimal it represents a concentration that can be reliably reproduced in all experiments.

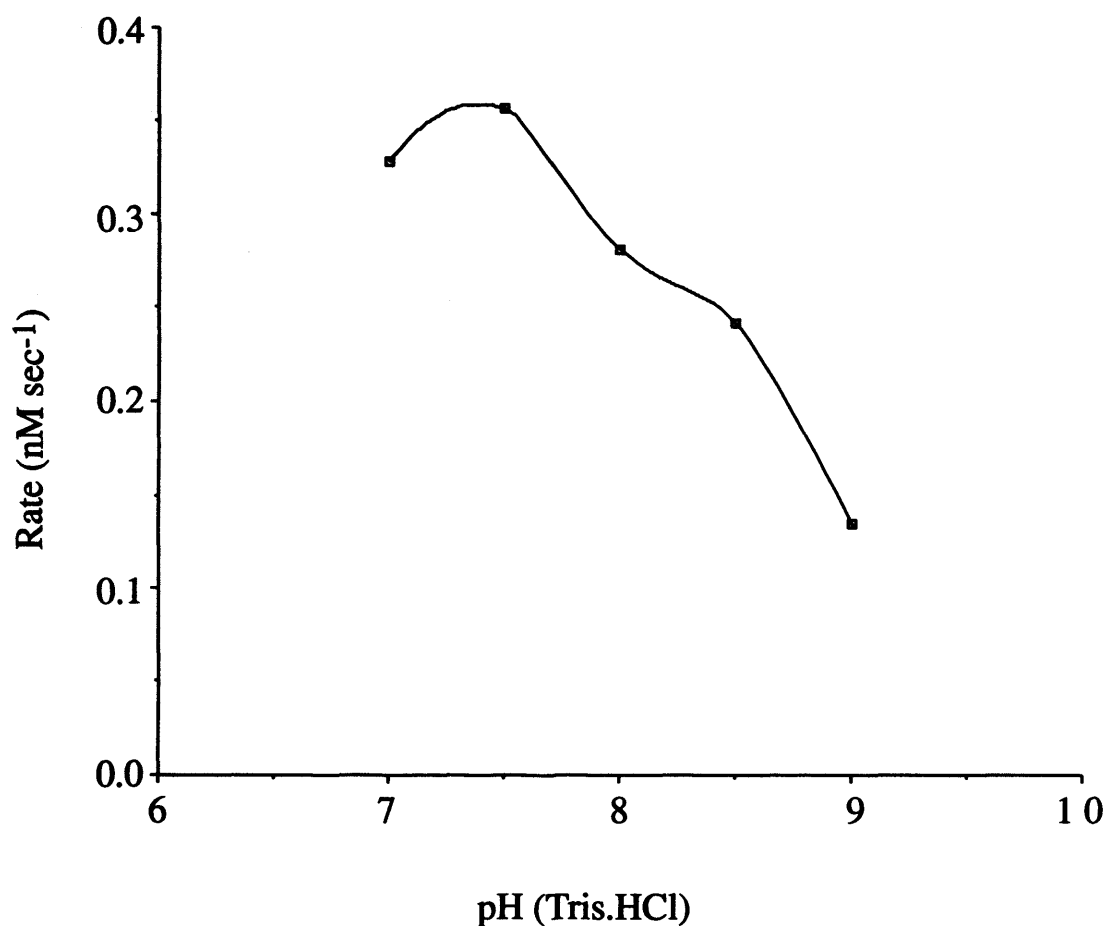
4.1.3 The effect of MgCl₂ concentration on the ATPase activity of the 52 kDa fragment.

The hydrolysis of ATP was assumed to be dependent on the presence of Mg^{2+} in the assay. This assumption was based on evidence from a range of ATPases including DNA gyrase and full-length human topo II α that have been shown to be dependent on Mg^{2+} for their activity. To examine this effect more closely, a series of experiments were performed assaying the protein at a range of Mg^{2+} concentrations. The range chosen was from 0 to 15 mM MgCl_2 . This range of concentrations was used as it represent a range around what had been our normal assay concentration e.g. 10 mM. The results of these assays were plotted (figure 4.3). This figure shows that the rate of ATP hydrolysis peaks at concentrations of Mg^{2+} between 1 and 3 mM. The fall in rate at high Mg^{2+} is quite marked and could not be accounted for in terms of ionic strength effects of increasing MgCl_2 concentrations. The rates of hydrolysis appeared to be highest when Mg^{2+} was in the range of 1:1 to 2:1 against ATP. Excess Mg^{2+} appears to lead to lower rates of ATP hydrolysis. In all further assays we endeavoured to keep the ATP and Mg concentrations equi-molar. A possible explanation for this observation is that free Mg^{2+} are in some way acting to inhibit the enzymatic activity when in significant excess with regard to the ATP, possibly through competition for the active site with the ATP-Mg complex. Such competition would lead to the observed loss of activity.

4.1.4 Summary of optimised conditions.

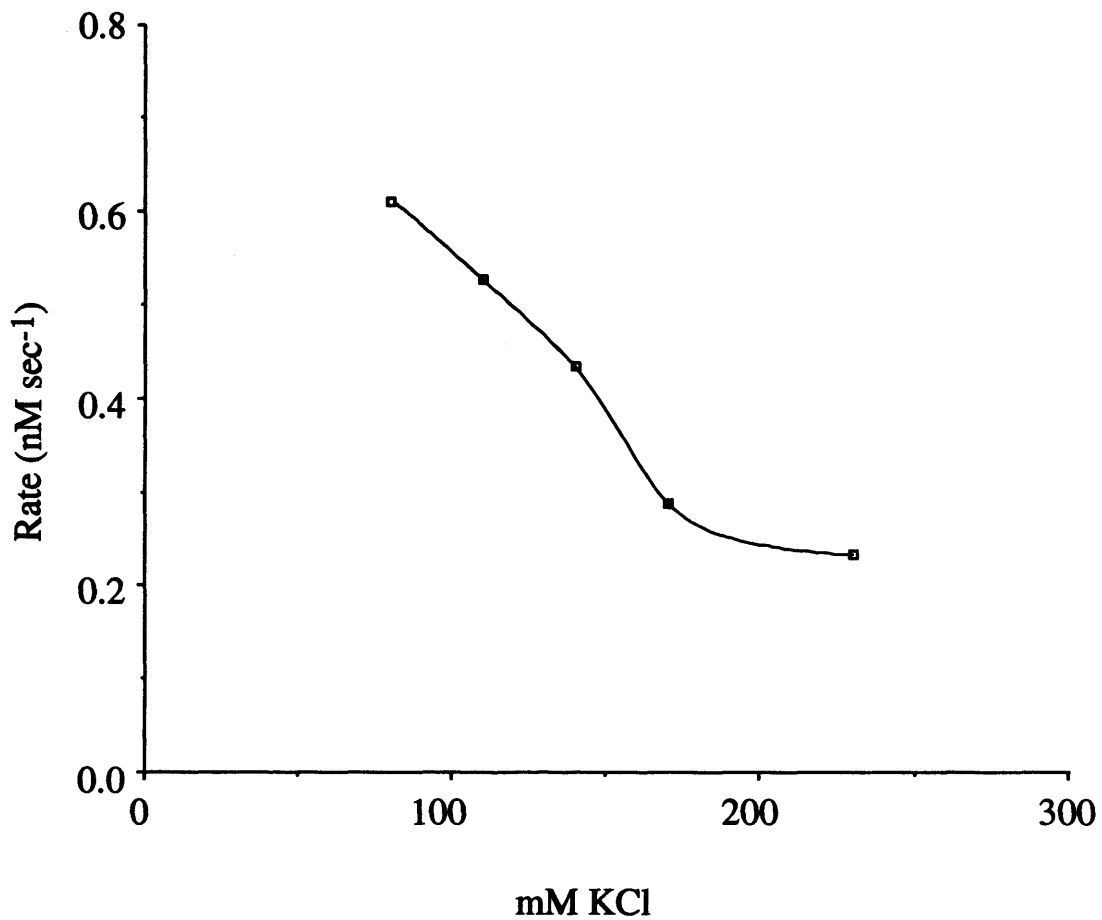
The optimisation experiments were used to generate a new set of standard conditions for ATPase assays, these were: KCl at 100 mM, this represents the lowest KCl concentration that can be reliably reproduced. The MgCl_2 concentration was set at 2 mM and the ATP concentration was also altered to 2 mM to provide an equimolar concentration with the MgCl_2 . The pH of the assay buffer was altered to 7.5.

Figure 4.1 ATPase of the 52 kDa protein vs pH



The above figure shows the effect of a range of pH conditions on the intrinsic ATPase of the 52 kDa fragment. The optimal pH of this reaction was 7.5. Carried out at 50 mM Tris.HCl, 10 mM MgCl₂, 1.25 mM ATP and 200 mM KCl. The assay was conducted at 37° C and the concentration of the protein was 0.6 μM.

Figure 4.2 52 kDa protein ATPase vs KCl



The above figure shows the effect of increasing KCl concentration on the intrinsic ATPase of the 52 kDa fragment. The reaction conditions were as described in figure 4.1 with regard to temperature MgCl_2 and ATP. The pH was 7.5 (50 mM Tris.HCl). The concentration of the protein was 0.6 μM .

Under these conditions it was found that typically 0.1 μM protein had an activity of $\sim 1 \text{ nM.s}^{-1}$.

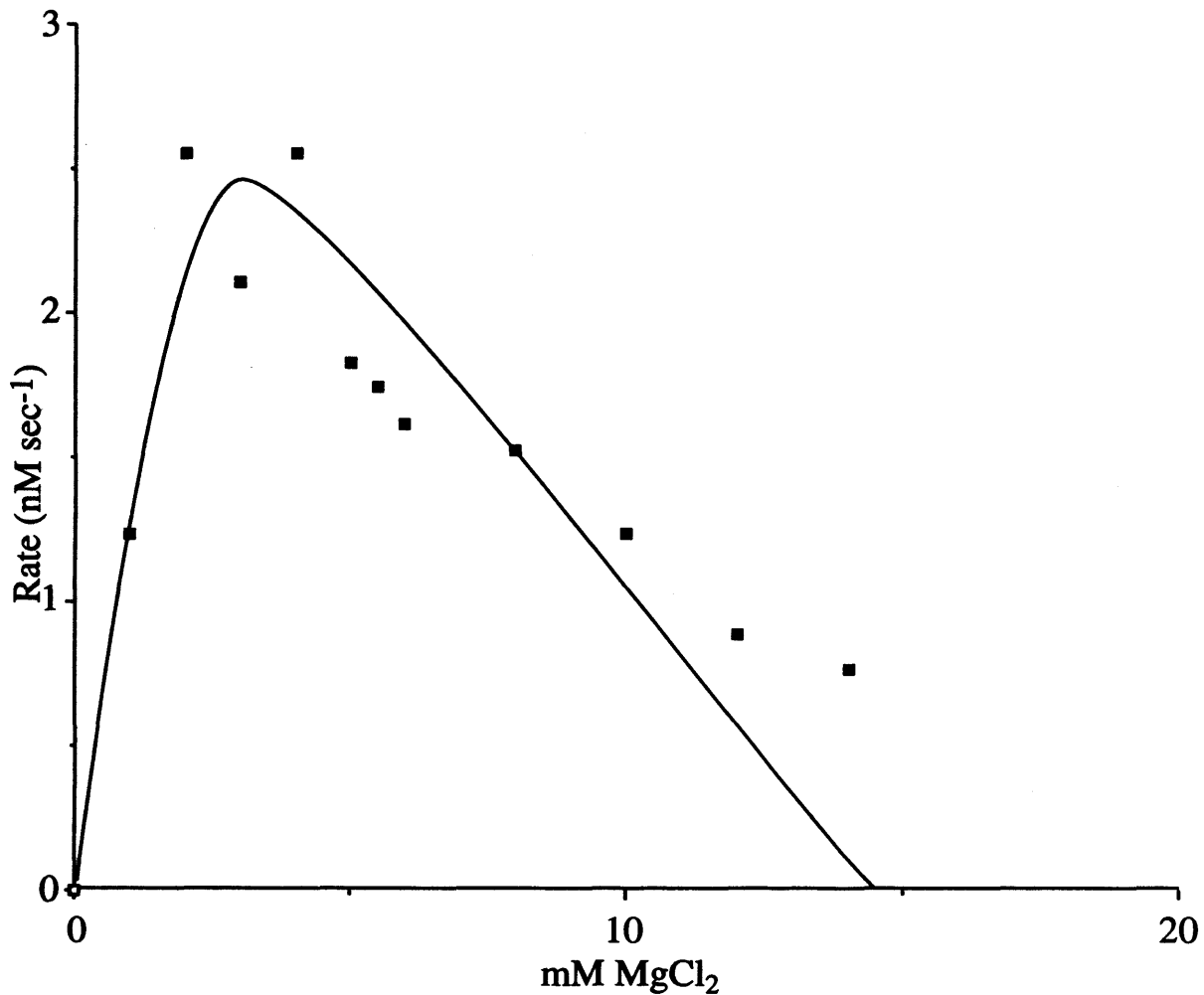
4.2 INTRINSIC ATPase ACTIVITY.

The initial experiments were to investigate the observed intrinsic ATPase activity of the 52 kDa fragment. Primarily these experiments were to examine the basic kinetics of this fragment. The following section outlines two kinetic experiments, in which ATPase activity was measured as a function of enzyme concentration and as a function of substrate concentration as well as a more speculative examination of the effects of DNA on the intrinsic rate. It was hoped that these experiments would provide insights into the mechanism in this fragment and thus the full-length enzyme.

4.2.1 ATP hydrolysis as a function of enzyme concentration.

The intrinsic ATPase activity of the 52 kDa protein was investigated as a function of enzyme concentration in a range of 75–450 nM. The data from this experiment are shown in figure 4.4. It must be noted that due to the relatively low activity of this protein large volumes of protein solution had to be added to the assay. This low intrinsic activity imposed a lower limit on the concentration of the protein that could be reliably assayed. The upper limit for the assay was defined by the maximum volume of sample that could be added to the assay before it became unreliable, this upper limit being 80 μl in a 200 μl total assay volume. The data from this experiment appear to indicate a linear dependence on enzyme concentration. This observation is significant in

Figure 4.3 52 kDa ATPase rate vs MgCl_2 at 1.25 mM ATP.



The above figure shows the affect of Mg^{2+} concentration on the rate of ATP hydrolysis by the 52 kDa fragment. It is clear from the above data that the rate peaks at about 1 - 4 mM. Reaction conditions were 50 mM Tris.HCl (7.5), 1.25 mM ATP, 100 mM KCl. Concentration of the protein was $0.6\mu\text{M}$. This assay was performed at 37°C .

that it is in marked contrast to the 43 kDa N-terminal domain of gyrase, which exhibits a non-linear dependence of ATPase on enzyme concentration (Ali *et al*, 1993).

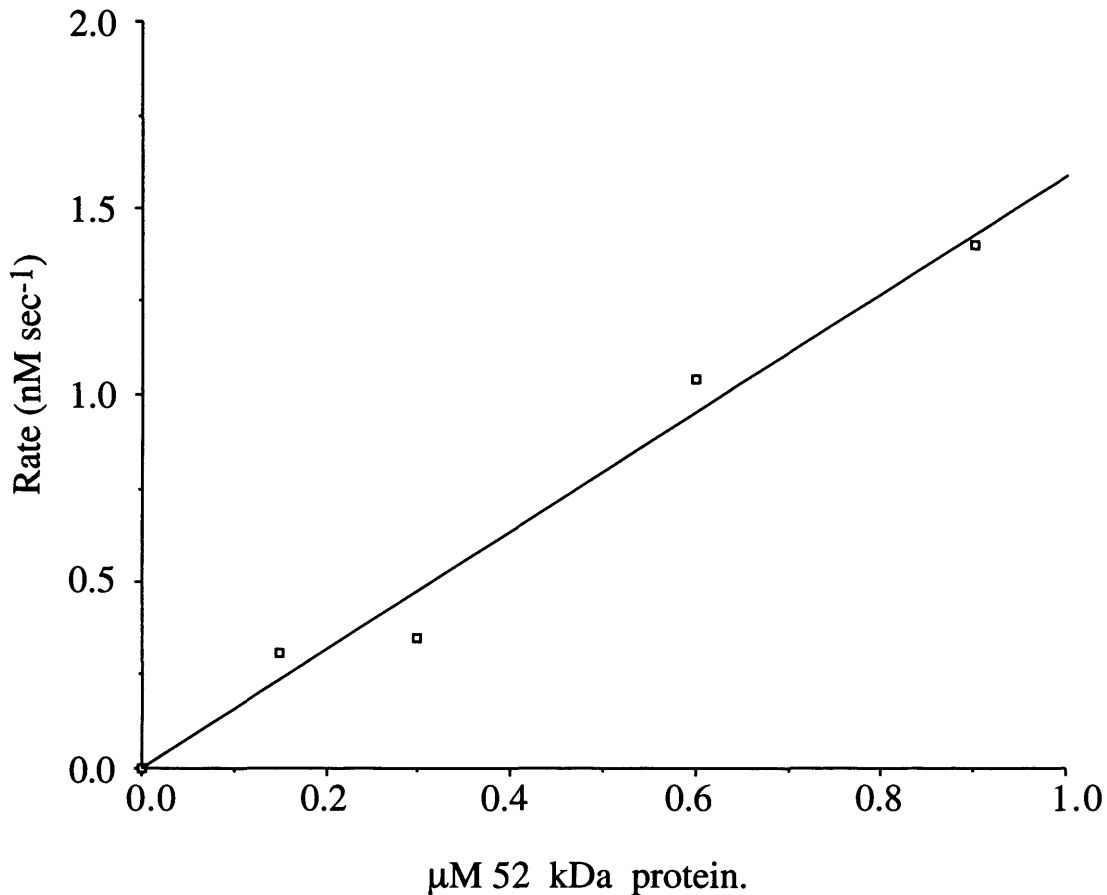
4.2.2 ATP hydrolysis as function of substrate concentration.

A series of experiments were performed to investigate the intrinsic ATPase activity of the 52 kDa fragment as a function of substrate concentration. These data were analysed by fitting to rectangular hyperbolic curve (MacCurveFit, Kevin Raner software). From these data values of K_M and k_{cat} (0.47 mM and 0.018 s^{-1}) were determined. These data are shown in figure 4.5. These data indicate that the 52 kDa fragment shows hyperbolic dependence of rate on substrate concentration, indicative of Michaelis-Menten kinetics. Again this differs from the 43 kDa fragment of gyrase which demonstrates non -Michaelis-Menten kinetics (Ali *et al*, 1993).

4.2.3 The DNA dependence of ATPase activity.

As part of the characterisation of the ATPase of the 52 kDa fragment it was decided to look for any DNA dependence the fragment might show. Unexpectedly upon the addition of DNA the ATPase activity of the fragment was significantly stimulated (figure 4.6). These experiments were performed with linear, supercoiled and relaxed pBR322 and it was found that all three stimulated the ATPase activity to a similar extent (data not shown). Further experiments using a variety of different preparations of the enzyme demonstrated an average maximum stimulation in ATPase rates of between 5- and 10- fold above the intrinsic rate. The exact level of stimulation appears to vary between preparations of the enzyme. We investigated the stimulation of ATPase activity across a range of DNA concentrations; these data are shown in figure 4.6. This experiment indicated that a significant excess of DNA was needed to fully stimulate the

Figure 4.4 ATP hydrolysis as a function of enzyme concentration.



The above figure shows the results of investigations into the dependence of the intrinsic ATPase rate on enzyme concentration. The above results indicate a linear dependence of rate on enzyme concentration. This experiment was carried under standard conditions (50 mM Tris.HCl (pH7.5), 100 mM KCl, 2 mM MgCl_2 , 2 mM ATP and conducted at 37°C in a total volume of 200 μl).

DNA-dependent ATPase rate. These data can be treated as a binding isotherm and an approximate value for the equilibrium dissociation constant for the binding of the 52 kDa fragment to DNA can be calculated (see Discussion). The behaviour of the 52 kDa fragment differs significantly from the 43 kDa domain of gyrase whose ATPase activity is independent of DNA (Ali *et al*, 1993), however it shows marked similarities to the full-length enzyme (Hammonds and Maxwell, 1997). These data suggest that a significant portion of the DNA-stimulated ATPase rate observed in the full-length enzyme can be attributed to DNA interacting with the N-terminal portion of the protein (see Discussion). The observation of DNA dependence in this fragment led to series of experiments to investigate this behaviour in more detail.

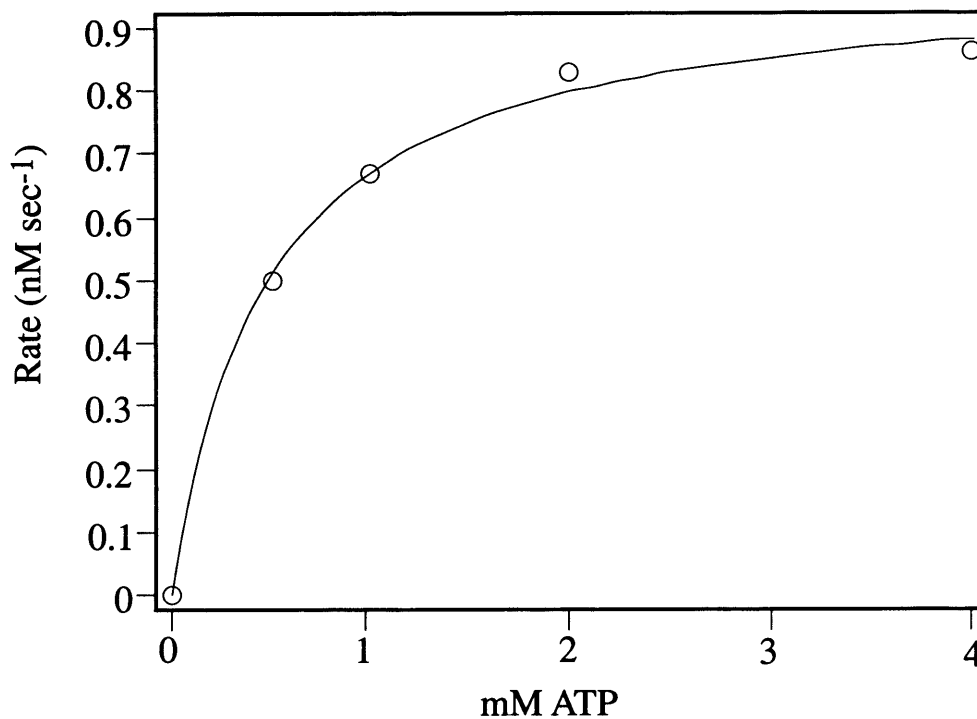
4.3 CHARACTERISATION OF THE DNA- DEPENDENT ATPase OF THE 52 kDa FRAGMENT.

Following the observed stimulation of ATPase activity in the presence of DNA, a series of experiments were conducted into the basic kinetics of the DNA-stimulated ATPase activity of this fragment. The following section outlines investigations of DNA-dependent ATPase activity as a function of enzyme concentration.

4.3.1 DNA dependent ATPase as a function of enzyme concentration.

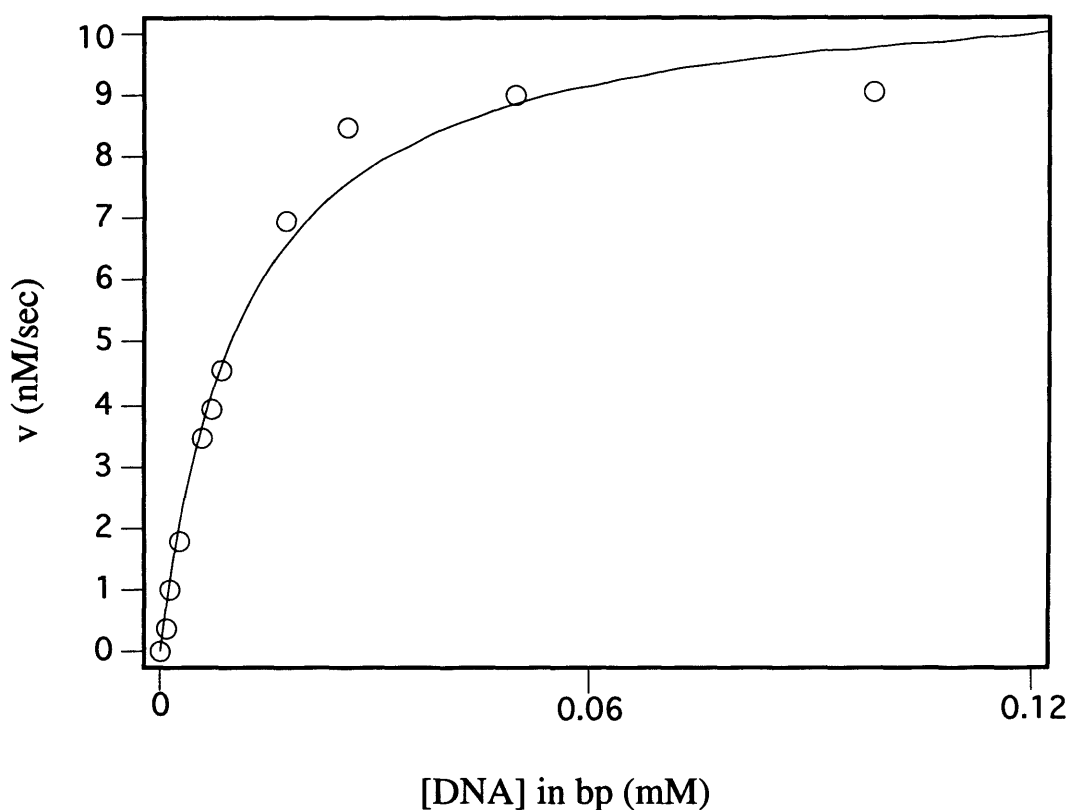
The DNA dependent ATPase was investigated as a function of enzyme concentration. These data are shown in figure 4.7. Again these data indicates a linear dependence of ATPase activity on enzyme concentration and so is consistent with the previous observation on the non-DNA dependent data (section 4.2.1).

Figure 4.5 ATP hydrolysis as a function of substrate concentration.



The above figure show the affect of increasing substrate on the intrinsic ATPase of the 52 kDa fragment. The enzyme shows hyperbolic dependence indicating that Michaelis-Menten kinetics apply. This experiment was performed under standard reaction condition (see fig 4.4); the enzyme concentration was 80 nM. The calculated values of K_M and K_{cat} were 0.47 mM and 0.018 s⁻¹ respectively.

Figure 4.6 ATP hydrolysis of the 52 kDa fragment as function of DNA concentration.



The above figure shows the stimulation of the ATPase rate of the 52 kDa fragment by DNA. This experiment was carried out under standard reaction conditions. The concentration of protein in this experiment was 0.6 μ M. This experiment indicates significant DNA stimulation. This experiment indicated that ~80 μ g/ml (0.12 mM) of DNA(supercoiled pBR322) was necessary to stimulate the enzyme to the greatest extent.

4.3.2 DNA-dependent ATP hydrolysis as function of substrate concentration

A series of experiments were conducted to examine the effect of substrate concentration on the DNA-dependent ATPase activity of the 52 kDa fragment. These data were analysed by fitting to a rectangular hyperbolic curve (MacCurveFit, Kevin Raner software) data shown in figure 4.8. The protein again shows a hyperbolic dependence indicating Michaelis-Menten kinetics. The calculated values for K_m and k_{cat} (0.40 mM and 0.11 s^{-1}) for this experiment suggest that in the presence of DNA the K_m of the enzyme is approximately the same whilst the k_{cat} increases by 6-fold. This indicates that while the rate of enzyme turnover is increased the affinity of the enzyme for the substrate remains the same.

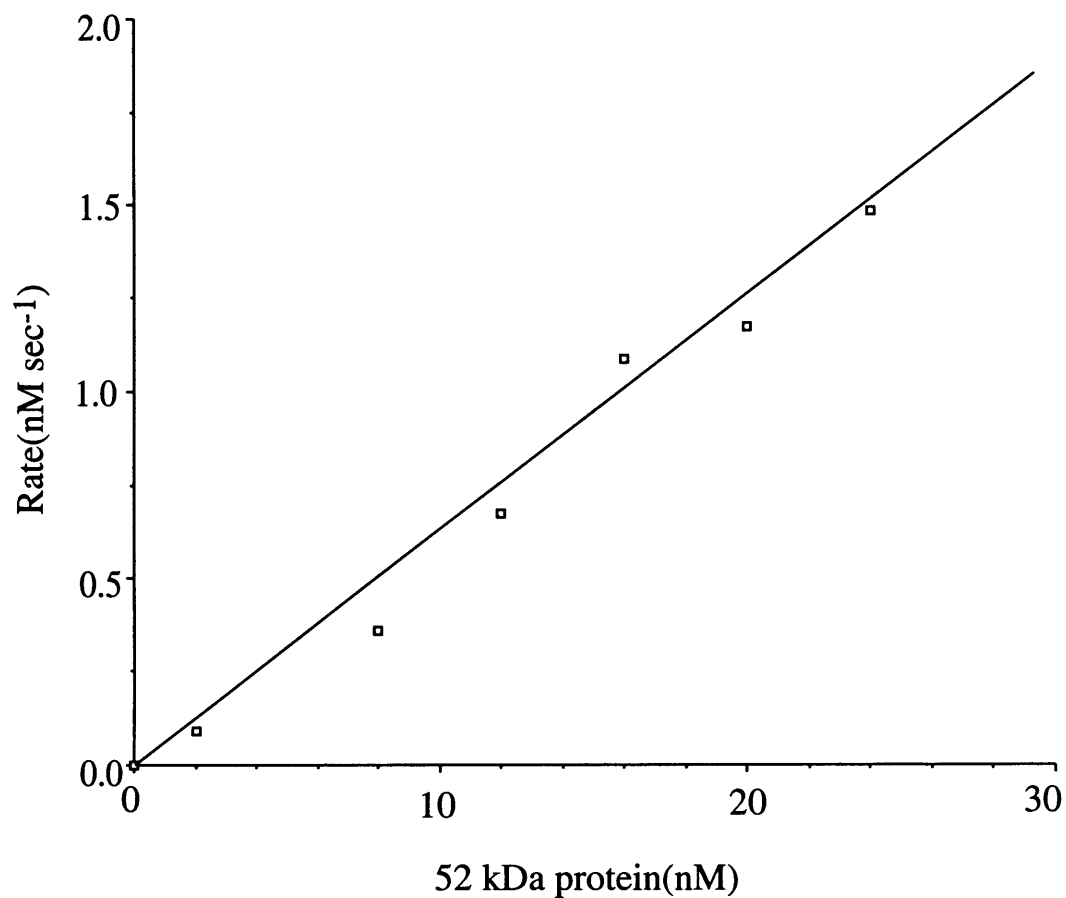
4.3.3 Effect of Mg^{2+} concentration on DNA-dependent ATP hydrolysis

A series of experiments were conducted to examine the effect of Mg^{2+} concentration on the DNA-dependent ATPase activity of the 52 kDa fragment (figure 4.9). The result of these studies appeared to indicate an apparent loss of activity at about 6 mM Mg^{2+} , the activity then appears to recover. This experiment was repeated on several occasions yielding the same result. In addition the experiment was repeated varying the DNA concentration in the assay and varying the concentration of the protein yielding the same result. There is no clear reason for this observation but it seems worthy of further study.

4.3.4 Removal of DNA during ATPase assay

It had been suggested that the apparent DNA stimulation that was observed with the 52 kDa protein was due to the protein folding on the DNA leading to a better protein conformation with respect to ATP hydrolysis. In order to examine this idea an

Figure 4.7 Concentration of 52 kDa protein vs DNA-dependent ATPase activity.



The above figure shows the result of investigations into DNA-dependent ATPase as function of enzyme concentration. These assays were conducted at 37°C under standard conditions in the presence of DNA (pBR322) at 80 µg/ml (0.12 mM bp). These data demonstrate that the ATPase activity is linear with respect to enzyme concentration.

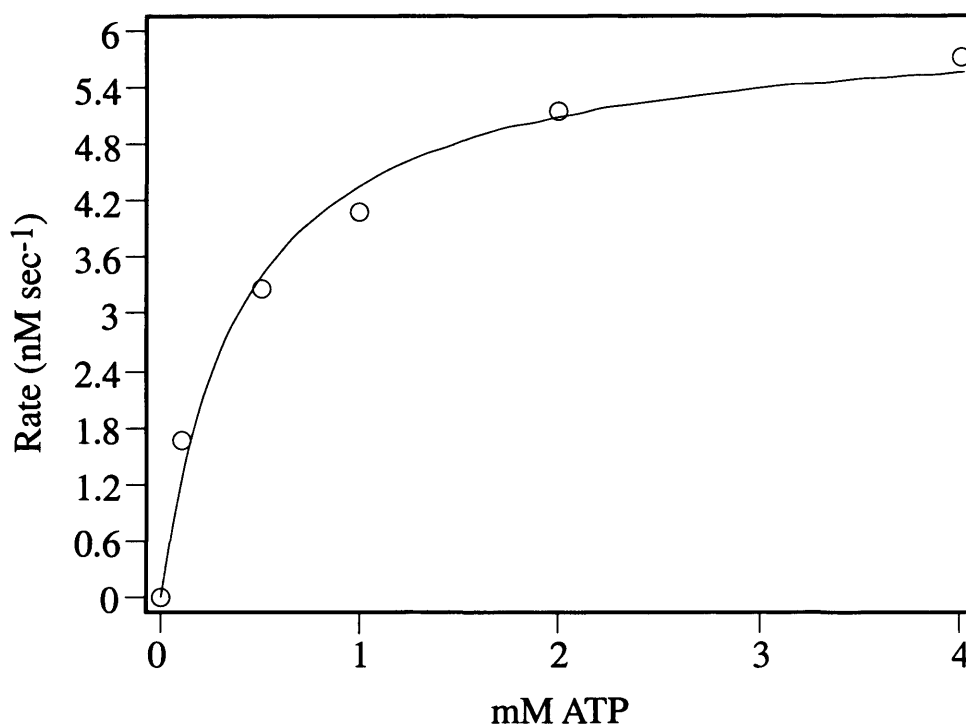
experiment was devised in which the ATPase assay would run initially in the absence of DNA, then DNA would be added to the assay and the rate observed. Following this DNase I would be added to the assay and any change of rate observed. The data for this experiment are summarised in figure 4.10 As these data show the rate of hydrolysis falls markedly upon the addition of DNase I, i.e. the removal of DNA. To ensure the rapid removal of all DNA (16 μ g pBR322) 30 units of DNase I (1 unit completely degrades 1 μ g of DNA (pBR322) at 37°C in 20 mins) were added and the assay left for 30 minutes. This experiment suggests that the enzyme requires DNA for increased ATPase activity and that no other component of the reaction mixture is responsible for the rate increase.

4.3.5 Effect of KCl concentration on DNA-stimulated ATPase activity.

To follow the previous observation of the optimal KCl concentration for intrinsic ATPase activity of the 52 kDa fragment (section 4.1.2) we decided to examine the effect of KCl on the DNA-dependent ATPase rate. These data (figure 4.11) show that a very similar pattern is evident. Due to the increased rate of ATPase activity seen as a result of DNA stimulation, a smaller volume of 52 kDa protein needs to be added to the assay to generate a reliable rate. This allows the concentration of KCl in the assay to be varied over greater range (0 to 200 mM). This experiment reveals that the rate of ATP hydrolysis rises from 0 to approximately 80 mM KCl then rapidly falls away. These data show that the concentration of 100 mM KCl suggested by figure 4.2 is near optimal for the ATPase activity of this enzyme.

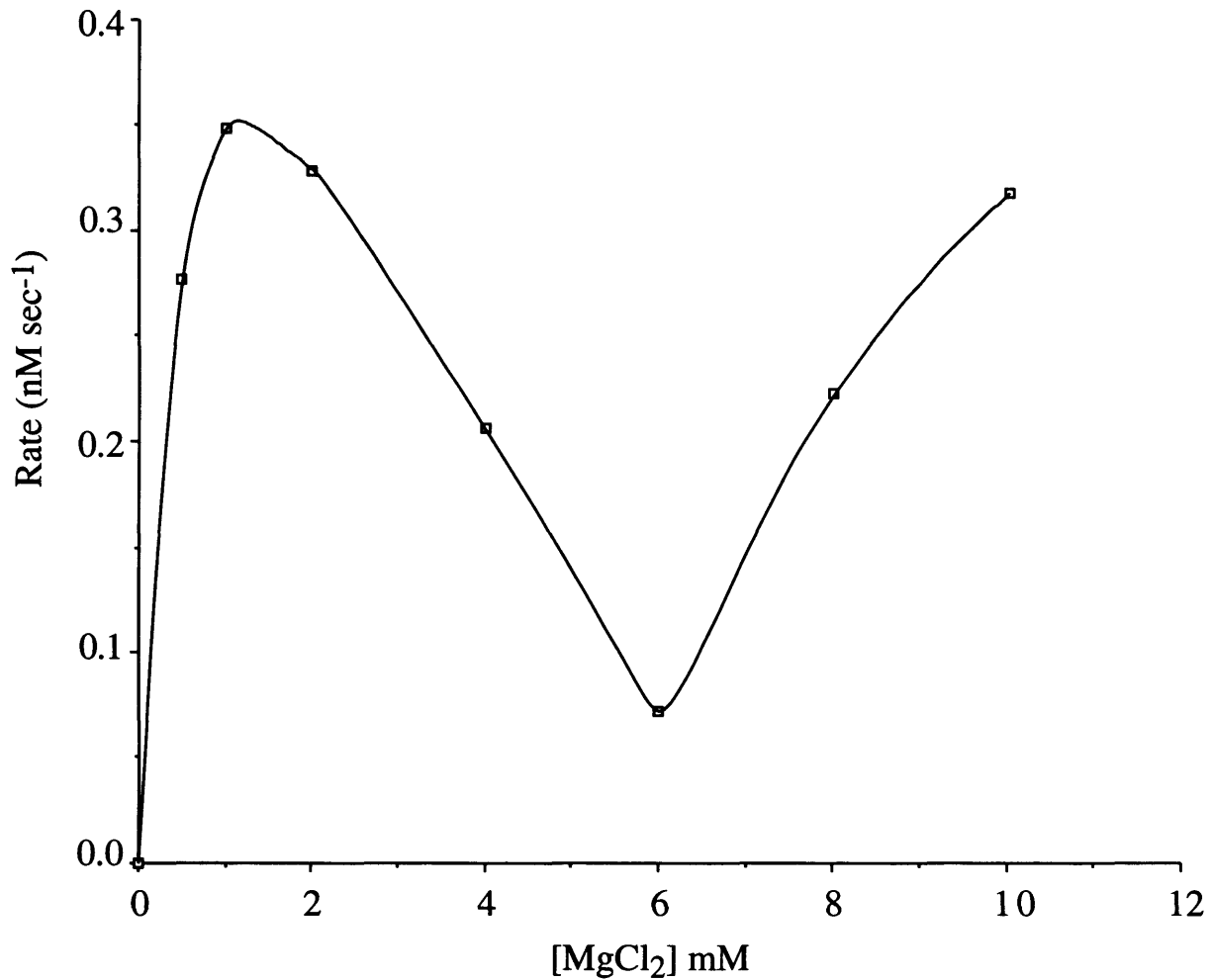
4.4 STUDIES TO EXAMINE THE 52 kDa FRAGMENT'S INTERACTION WITH DNA.

Figure 4.8 DNA-dependent ATP hydrolysis as a function of substrate concentration.



The above figure shows the DNA-dependent ATP hydrolysis as a function of substrate concentration. From these data it is clear that the protein shows hyperbolic dependence on the substrate concentration indicating Michaelis-Menten kinetics. This experiment was performed under standard experimental conditions. The enzyme concentration was 80 nM. The calculated values of K_M and K_{cat} were 0.40 mM and 0.11 s⁻¹ respectively.

Figure 4.9 The affect of MgCl_2 on the DNA-dependent ATPase of the 52 kDa fragment.

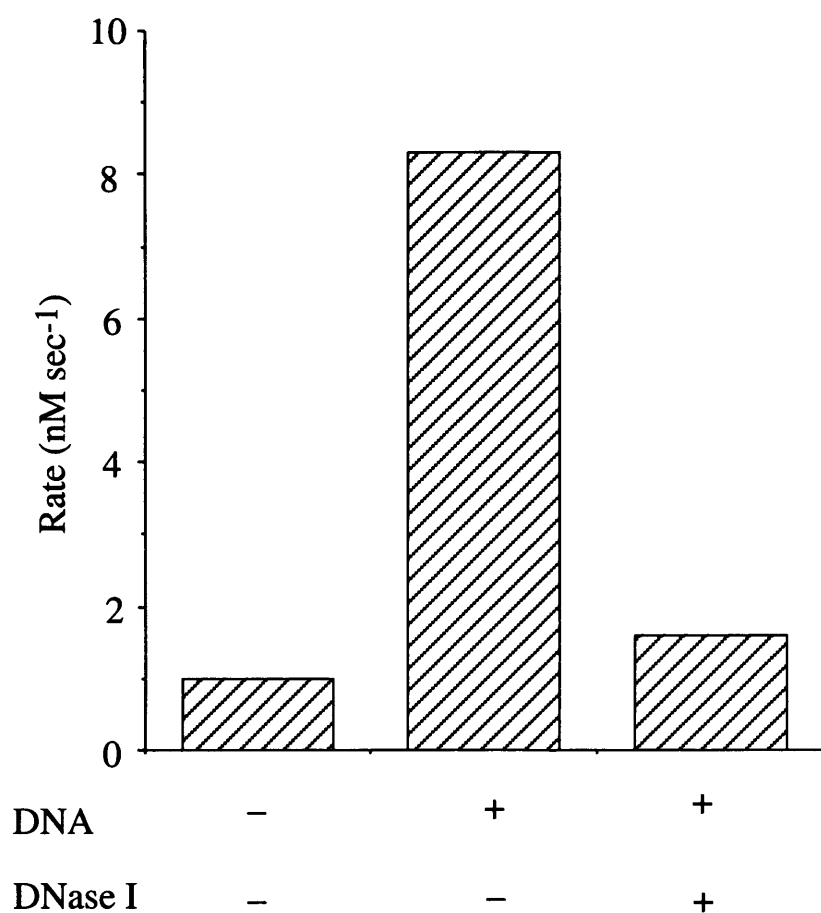


The above figure shows the result of experiments looking the affect of Mg^{2+} on the DNA-dependent ATPase. The result is a dip in activity at about 6 mM Mg^{2+} . This experiment was performed under standard experimental conditions plus the presence of DNA(pBR322) at $80\mu\text{g/ml}$ (0.12 mMbp). The enzyme concentration was 8 nM.

Following confirmation of the observed effect of DNA on the ATPase activity of the protein we next attempted to further study this interaction by examining the possibility that the protein would affect the mobility of a fragment of DNA on a non-denaturing polyacrylamide gel. Staining with ethidium bromide and examination under UV light would allow the observation of any alteration in the mobility of the DNA fragment as a result of protein binding. A 198 base pair fragment of DNA was used in these studies. The results were generally unsatisfactory due to smearing of the DNA and difficulties in successfully capturing an image. However it was observed that following incubation with 52 kDa protein the DNA was often not observed on the gel. This suggested that protein-DNA interactions were occurring, however under native conditions the intrinsic charge on the protein could prevent the DNA fragment from entering the gel (data not shown). It also possible, given the observed insolubility of the protein, that under the conditions used in running native gels the 52 kDa fragment had fallen out of solution. In order to look more closely at possible DNA-protein interactions a sample of the 52 kDa protein was provided for analysis on a BIAcore™. For details of this method see Szabo et al (1995). DNA was crosslinked to the sensorchip and a sample of protein flowed over the surface of the chip. Interactions between the DNA, immobilised on the chip, and the protein can be measured. This approach failed to generate usable data as there was too much non-specific binding associated with the sample.

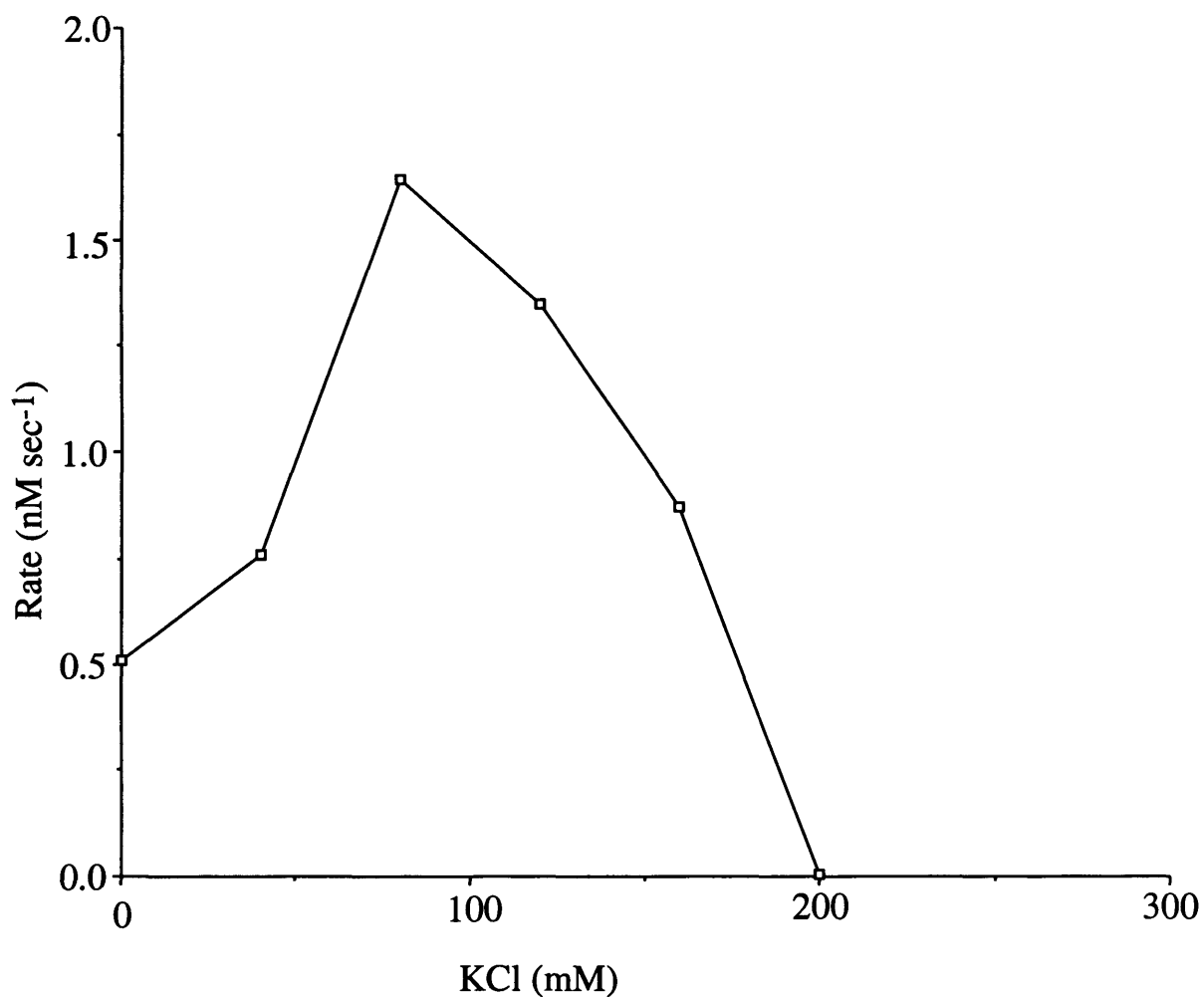
4.5 DIMERISATION STUDIES ON THE 52 kDa FRAGMENT

Figure 4.10 Effect of DNase I on the DNA-dependent ATPase of the 52 kDa fragment.



The above figure shows the result of an experiment to examine the dependence upon the presence of DNA of the DNA-dependent ATPase. The experiment was carried out under standard assay conditions in the presence of 80 $\mu\text{g/ml}$ (0.12 mM bp) of DNA (supercoiled pBR322). The enzyme concentration was 80 nM. 3 μl of DNase I (this comprises 30 units were one unit completely degrades 1 μg of DNA (pBR322) at 37°C) were added to the assay to ensure the removal of the DNA.

Figure 4.11 ATPase rate of the 52 kDa protein vs KCl concentration.



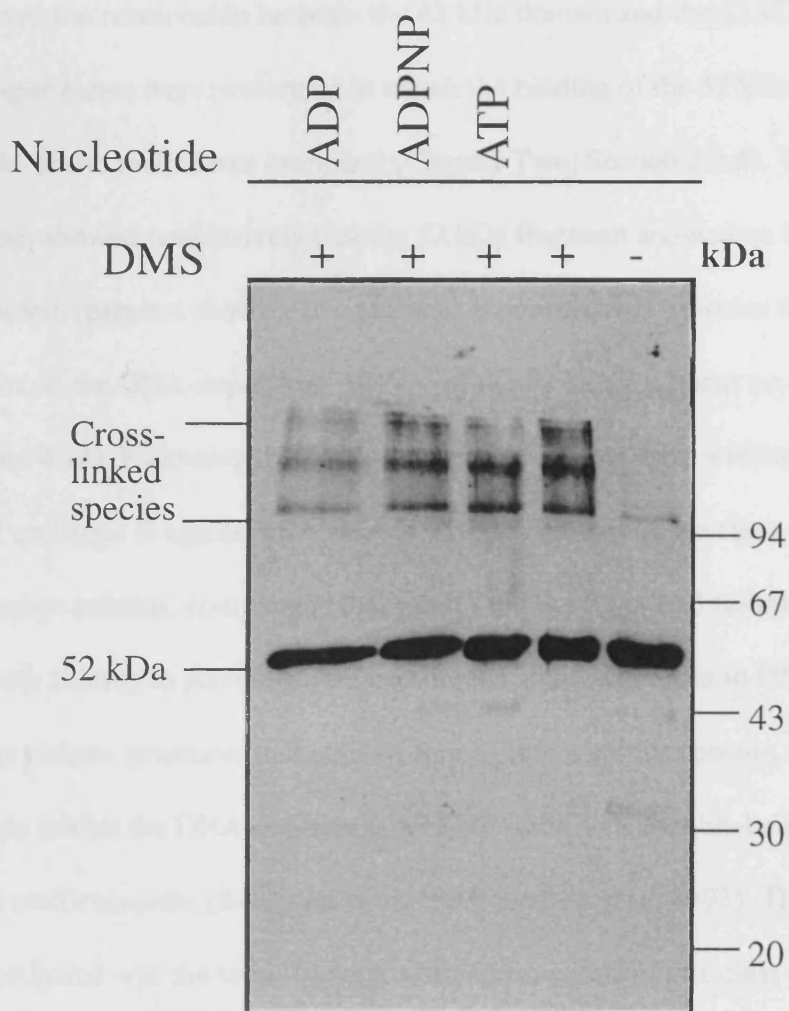
The above figure shows the effect of increasing KCl concentration on the rate of DNA-dependent ATP hydrolysis by the 52 kDa protein. This experiment was conducted under standard conditions in the presence of 80 $\mu\text{g/ml}$ (0.12 mM bp) DNA (supercoiled pBR322).

A salient feature of the 43 kDa N-terminal fragment of the GyrB domain of gyrase is the part played by dimerisation in the turnover of ATP (Ali *et al*, 1995). There is strong evidence from both kinetic and structural studies to support the idea that this domain dimerises in the presence of nucleotide. The observation that the 52 kDa fragment shows a linear dependence of ATPase activity on enzyme concentration in both the presence and absence of DNA suggested a number of possibilities: (1) the 52 kDa protein is predominantly dimeric in solution, (2) that dimerisation was not occurring or (3) dimerisation was not a rate-limiting step in the reaction cycle. This area required further study. In order to investigate the state of the enzyme a series of cross-linking experiments was performed on the protein using the cross linking agent DMS. The agent cross-links lysine residues. Dimers can then be resolved on an SDS-polyacrylamide gel then detected by Western blotting. Figure 4.12 shows the result of such an experiment. The protein was found to form dimers in both the presence and the absence of the non-hydrolysable analogue ADPNP and in the presence of ADP and ATP. This observation suggests that the protein can form dimers both in the presence and the absence of nucleotide triphosphate. This suggests that the protein may be predominantly a dimer in solution.

4.6 THE EFFECT OF DRUGS ON THE DNA-DEPENDENT ATPase ACTIVITY OF THE 52 kDa FRAGMENT.

Topoisomerase IIs are the targets of several clinically important classes of drugs (Froelich-Ammon and Osheroff, 1995; Chen and Liu, 1994; Isaacs *et al*, 1995). The activity of these drugs were tested against the ATPase activity of the 52 kDa fragment. Initial studies involved novobiocin, an anti-gyrase compound that is known to bind

Figure 4.12 Cross-linking studies on the 52 kDa fragment.



The above figure shows the result of studies on the 52 kDa protein using DMS, a chemical cross-linking reagent. Cross linked species are seen in all lanes containing the reagent. This data suggests that the protein can form dimers both in the presence and absence of nucleotide.

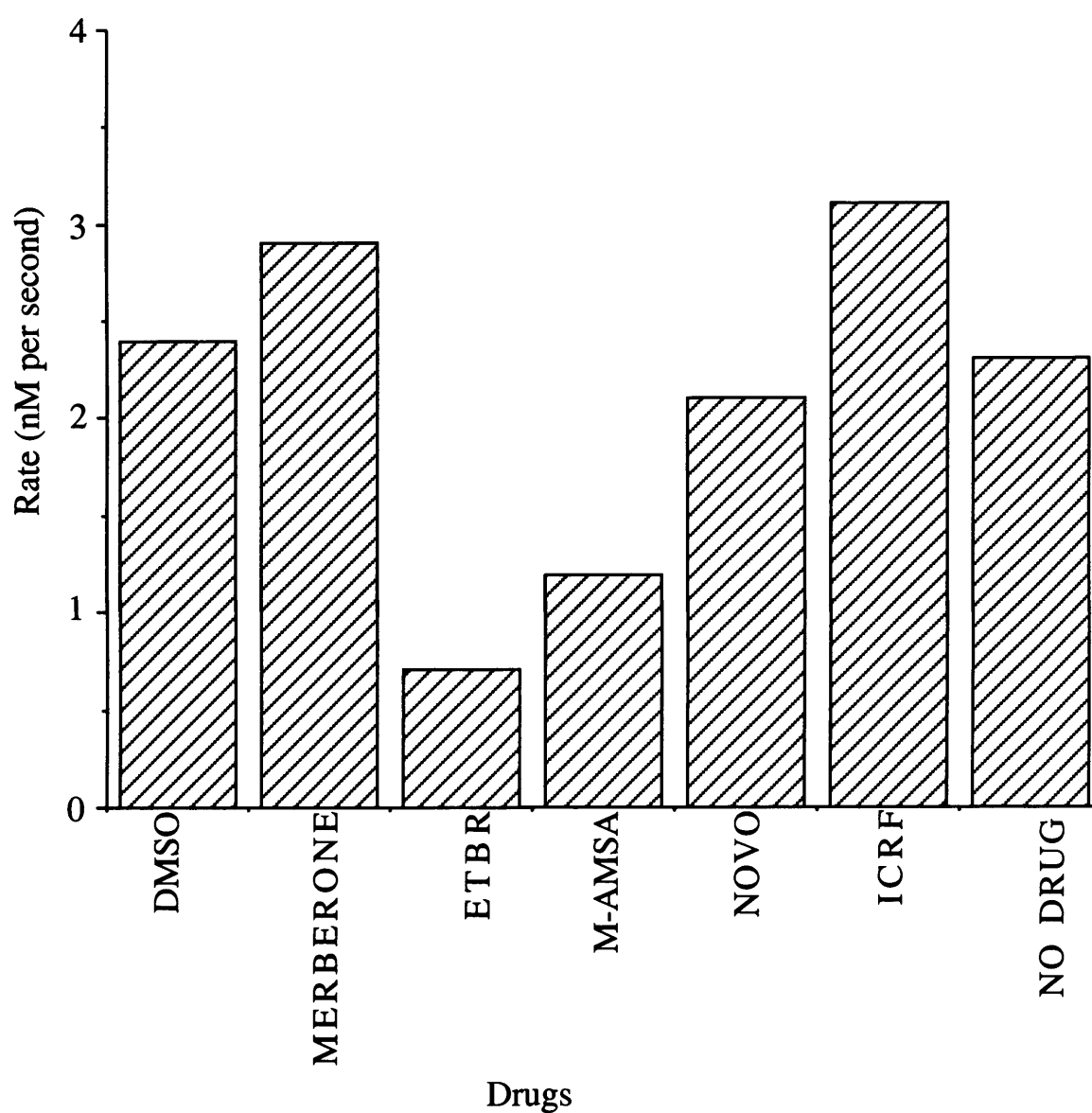
strongly to the 43 kDa N-terminal domain of GyrB and to inhibit the ATPase activity of that fragment (Ali *et al*, 1993). In addition there had been reports that suggested topo II in *Drosophila* could be inhibited by the presence of novobiocin (Robinson *et al*, 1993). Given the relationship between the 43 kDa domain and the 52 kDa fragment of topo II, experiments were performed in which the binding of the 52 kDa fragment to a novobiocin-bound matrix was examined (Chapter Two, Section 2.2.4). These experiments showed conclusively that the 52 kDa fragment showed no binding capacity for novobiocin (data not shown). In additional experiments to examine the affect of novobiocin on the DNA-dependent ATPase of the 52 kDa fragment no inhibition was seen (figure 4.13). Following these results, the experiments were widened to include two classes of anti-topo II agents. m-AMSA is a representative of the class of topoisomerase poisons, compounds that inhibit the breakage and re-union step of the topo II cycle leading to protein-associated double stranded breaks in DNA. This interaction creates structures that convert topo II into a cellular poison. These compounds inhibit the DNA-dependent ATPase activity of the full-length eukaryotic enzyme from *Drosophila* (Robinson *et al*, 1993; Corbett *et al*, 1993). The second class to be investigated was the topo II antagonists. Compounds in this class are specific inhibitors of topo II activity. The representative compounds of this class were merbarone and ICRF-193. The initial investigations showed that the topo II antagonists had no effect on the DNA-dependent ATPase of the enzyme, however m-AMSA appeared to be reducing the observed rate. As an explanation for this observation it was suggested that the compound might be binding non-specifically to the DNA thus interfering with the observed rate. To test this theory the DNA-dependent activity of the enzyme was tested against a non-specific DNA binding compound ethidium bromide. This compound was also observed to reduce the DNA-dependent ATPase

activity of the enzyme. It was concluded that the reduction in rate seen with m-AMSA was as a result of it binding to DNA and not to any specific interaction with the enzyme. The mode of binding for both ethidium bromide and m-AMSA is intercalation. In these studies supercoiled DNA (pBR322) was used to stimulate ATPase activity of the enzyme. At the concentration of DNA used, m-AMSA and ethidium bromide would saturate the DNA. This could lead to the distortion of the DNA and it is possible that this distortion is responsible for the loss of DNA-dependent activity. These data are summarised in figure 4.13.

4.7 PHOSPHORYLATION STUDIES ON THE 52 kDa FRAGMENT.

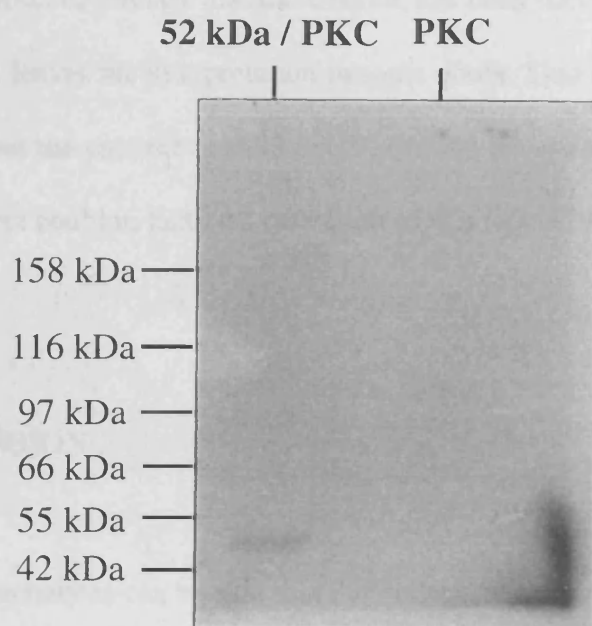
It has been shown that the full-length human topo II α is modified by phosphorylation in vivo (Wells *et al*, 1994). The majority of the sites for phosphorylation are located in the extreme C-terminus of the enzyme. A single potential phosphorylation site is located at Ser 29 in the N-terminal portion of the enzyme and thus is contained in the 52 kDa fragment. Initial experiments were designed to investigate whether the protein is a target for kinases. The two kinases that were used were casein kinase II (CKII) and protein kinase C (PKC). ATP containing [γ -³²P] was used as a substrate in the reaction. The samples of protein were then run on SDS-polyacrylamide gel which was then vacuum dried. Modification of the protein by the incorporation of [γ -³²P] would be detected by exposing the dried gel to Fuji X-ray film. The result of this experiment are seen in figure 4.14. This experiment shows that the protein is clearly modified by protein kinase C. The next step was to repeat the experiment with PKC using non-labelled ATP and run the resulting sample in a standard ATPase assay. The result of

Figure 4.13 The effects of anti-topo drugs on the ATPase of the 52 kDa fragment.



The above figure shows the effects of a variety of anti-topoisomerase compound on the 52 kDa fragment of topo II. The protein was at 100 nM and each of the compounds was added to a concentration of 20 $\mu\text{g/ml}$. The experiment was performed under standard conditions with addition of 80 $\mu\text{g/ml}$ pBR322 DNA.

Figure 4.14 Phosphorylation of the 52 kDa protein by PKC.



The above figure shows the phosphorylation of the 52 kDa protein by PKC. In the first lane shows the phosphorylation of the 52 kDa fragment by PKC, the second lane shows the auto phosphorylation of PKC.

this assay indicated that the phosphorylation of the enzyme had little effect on the rate of ATP hydrolysis by the fragment (for 80nM 52 kDa protein in the presence of PKC the rate was 1nM s^{-1} , in the absence of PKC the rate was 0.8nM s^{-1}). Although this approach is able to provide an indication of the effect of phosphorylation of Ser 29, the inability to observe directly that the enzyme has been successfully phosphorylated at this position, leaves the interpretation in some doubt. This experiment allows the possibility that the enzyme has not been correctly phosphorylated so the lack of apparent effect could in fact be a reflection of this lack of phosphorylation.

4.8 DISCUSSION

In summary it can be said that the optimal reaction conditions for the ATPase of the 52 kDa N-terminal fragment of human topo II α are broadly similar to those for the full-length enzyme i.e. 50 mM Tris.HCl (pH 7.5), 2 mM MgCl_2 , 2 mM ATP and 100 mM KCl. The observation that the intrinsic rate shows a preference for $[\text{Mg}^{2+}]$ in the range equi-molar with [ATP] to double the [ATP] might suggest that free Mg^{2+} may compete for the binding site on the enzyme with the Mg-ATP complex, excess Mg^{2+} leading to partial inhibition of the enzyme. This observation may suggest a mechanism for inhibition of the enzyme by Ni^{2+} (Chapter 3, section 3.3.5) as Ni^{2+} may bind in the Mg^{2+} binding site and prevent the binding of the Mg-ATP complex. The linear dependence of both the DNA-dependent and intrinsic rates on enzyme concentration coupled with the results of the cross-linking experiments suggest that the enzyme exists as predominantly a dimer in solution. This observation is in contrast to the N-terminal domain of GyrB, the 43 kDa protein, which shows non-linear dependence of rate on

enzyme concentration (Ali *et al*, 1993). This has been interpreted as a consequence of monomer-dimer equilibrium. The ATP binds to the monomer followed by the dimerisation, only the dimer form can turn over ATP. This is followed by product release and the enzyme returning to a monomeric state. In this system dimerisation is the rate limiting step. The linear kinetics seen in the 52 kDa protein suggested three possibilities: (1) the 52 kDa protein is predominantly dimeric in solution, (2) that dimerisation was not occurring or (3) dimerisation was not a rate-limiting step in the reaction cycle. Evidence from cross linking studies showed dimers in the presence and the absence of the non-hydrolysable analogue ADPNP and in the presence of ADP and ATP suggest that the 52 kDa protein is predominantly a dimer in solution. This may suggest differences between the prokaryotic and eukaryotic enzymes.

The observation of DNA-dependent ATP hydrolysis was unexpected. The level of stimulation by DNA is 5-to 10-fold (6-fold as judged by k_{cat} comparisons) compares well to stimulation of full-length topo II α of ~10-fold (Hammonds and Maxwell, 1997). DNA stimulation of other type II enzymes this been shown to be in the 3- to 17- fold range, depending on the enzyme to DNA ratio. The K_M values in the absence and presence of DNA were found to be essentially the same (0.4-0.47 mM) whereas the k_{cat} values were 0.018 and 0.11 s⁻¹ in the absence and presence of DNA respectively. It is interesting to compare these values with those found for full-length topo II α : k_{cat} and K_M values of 2.17 s⁻¹ and 0.78 mM respectively at low DNA to enzyme ratios, and 0.59 s⁻¹ and 0.56 mM respectively at high enzyme to DNA ratio (Hammonds and Maxwell, 1997). Thus the K_M value for the ATPase domain of topo II α is in keeping with the values for the full-length enzyme and also with those for other type II topoisomerases such as DNA gyrase (0.21-0.45 mM; (Maxwell and Gellert, 1984). The k_{cat} values for

the ATPase domain are somewhat less than that for the full-length enzyme suggesting that binding of DNA at the DNA “gate” may be required for full DNA stimulation of the ATPase activity.

Figure 4.6 shows the stimulation of the ATPase activity of the 52 kDa protein as a function of DNA concentration. If it is assumed that the reaction velocity is directly proportional to the concentration of DNA-bound enzyme molecules then these data can be treated as a binding isotherm i.e. the concentration of DNA-bound enzyme is directly proportional to the rate of reaction. This yields an equilibrium dissociation constant (K_d) of 14.3 (+/- 2.5) μM . Although this binding constant is weak it is based on a DNA concentration in base pairs as we do not know the binding-site size for the ATP-operated clamp. If we were to assume that a 10 bp segment of DNA binds in the clamp, i.e. the DNA-binding site accommodates 10 bp (such a value would be consistent with the crystal structure of the N-terminal domain of GyrB (Wigley *et al*, 1991) then the K_d would be $\sim 1.4 \mu\text{M}$. However further experiments are required to establish the DNA-binding characteristics of this domain. These studies might include the limited proteolysis of the protein in the presence of DNA. Such a study would provide evidence for interactions between the protein and the DNA by showing any conformational changes in the enzyme in the presence of DNA. An investigation in to the minimum length of DNA needed to stimulate ATPase activity in the 52 kDa protein would provided an insight into the mechanism in which the protein and DNA interact e.g. a clamp like interaction might be expected to require a short length of DNA.

The 52 kDa fragment is clearly a target for protein kinase C (Wells *et al*, 1995) but phosphorylation [of the site at Ser 29] had no apparent effect on the ATPase activity of enzyme. This indicates that this site may have another role in the function of the full-length enzyme or any effect may only be apparent in the full-length enzyme.

Controls indicated that the increased rate in the presence of PKC was apparently due to ATP usage by PKC in the assay and not a result of modification of the 52 kDa protein. The affects of phosphorylation were further studied by mutational analysis, Chapter 5.

We have conclusively shown that the 52 kDa fragment is not a target for novobiocin. The protein does not bind to a novobiocin matrix and novobiocin has no apparent effect on ATP hydrolysis by the 52 kDa protein. Eukaryotic topo II inhibitors do not appear to have any direct effect on the DNA-dependent ATP hydrolysis rate of the 52 kDa fragment thus providing evidence for an indirect inhibition of ATPase function in the full-length enzyme i.e. the drugs are interacting elsewhere (outside the 52 kDa domain) on the full-length enzyme and these interactions are leading to the loss of ATPase activity as a secondary effect.

It must be noted that a persistent problem encountered during this project was the lack of consistent rates between different preparations of the 52 kDa protein. This can be seen by a comparison between the data seen in figure 4.6 and that seen in figure 4.8. In figure 4.6 at 2mM ATP 600nM protein shows a DNA-stimulated rate of 10 nM sec⁻¹. In figure 4.8, under the same conditions, 80nM protein shows a DNA-stimulated rate of 5.4 nM sec⁻¹. The second batch of protein had therefore approximately 4 fold greater ATPase activity. This made direct comparisons between batches of enzyme difficult. It is however possible to examine general trends in the activity of the enzyme. The differences seen between batches of protein are possibly the result of differences in re-folding efficiency during preparation.

CHAPTER FIVE

IDENTIFICATION OF THE ACTIVE SITE-RESIDUE OF THE 52 kDa N-TERMINAL FRAGMENT OF HUMAN TOPO II α .

5.1 INTRODUCTION.

It was decided to follow the characterisation of the hydrolysis of ATP by the 52 kDa fragment by using site-directed mutagenesis to examine the catalytic residue involved in this reaction. Previous work on the related 43 kDa domain of DNA gyrase had identified Glu 42 as the catalytic residue in the ATPase reaction (Jackson and Maxwell, 1993) in that enzyme. A second conserved residue, His 38, is thought to mediate the action of Glu 42 through hydrogen bonding. As the amino acid sequences in this region are conserved between the type II topoisomerases, figure 5.1, it was possible to postulate that Glu 86 in human topo II α might be the corresponding catalytic base. In order to verify this proposal it was suggested that site-directed mutagenesis of the Glu 86 residue be performed. We decided to attempt to mutate Glu 86 to Ala and Asp. The reason for the creation of these mutants was that the proposed mechanism of ATP hydrolysis for the 43 kDa domain of gyrase suggests that an Ala mutant would be completely inactive whereas the Asp mutant's charge would allow some limited hydrolysis to take place (Jackson and Maxwell, 1993). In addition following the results of our analysis of the phosphorylation of the 52 kDa fragment we decided to extend the mutagenesis study to generate two mutants of Ser 29. This residue had been shown to be phosphorylated in the full-length enzyme (Wells *et al*, 1995). This residue would be

changed to an Ala or an Asp. The choice of these residues reflects that the lack of charge in the Ala mutant would mimic the non-phosphorylated state of the enzyme and the charge on the Asp mutant could mimic the phosphorylated state of the enzyme.

5.1.1 Quikchange™ site directed mutagenesis

The Quikchange mutagenesis method is performed by preparing a double-stranded plasmid template containing the insert of interest. Two oligonucleotide primers complementary to opposite strands of the template vector are synthesized containing the desired mutation. By means of temperature cycling the primers can be extended using *Pfu* DNA polymerase, a high fidelity DNA polymerase. This process creates a mutated plasmid that contains two staggered nicks. Following this process the sample is treated with *Dpn* I. *Dpn* I is a DNA endonuclease that is specific for methylated and hemimethylated DNA and thus digests the template DNA, effectively leading to the selection of only mutated DNA. The nicked mutated plasmid DNA can then be transformed into *E. coli* where the nicks will be repaired leading to the production of whole plasmid containing the desired mutation. A diagrammatic view of this process is seen in figure 5.2.

5.1.2 Designing the mutagenic oligonucleotides.

When designing the mutagenic oligonucleotides to be used with the Quikchange protocol several general features must be taken into account. The mutagenic oligonucleotides must be complementary annealing to the same site on opposite strands of the template plasmid. The oligonucleotides must be between 25 and 45 base pairs in length and the melting temperature (T_m) of the oligonucleotides must be ~10°C above the

Figure 5.1

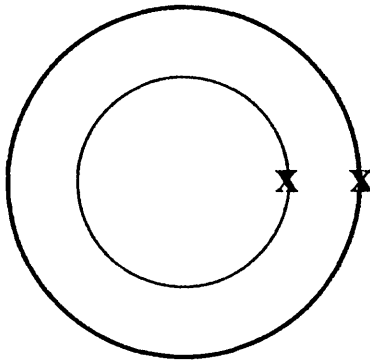
<i>E. coli</i> GyrB	G ₃₅	L	H	H	M	V	F	E	V	V	D	N	A	I	D ₄₉
<i>P. putida</i> GyrB	G ₃₇	L	H	H	M	V	F	E	V	V	D	N	S	I	D ₅₁
<i>N. gonorrhoeae</i> GyrB	G ₃₉	L	H	H	M	V	F	E	V	L	D	N	A	I	D ₅₃
<i>B. subtilis</i> GyrB	G ₃₆	L	H	H	L	V	W	E	I	V	D	N	S	I	D ₅₀
<i>Pr. mirabilis</i> GyrB	G ₃₅	L	H	H	M	V	F	E	V	V	D	N	A	I	D ₄₉
<i>S. aureus</i> GyrB	E ₄₂	L	H	I	S	V	.	E	I	V	D	N	S	I	D ₅₆
<i>Haloferax</i> GyrB	G ₃₆	L	H	H	L	V	Y	E	V	V	D	N	S	I	D ₅₀
<i>M. pneumoniae</i> GyrB	G ₃₉	L	H	H	M	I	W	E	I	I	D	N	S	I	D ₅₃
<i>E. coli</i> ParE	R ₃₁	P	N	H	L	G	Q	E	V	I	D	N	S	V	D ₄₅
bacteriophage T4 gp 39	G ₄₇	L	V	K	L	I	D	E	I	I	D	N	S	V	D ₆₁
bacteriophage T2 gp 39	G ₄₇	L	V	K	L	I	D	E	I	I	D	N	S	V	D ₆₁
<i>H. sapiens</i> Top II α	G ₇₉	L	Y	K	I	F	D	E	I	L	V	N	A	A	D ₉₃
<i>H. sapiens</i> Top II β	G ₇₉	L	Y	K	I	F	D	E	I	L	V	N	A	A	D ₉₃
<i>D. melanogaster</i> Top II α	G ₆₀	L	Y	K	I	F	D	E	I	L	V	N	A	A	D ₇₄
<i>Sa. cerevisiae</i> Top II α	G ₅₈	L	F	K	I	F	D	E	I	L	V	N	A	A	D ₇₂
<i>Sc. pombe</i> Top II α	G ₇₀	L	Y	K	I	F	D	E	I	I	V	N	A	A	D ₈₄
<i>T. brucei</i> Top II α	G ₅₃	L	L	K	I	V	D	E	I	L	L	N	A	S	D ₆₇
<i>C. fasciculata</i> Top II α	G ₅₃	L	L	K	I	V	D	E	I	L	L	N	A	A	D ₆₇

The above figure shows the sequence alignment of several type II topoisomerases. As can be clearly seen there is a considerable degree of homology between them in this region. Experiments on the 43 kDa fragment of *E. coli* GyrB has provided good evidence that Glu 42 acts as the catalytic base during the ATPase reaction of that enzyme. This evidence suggests that Glu 86 would fulfill a similar role in human topoisomerase II α . There is evidence that His 38 in *E. coli* GyrB is important, it has been suggested that a hydrogen bond formed by this residue to Glu42 allows Glu 42 to act as a general base. A similarly charged amino acid (Lys 82) is found in the human sequence.

Figure 5.2 Mutagenesis strategy.

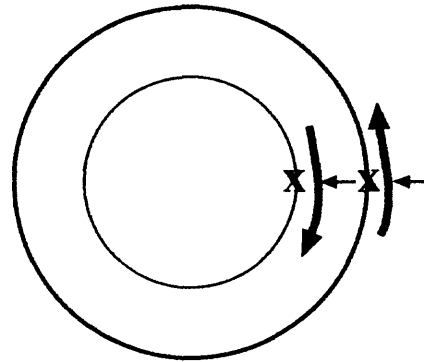
Step 1

Template plasmid, (x) shows target site for mutation.



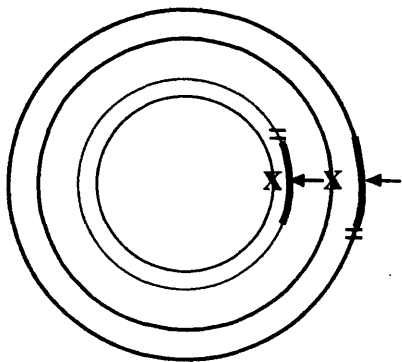
Step 2

The plasmid is denatured and mutagenic primers anneal containing the desired mutation (←).



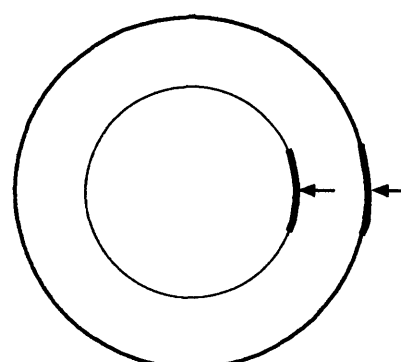
Step 3

Using *Pfu* DNA polymerase the primers are extended to form nicked (=) circular strands incorporating the mutations.



Step 4

The non-mutated methylated parental DNA is digested away with *DpnI*. This results in double stranded nicked plasmid incorporating the mutation of interest.



extension temperature of 68°C. The T_m of the oligonucleotides can be estimated using the following formula:

$$T_m = (2^\circ\text{C})(A+T) + (4^\circ\text{C})(G+C)$$

The mutation desired must have 10 to 15 base pairs of flanking sequence to ensure good annealing. It is preferable to have a GC content that is at a minimum 40% of the oligo sequence and the oligo should end in a G or C. In addition to fulfilling these conditions it was considered sensible to introduce two mutations, one that would lead to the point mutation when incorporated into the sequence and one that although silent, i.e. introducing no amino acid change, would lead to the removal of a restriction site within the plasmid. This could then be used in a restriction analysis experiment to screen for mutagenic plasmids. The oligonucleotides used in these experiments are seen in figure 5.3.

5.1.3 PCR conditions for the oligonucleotide extension.

It was important to ensure that oligonucleotides to be used in the extension are kept in excess over the template DNA. The basic PCR protocol for these mutagenesis experiments is seen in table 5.1

Table 5.1 Condition for oligonucleotide extension.

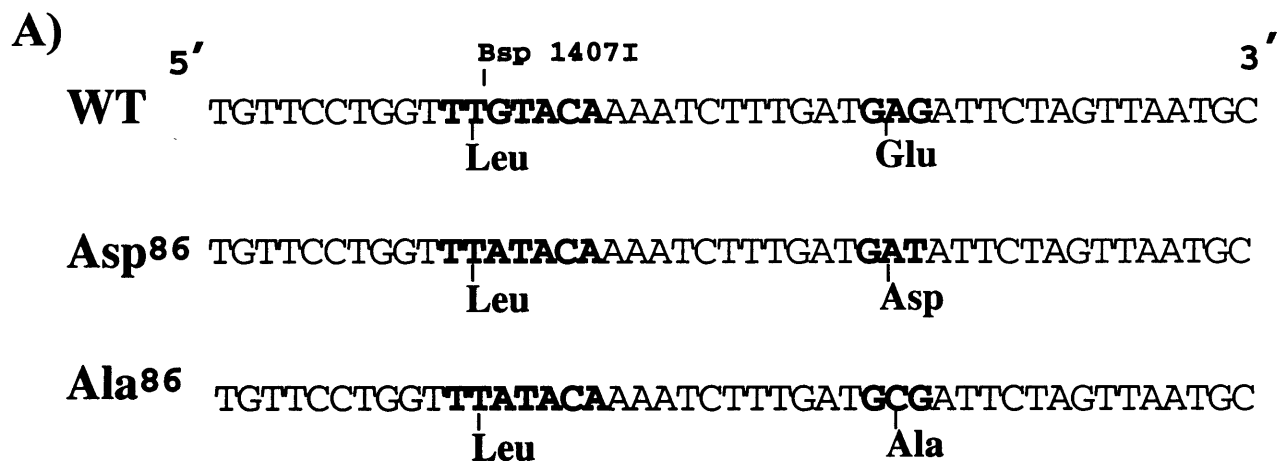
Segment	Cycles	Temperature	Time	Comment
1	1	95°C	30 seconds	To melt oligo and template DNA.
2	10-16	95°C	30 seconds	Re-melting following extension.
		55°C	1 minute	Annealing oligo to template.
		68°C	2 minute per kb of plasmid	Extension of the mutagenic oligo.

The template plasmid that was used in these extensions was 6.7 kb so the extension time used was 14 minutes. For the nucleotide changes we were hoping to introduce to the plasmid we repeated the PCR cycle 16 times.

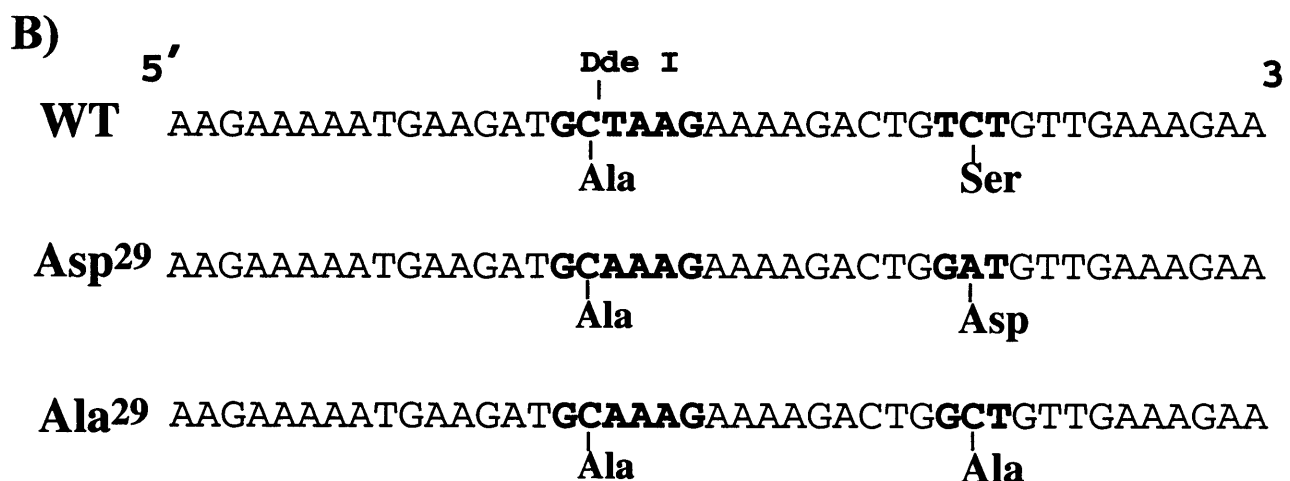
5.2 ANALYSIS OF THE MUTATED PLASMIDS.

As has been mentioned before, the mutated plasmids should contain both the mutation of interest and a silent mutation that deleted a restriction site in the template DNA. Following transformation of the PCR products, the plasmid was prepared. The next step was to cut the plasmid with the appropriate restriction enzyme, i.e. the one for which a site has been deleted in the mutant plasmid, then by analysing the resulting fragments of DNA it is possible to tentatively identify the plasmids of interest. Figure 5.4 shows the result of the restriction analysis of the first set of mutated plasmids. In these plasmids containing a mutation at position 86, a *Bsp* 1407I restriction site had been removed. This site is unique in the plasmid sequence leading to linearisation of the wild-type plasmid. Therefore cleavage is a clear indication that the mutation strategy has not been successful. Figure 5.5 shows the plasmids containing a mutation at position 29, a *Dde* I site was removed, this site was not unique but gave rise to a detectable difference in the restriction pattern in the mutated plasmid. In plasmids with the *Dde* I site removed the largest fragment will be 1.6 Kb other wise it will be approximately 1000 bp. By the selection of those plasmids that had given rise to the expected restriction pattern for the incorporation of mutations we were better able to select likely candidates for DNA sequencing.

Figure 5.3

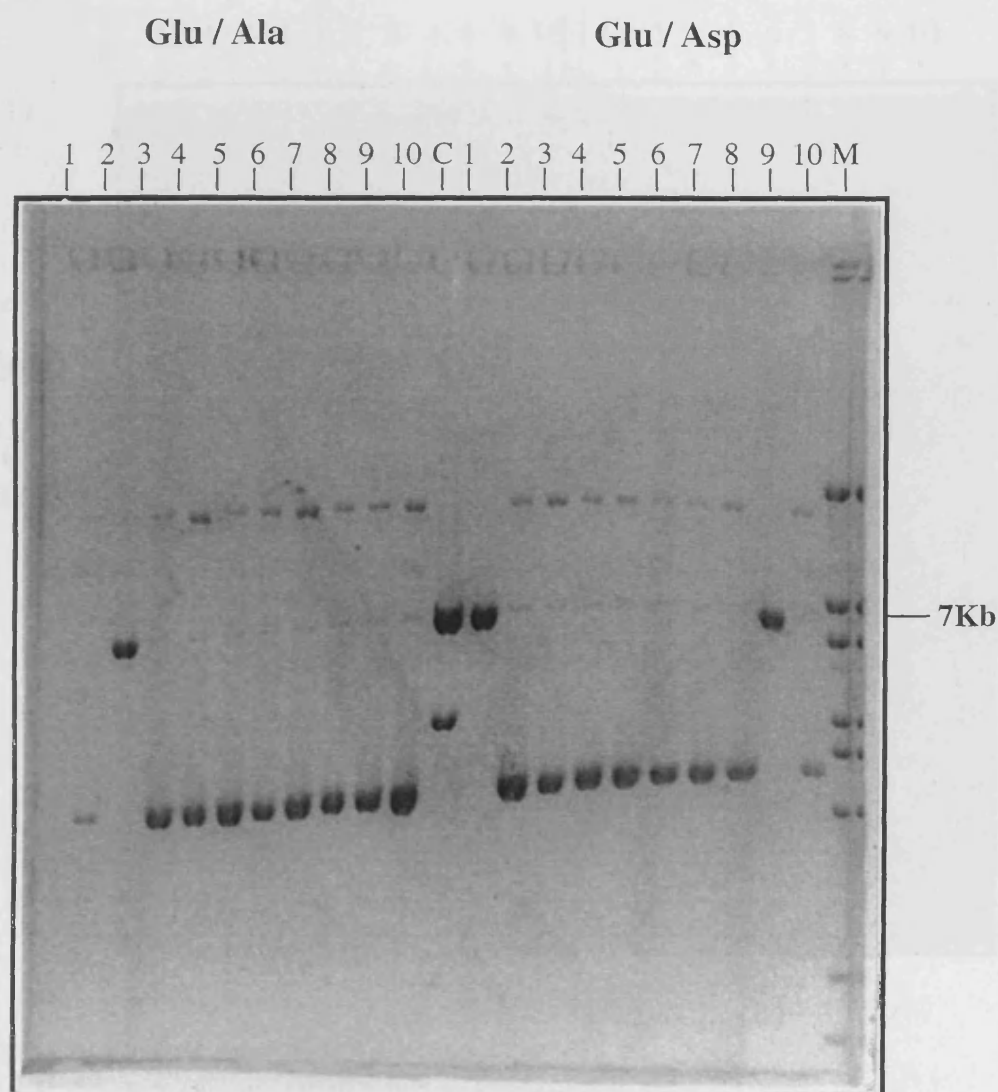


The sequences seen above represent the oligos generated to introduce point mutations at position 86, the putative catalytic base in human topo II α . The top sequence (WT) is the original DNA sequence from the wild type protein in this region. The centre sequence (Asp⁸⁶) is the oligo for the Glu-Asp mutation incorporating a silent mutation removing a *Bsp* 1407I restriction site. The lower sequence (Ala⁸⁶) is the oligo for the Glu-Ala mutant.



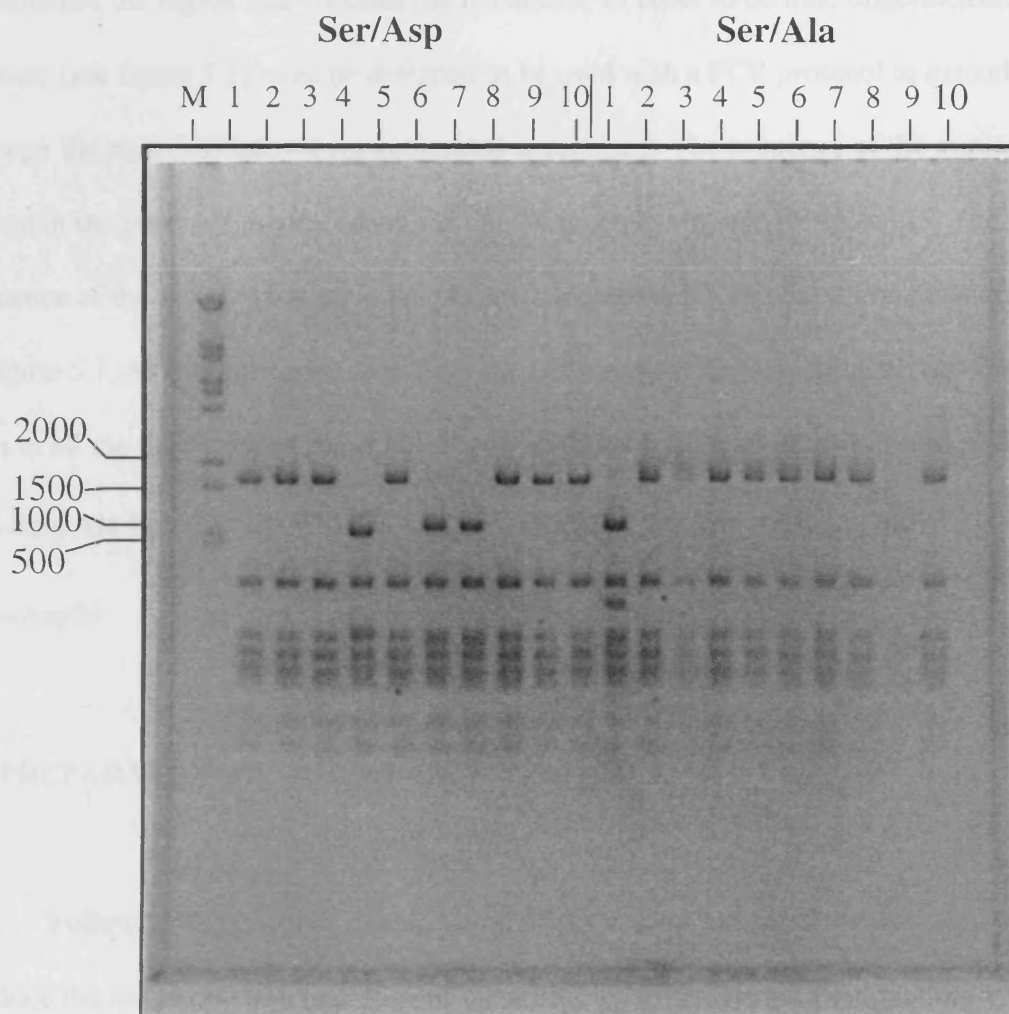
The sequences seen above represent the oligos generated to introduce point mutations at position 29, the putative phosphorylation site. The top sequence (WT) is the original DNA sequence from the wild type protein in this region. The oligos Asp²⁹ and Ala²⁹ represent sequences designed to introduce point mutations for Ser-Asp and Ser-Ala respectively at position 29. Both of the mutant oligos once again have an additional silent mutation that will abolish the *Dde* I site.

Figure 5.4 Restriction analysis of plasmids containing a mutation at position 86.



The above gel shows the result of a restriction analysis of plasmids containing a mutation at position 86. The removal of a unique restriction site in plasmids incorporating this mutation will result in a failure to linearise on incubation with the restriction enzyme.

Figure 5.5 Restriction analysis of plasmids mutated at position 29



The above gel shows the result of the restriction analysis of the plasmids containing a mutation at position 29. Successful mutation will result in the removal of a *Dde* I restriction site. On restriction with this enzyme the plasmids incorporating the mutation will yield a largest fragment of 1.6 Kb. Those that have failed to incorporate the mutation will yield a fragment of 1000 bp. All samples are run on a 1% agarose gel.

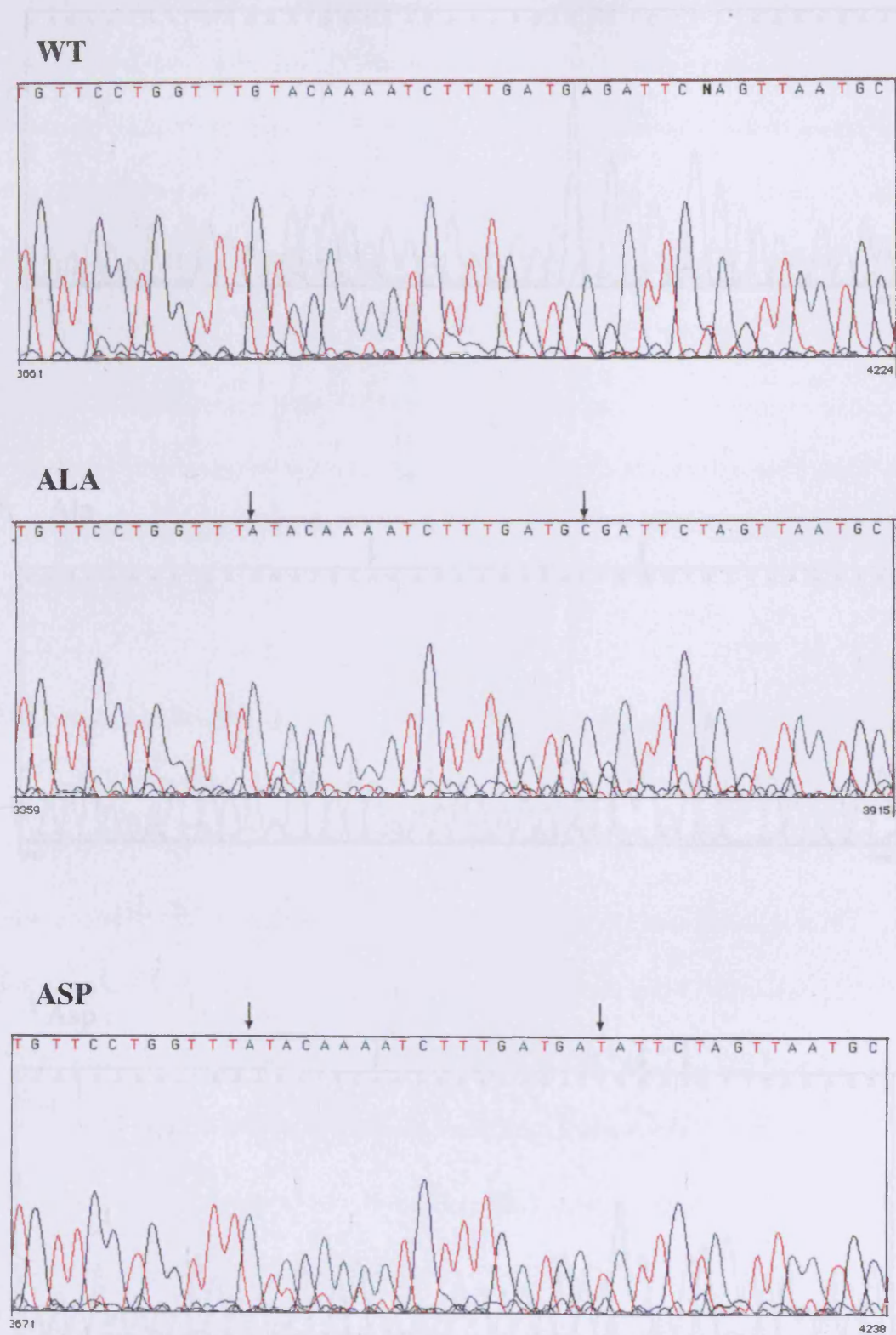
5.2.1 DNA sequencing.

Following the putative identification of the mutated plasmids, the next step was to sequence the region that contains the mutations. In order to do this, oligonucleotide primers (see figure 5.3) must be designed to be used with a PCR protocol to extend through the region of interest for automated sequencing. The sequence of the mutated region in the plasmids incorporating the Glu 86 mutants are seen in figure 5.6. The sequence of the mutated region in the plasmids incorporating the Ser 29 mutants are seen in figure 5.7. As can be clearly seen from the DNA sequencing the correct mutations are seen in all the four mutated plasmids. These plasmids were named as followed pLPG1= Glu 86→Ala 86, pLPG2= Glu 86→Asp 86, pLPG3 = Ser 29 →Ala 29 and pLPG4=Ser 29→Asp29.

5.3 PREPARATION OF THE MUTATED PROTEIN.

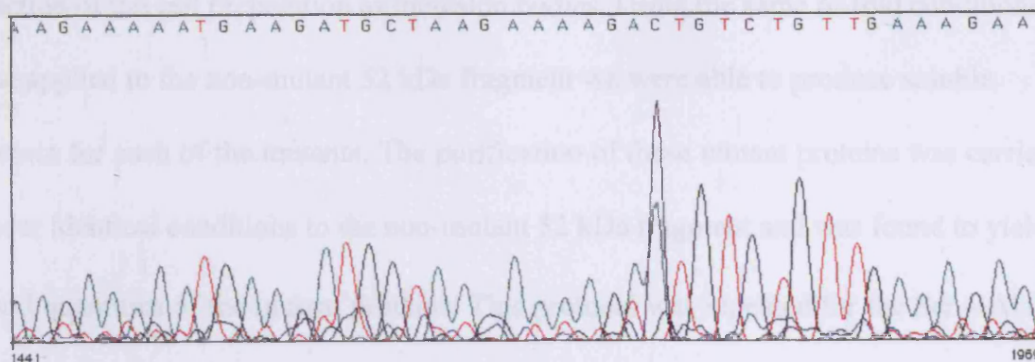
Following the positive identification of the mutant plasmids the next step was to produce the mutant protein in sufficient quantities for experimental examination. We decided to work on the Glu 86 mutants in the first instance. To achieve this the expression strain (B834(DE3)pLysS) was transformed using plasmids pLPG1 and pLPG2. The production of these proteins was examined using standard trial induction conditions developed for the 52 kDa fragment (10 ml of NB broth inoculated with 200 µl of an overnight culture were induced at (OD₅₆₀)=0.5 with 50 µM IPTG grown for a further 3 hours then harvested by centrifugation). Both mutant proteins were produced in good quantities under the same induction conditions used for the production of the 52 kDa fragment. Both proteins were found to be almost exclusively in the insoluble

Figure 5.6 Sequence of Glu 86 mutations

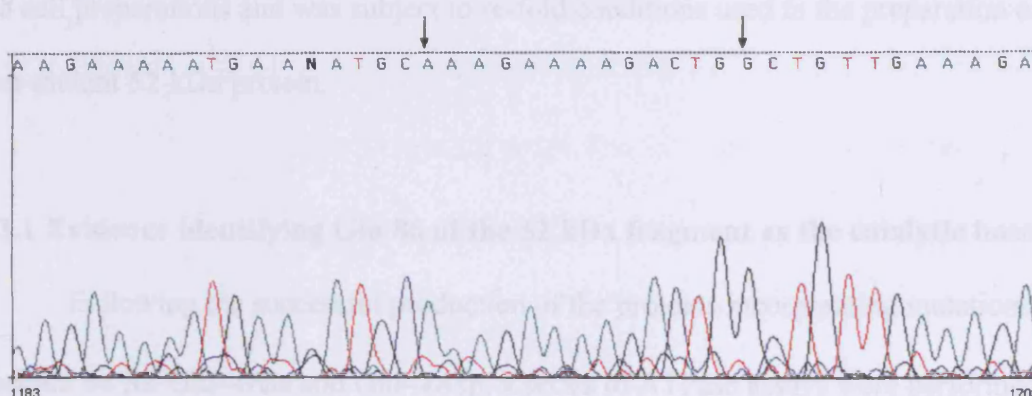


The above figures show the chromatograms and associated sequence for the mutated region containing Glu 86. The wild-type sequence is shown in the top panel, the two mutants are shown in the lower panels. The arrows show the incorporation of point mutations. Approximately 800 bases of sequence were returned. This sequence was checked for random mutations and none were found.

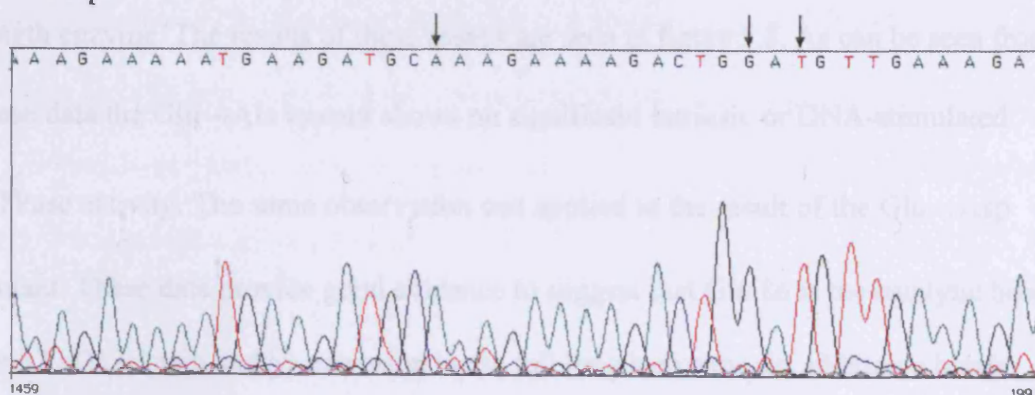
WT



Ala



Asp



The above panels show the chromatograms resulting from the sequencing of the region of the plasmid coding for Ser 29. The first panel shows the sequencing of the wild type protein. The following panels show the sequence of the Ala and Asp mutants respectively. This data confirms that the mutagenesis has been successful. The arrows indicate the positions of the point mutations.

fraction of the cell preparation as inclusion bodies. Using the same re-fold conditions that applied to the non-mutant 52 kDa fragment we were able to produce soluble protein for each of the mutants. The purification of these mutant proteins was carried under identical conditions to the non-mutant 52 kDa fragment and was found to yield good quantities of the mutant proteins. This protocol was repeated for the Ser→Ala and Ser→Asp mutations using the plasmids pLPG3 and pLPG4. Once again the protein was produced in sufficient quantities for experimental examination. The protein resulting from these clones was once again found almost exclusively in the insoluble fraction of the cell preparations and was subject to re-fold conditions used in the preparation of the non-mutant 52 kDa protein.

5.3.1 Evidence identifying Glu 86 of the 52 kDa fragment as the catalytic base.

Following the successful production of the proteins incorporating mutations at position 86 for Glu→Ala and Glu→Asp, a series of ATPase assays were performed in order to examine the suggestion that Glu 86 was the catalytic base involved in the ATPase reaction of the 52 kDa fragment of human topo II α and by extension in the full length enzyme. The results of these assays are seen in figure 5.8. As can be seen from these data the Glu→Ala mutant shows no significant intrinsic or DNA-stimulated ATPase activity. The same observation can be applied to the result of the Glu→Asp mutant. These data provide good evidence to suggest that Glu 86 is the catalytic base in the 52 kDa protein and by extension in the full length enzyme. In addition a blank preparation was conducted, cells were grown in the normal way but the protein was not induced. This preparation was then processed identically to the preparations containing recombinant protein and the resulting fractions assayed. None of these fractions showed

any ATPase activity. This indicates that all ATPase activity seen was due to the presence of the recombinant proteins. This experiment provided an effective control for background ATPase rates.

5.3.2 Evidence that phosphorylation at Ser 29 has no direct effect on the rate of ATP hydrolysis of the 52 kDa fragment.

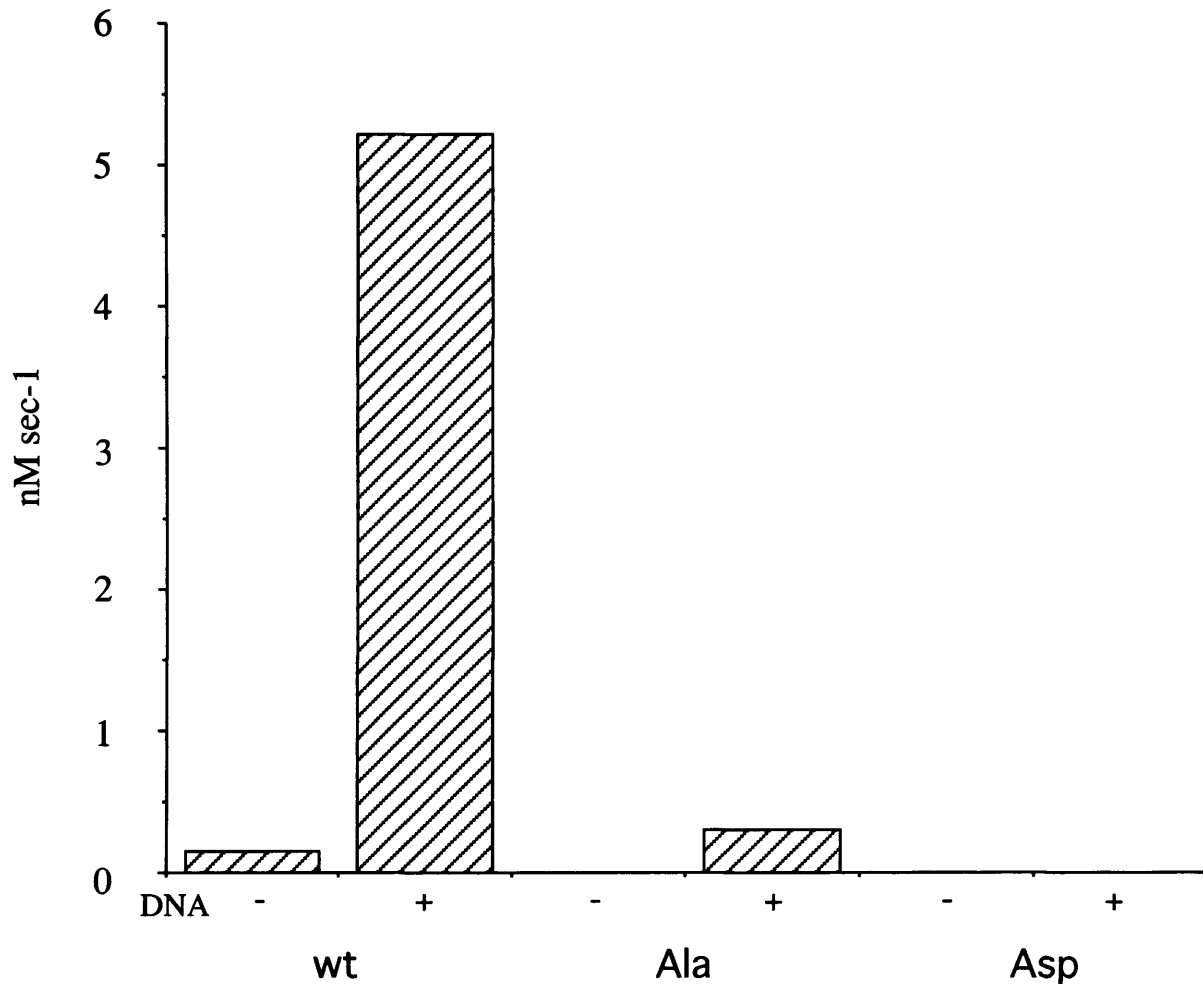
Following the successful production of recombinant protein incorporating the two mutations at position, 29 Ser→Ala and Ser→Asp, a series of assays were performed to examine the affect of mutating this phosphorylation site. These data are seen in figure 5.9. These data suggest that neither mutation has affected the DNA-dependent ATPase rate of the 52 kDa fragment. The Ser→Ala mutation effectively produces a protein that can not be phosphorylated. The observation that this protein has a rate that is approximately the same as the wild type protein, prepared in parallel, suggest that it is not being affected by phosphorylation at position 29 in vivo, perhaps by a contaminating kinase.

The Ser→Asp mutant may mimic the effect of phosphorylation on the 52 kDa protein at position 29. The observation that this protein is little different in terms of its ATPase activity compared to wild type protein suggest that either the ATPase activity of the protein is unaffected by phosphorylation at this site or that an aspartate residue fails to imitate phosphorylation at position 29.

5.4 DISCUSSION.

The observation that the N-terminal fragment of human topo II α , represented by the 52 kDa protein was an active ATPase having both an intrinsic and DNA-

Figure 5.8 Result of point mutations at position Glu 86 on ATPase activity

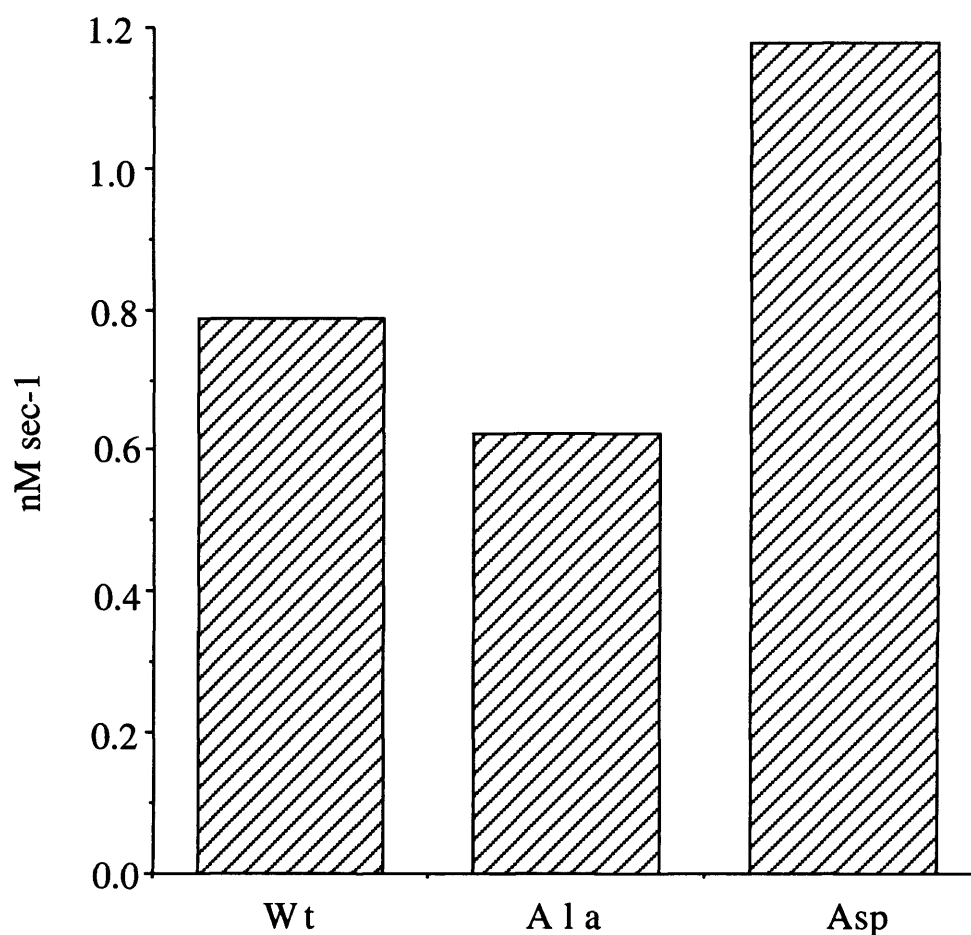


The above figure shows the results of the ATPase assays run using the two Glu 86 mutants of the 52 kDa N-terminal fragment. As is clearly seen both of the mutated proteins have significantly reduced ATPase, both intrinsic and DNA dependent in comparison to the wild-type protein. The concentration of protein used in this assay was 0.78 μ M. Overall these data provide good evidence in support of the suggestion that Glu 86 is an essential residue in the in the hydrolysis of ATP.

stimulated ATPase activity allow us the opportunity to examine the catalytic site in this enzyme, and by extension the full length enzyme, in greater detail. The reasoning behind this was two fold : a) to confirm the identity of the catalytic base as Glu 86 as suggested by the sequence alignments and, b) mutations that disable the catalytic function of the enzyme would further rule out the possibility of the observed ATPase rates being the result of a unknown contaminant. The two mutants of the Glu 86 residue provided good evidence that Glu 86 does have an important role in the hydrolysis of ATP by human topo II α possibly by acting as a catalytic base. This would seem to provide evidence that the mechanism suggested for DNA gyrase (Jackson and Maxwell, 1993) supported by amino acid sequence alignment, can be extended as the general mechanism for ATP hydrolysis in type II topoisomerases. In the absence of any specific inhibitor of the ATPase activity of human topo II the ability to abolish the ATPase activity of this fragment by mutation strongly suggests the observed activity is due to the 52 kDa fragment and not an unknown contaminant.

The mutation of the Ser 29 residue was to provide additional evidence for the previous observation that phosphorylation had no discernible affect on ATPase rate. The assays that were performed using these mutants provided evidence that the previous observations regarding the phosphorylation of Ser 29 were correct (section 4.7). Neither mutant showed any significant alteration in ATPase rate compared to wild type protein prepared in parallel. It was possible that the native protein prepared from *E.coli* could be phosphorylated at position 29 in vivo. The protein containing the Ser→Ala mutation effectively provides a control for this possibility. As both the Ser→Ala and the Ser→Asp mutants do not effect the ATPase activity of the 52 kDa protein it can be said that Ser 29 is not a vital residue in the ATPase activity of this

Figure 5.9 Result of point mutations at position Ser 29 on ATPase activity



The above figure shows the results of ATPase assays that were conducted using the two Ser mutations of the 52 kDa protein. The concentration of the proteins used in this assay was 0.25 μ M. As can be clearly seen for both mutations there was very little effect on the overall rate of the enzyme.

enzyme. The role of phosphorylation of this site in the context of the full -length enzyme is still a matter of speculation. There is clearly scope for moving these mutations into the full length enzyme to examine their effect.

CHAPTER 6

DISCUSSION

6.1 Production and purification of 52 kDa protein.

The object of the first part of this project was to produce and purify protein representing the N-terminal domain of human topo II α . Amino acid alignment suggested that this domain could be responsible for the binding and hydrolysis of ATP in the full length enzyme. After initial difficulties with protein production it was found that the protein produced from our chosen clone was almost exclusively in the insoluble fraction of the cell preparation, this was possibly the result of expressing a fragment of a eukaryotic protein in prokaryotic expression system. All attempts to produce soluble protein directly failed. We were therefore forced to address the problems associated with developing a reliable protocol for re-folding the protein from inclusion bodies prior to purification.

Following the development of a successful re-fold protocol we attempted to purify the protein on a Mono SP column; this choice reflected the pI (isoelectric point) of the enzyme which had been predicted to be 9.3. This would suggest a very basic protein so a strong cation exchanger was used. These attempts failed, the protein becoming irreversibly bound to the column. The reason for this was probably due to the limited solubility of the recombinant protein. As the protein bound to the column the local concentration rose to beyond that which could remain in solution, this would result in the protein precipitating out of solution. This explanation matches our observation of apparently irreversible binding to the Mono SP column often followed by an increase in

back pressure, typical of the column becoming blocked. This explanation is also supported by observations made during our attempts to concentrate soluble re-folded protein, these attempts also resulted in a loss of protein as it precipitated from solution.

The use of protein that incorporated a His tag allowed the purification of the protein under denaturing conditions on a Ni^{2+} column. Purification of the protein under denaturing conditions overcame problems associated with the low solubility of the protein and the Ni^{2+} matrix provided a single step purification strategy.

The protein could be re-folded following purification to generate purified soluble protein. Protein purified this way proved to be inactive, this was found to be due to the leeching of Ni^{2+} ions which effectively inhibited the ATPase activity. This inhibition was also seen with the full-length enzyme (personal communication from Tim Hammonds, this lab). This inhibition may be due to the interactions between the Ni^{2+} ions and the Mg^{2+} -binding site on the enzyme. Once the Ni^{2+} metal affinity column was replaced with a cobalt affinity column, the problems of inhibition due to metal leaching were overcome.

It must be noted that a persistent problem encountered during this project was the lack of consistent rates between different preparations of the 52 kDa protein. This can be seen by a direct comparison between the preparations of proteins used in the studies of the DNA-dependent ATPase activity. In the preparation in which the DNA-dependent rate was first observed (Chapter 4, section 4.2.3, figure 4.6) 600 nM enzyme gave a maximum rate of 10 nM sec^{-1} ; in the subsequent preparation of 52 kDa protein, 80 nM enzyme in the same conditions gave a maximum rate of 5.4 nM sec^{-1} (Chapter 4, section 4.3.2., figure 4.8). This indicates that the second batch of protein has a DNA-dependent rate that is ~ 4 fold faster than the initial batch.

These differences made direct comparisons between batches of enzyme difficult. Efforts to minimise these differences included preparing protein in parallel where direct comparisons were necessary, e.g. when preparing the mutant proteins (Chapter 5) wild type protein was prepared and re-folded in parallel with the mutant protein preparations to minimise the differences. In spite of these variations it is possible to examine general trends in the activity of the enzyme. The differences seen between batches of protein are possibly the result of differences in re-folding efficiency during preparation. The low rate of ATPase activity seen when examining the intrinsic rate of the enzyme often meant that a large volume of protein solution had to be added to the total assay volume, typically 40 μ l in 200 μ l. At volumes above 60 μ l the assay becomes unreliable, this is possibly due to glycerol in the assay in the buffer. This effectively imposes a limit on the concentration of protein that can be successfully assayed.

Overall the protein proved difficult to work with, presenting challenges in terms of successful expression, in producing a purification protocol and in the generation of active protein.

6.2 OPTIMISATION OF CONDITIONS FOR ATPase ACTIVITY.

In summary it can be said that the optimal reaction conditions for the ATPase of the 52 kDa N-terminal fragment of human topo II α are broadly similar to those for the full-length enzyme, i.e. 50 mM Tris.HCl (pH 7.5), 100 mM KCl, 0.5 mM EDTA and 1 mM DTT (Hammonds and Maxwell, 1997). The observation that the intrinsic rate shows a preference for [Mg²⁺] in the range equi-molar with [ATP] to double [ATP]

might suggest that free Mg^{2+} may compete for the binding site on the enzyme with the Mg-ATP complex. This apparent sensitivity to $[\text{Mg}^{2+}]$ may account for the enzymes inhibition by Ni^{2+} during preparation (Chapter 3, section 3.3.5). It is possible that the Ni^{2+} ions are competing for binding with Mg^{2+} binding site on the enzyme. The linear dependence of both the DNA-dependent and intrinsic rates of ATP hydrolysis on enzyme concentration suggested that the protein may be a dimer in solution. Further evidence for the presence of dimer was provided by the results of cross-linking experiments suggesting that the enzyme exists predominantly as a dimer. In these experiments it was shown that DMS, an agent that cross-links lysine residues, was shown to be able cross-link 52 kDa protein in the presence and absence of nucleotide. This provides evidence for the view that the 52 kDa protein does not require the binding of nucleotide to dimerise. This observation is in contrast to the equivalent fragment of the prokaryotic enzyme gyrase, 43 kDa protein, this has been shown to be predominantly a monomer in solution, dimerising in the presence of ATP (Ali et al, 1993) and having non-linear kinetics. These difference may reflect a difference between the two clones e.g. the additional C-terminal amino acids in the 52 kDa protein making contacts that allow the formation of a dimer in the absence of nucleotide. This explanation is unlikely, it has been seen recently that two new constructs encompassing the 52 kDa protein also fail to show non linear kinetics (Spencer Campbell, personal communication). These observations may therefore reflect real differences between these two enzymes.

6.3 ANALYSIS OF THE DNA -DEPENDENT ATPase ACTIVITY OF THE 52 kDa FRAGMENT.

The observation of DNA-dependent ATP hydrolysis was unexpected (Chapter 4, section 4.2.3). The level of stimulation by DNA in the 52 kDa fragment is 5- to 10-fold (6-fold as judged by k_{cat} comparisons), and compares well to stimulation of full-length topo II α of 10-fold depending on enzyme to DNA ratio (Hammonds and Maxwell, 1997). DNA stimulation of other type II enzymes has been shown to be in the 3- to 17- fold range. The K_M values in the absence and presence of DNA were found to be essentially the same (0.4-0.47 mM) whereas the k_{cat} values were 0.018 and 0.11 s⁻¹ in the absence and presence of DNA respectively. It is interesting to compare these values with those found for full-length topo II α : k_{cat} and K_M values of 2.17 s⁻¹ and 0.78 mM respectively at low DNA to enzyme ratios, and 0.59 s⁻¹ and 0.56 mM respectively at high enzyme to DNA ratio (Hammonds and Maxwell, 1997). Thus the K_M value for the ATPase domain of topo II α is in keeping with the values for the full-length enzyme and also with those for other type II topoisomerases such as DNA gyrase (0.21-0.45 mM); (Maxwell and Gellert, 1984). The k_{cat} values for the ATPase domain are somewhat less than that for the full-length enzyme suggesting that binding of DNA at the DNA “gate” may be required for full DNA stimulation of the ATPase activity. If it is accepted that the 52 kDa fragment is acting as an ATP operated clamp then it can be assumed that the protein’s interactions with the DNA mimic the binding of the T segment in the full length enzyme. Clearly this would indicate a substantial role in the stimulation of ATPase activity by the binding of the T segment. Mechanistically this would lead to a model where the ATPase activity of the full length enzyme is coupled directly to strand passage by an ATP-operated, DNA-stimulated clamp.

The equilibrium dissociation constant (K_d) calculated from the ATPase activity of the 52 kDa protein as a function of DNA concentration has a value of 14.3 (+/- 2.5) μ M. Although this binding constant is weak it is based on a DNA concentration in base pairs as we do not know the binding-site size for the ATP-operated clamp. If we were to assume that a 10 bp segment of DNA binds in the clamp, i.e. the DNA-binding site accommodates 10 bp (such a value would be consistent with the crystal structure of the N-terminal domain of GyrB (Wigley *et al*, 1991), then the K_d would be $\sim 1.4 \mu$ M.

Although this suggests a weak interaction between the protein and the DNA this is perhaps not surprising. The role of the ATP operated clamp suggested by the current model would involve only a transitory contact with DNA. If the protein bound the DNA too strongly then the T segment might be unable to leave the clamp. The value that we have calculated is based on an assumption on the length of DNA it can interact with and it is possible that in the full length enzyme the binding characteristics may be significantly different. However further experiments are required to establish the DNA-binding characteristics of this domain.

6.4 EFFECTS OF PHOSPHORYLATION ON THE ATPase ACTIVITY OF THE 52 kDa FRAGMENT.

The 52 kDa fragment is clearly a target for protein kinase C (Wells *et al*, 1995). Our studies on the 52 kDa fragment showed that the enzyme was phosphorylated in the presence of protein kinase C but phosphorylation of the site at Ser 29 had no apparent effect on the ATPase activity of the enzyme. This indicates that this site may have another role in the function of the full-length enzyme or that the effect on the ATPase activity may only be apparent in the context of the full-length enzyme.

The experiments previously described (Chapter 4, section 4.7) were unable to show directly that the enzyme used in the ATPase assay had been phosphorylated. Given the possible significance of this site a second study using site directed mutagenesis was performed in an attempt to clarify the significance of these results.

6.4 EFFECTS OF DRUGS ON THE ATPase ACTIVITY OF THE 52 kDa FRAGMENT.

We have conclusively shown that the 52 kDa fragment is not a target for novobiocin. The protein shows no affinity for a novobiocin bound matrix and the drug has no effect on the ATPase activity of the enzyme (Chapter 4, section 4.6). This is in contrast to previous reports of an eukaryotic topo II, *Drosophila* topo II, showing inhibition by novobiocin (Robinson *et al*, 1993). These differences may reflect differences between the *Drosophila* and the human enzymes. Eukaryotic topo II inhibitors do not appear to have any direct effect on the DNA-dependent ATP hydrolysis rate of the 52 kDa fragment thus providing evidence for an indirect inhibition of ATPase function in the full-length enzyme, i.e. the drugs are interacting elsewhere (outside the 52 kDa domain) on the full-length enzyme and these interactions are leading to the loss of ATPase activity as a secondary effect. The observation that a non-specific DNA intercalator, ethidium bromide, was able to reduce the rate of DNA-dependent ATP hydrolysis may suggest one of the methods of indirect inhibition. Drugs such as m-AMSA which are known to be DNA intercalators can lead to distortion of the DNA molecule in such a way that the DNA stimulation of the ATPase rate is reduced. We believe this accounts for the reduced rate seen with m-AMSA in our study. In the context of the full length enzyme this situation is more complex, the binding of the G

segment and the breakage and re-union reactions being affected by the binding of drug.

The successful dissection of the domain responsible for ATP hydrolysis is able to provide a more simple system in which such indirect effects can be demonstrated.

6.5 MUTATIONAL ANALYSIS OF THE 52 kDa PROTEIN.

The observation that the N-terminal fragment of human topo II α , represented by the 52 kDa protein, was an active ATPase having both an intrinsic and DNA-stimulated ATPase activity allowed us the opportunity to examine the catalytic site in this enzyme, and by extension the full length enzyme. The rationale behind this was two fold : a) to confirm the identity of the catalytic base as Glu 86 as suggested by sequence alignments (Jackson and Maxwell, 1993) and, b) mutations that disable the catalytic function of the enzyme would further rule out the possibility of the observed ATPase rates being the result of a unknown contaminant. The two mutants of the Glu 86 residue provided good evidence that Glu 86 does have an important role in the hydrolysis of ATP by human topo II α possibly by acting as a catalytic base. This would seem to provide evidence that the mechanism suggested for DNA gyrase, supported by amino acid sequence alignment, can be extended as the general mechanism for ATP hydrolysis in type II topoisomerases. In the absence of any specific inhibitor of the ATPase activity of human topo II, the ability to abolish the ATPase activity of this fragment by a mutation strongly suggests the observed activity is due to the 52 kDa fragment and not an unknown contaminant.

The mutation of the Ser 29 residue was to provide additional evidence for the previous observation that phosphorylation had no discernible effects on ATPase rate. The choice of the replacement residues was important. The mutant protein carrying an

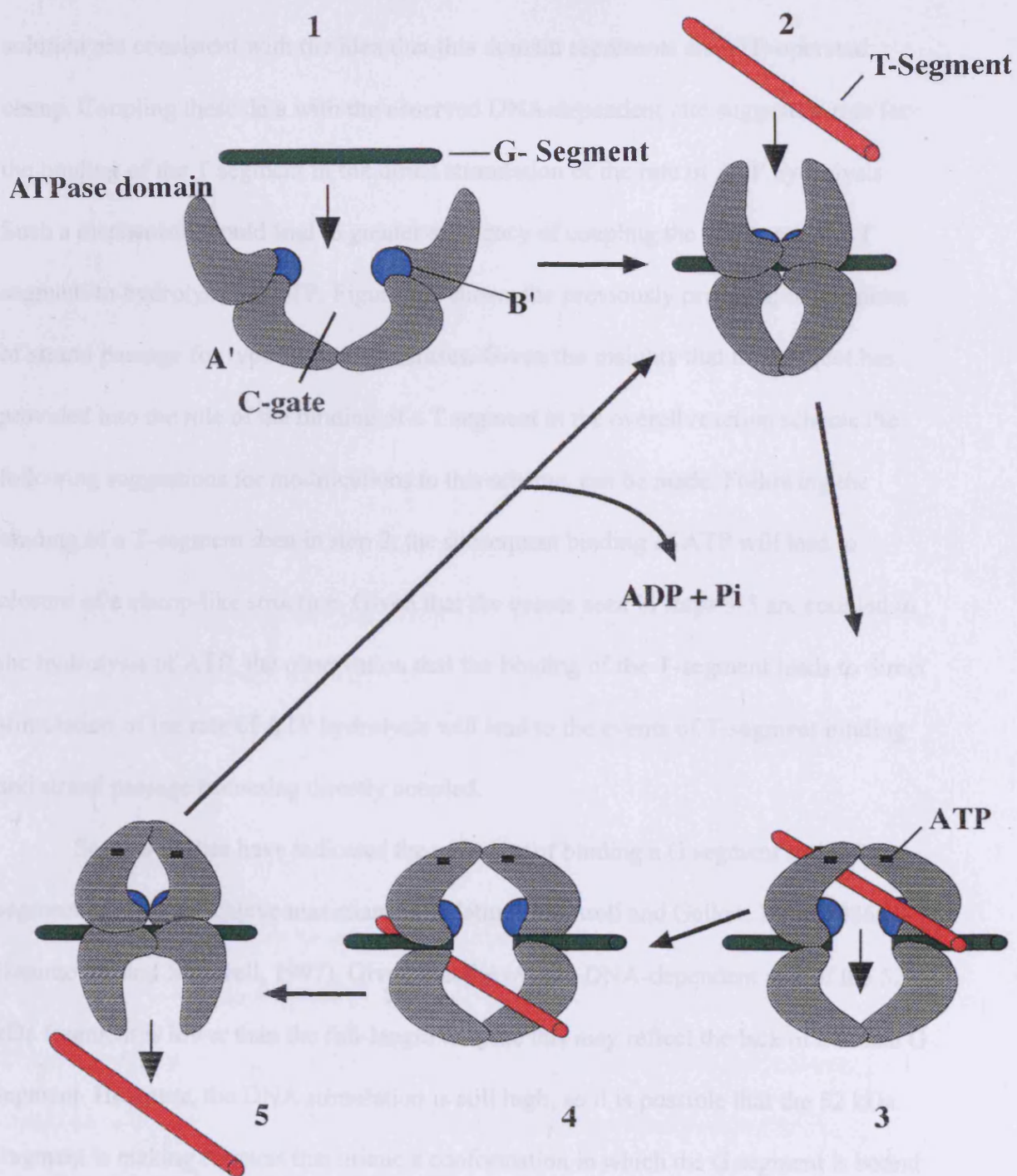
Asp residue could possibly mimic the wild type protein in which the Ser 29 residue was phosphorylated. The observation that this protein had approximately wild type DNA-dependent rate suggests two possibilities, that the protein does not mimic the phosphorylated wild type protein or that phosphorylation at this site does not have any effect on the DNA-dependent ATPase of the 52 kDa protein. Given the previous observation that phosphorylation of the wild type enzyme has no effect of DNA-dependent ATPase activity it is probable that the second explanation is the more likely. The second mutant incorporating an Ala at position 29 effectively produced a protein that could not be a target for phosphorylation at position 29. In effect this mutant provided two useful pieces of data, that the enzyme was not being affected by a contaminating kinase and that Ser 29 was not an important residue in the ATPase mechanism of this enzyme.

CONCLUSIONS

The production of the 52 kDa protein was dogged by difficulties: in finding the correct composition of broth, in the practical difficulties of dealing with an insoluble protein that required the development of refolding protocols, and in assaying protein that would not tolerate an increase in concentration above 0.15 mg/ml. These difficulties may reflect on the suitability of the clone. There is work ongoing within this lab to re-clone an equivalent fragment of human topo II α with respect to finding the C-terminal boundary of the domain with more precision, this it is hoped will generate a protein with greater solubility.

This project has however generated some interesting insights into the ATPase activity of human topo II α and by extension eukaryotic type II topoisomerases. The 52 kDa N-terminal fragment reflects the ATPase domain of the full-length enzyme. The

Figure 6.1 Mechanism of strand passage in topo II.



The above figure shows the proposed mechanism for strand passage by type II topoisomerases. Given the observation that T-segment binding is coupled to ATP hydrolysis then strand passage, steps 3-5 and the enzyme turnover will be directly coupled to the binding of a T-segment.

cross-linking and kinetic data that support the view that the fragment forms a dimer in solution are consistent with the idea that this domain represents an ATP-operated clamp. Coupling these data with the observed DNA-dependent rate suggests a role for the binding of the T segment in the direct stimulation of the rate of ATP hydrolysis. Such a mechanism would lead to greater efficiency of coupling the passage of the T segment to hydrolysis of ATP. Figure 6.1 shows the previously proposed mechanism of strand passage for type II topoisomerases. Given the insights that this project has provided into the role of the binding of a T segment in the overall reaction scheme the following suggestions for modifications to this scheme, can be made. Following the binding of a T-segment seen in step 2, the subsequent binding of ATP will lead to closure of a clamp-like structure. Given that the events seen in steps 3-5 are coupled to the hydrolysis of ATP, the observation that the binding of the T-segment leads to direct stimulation of the rate of ATP hydrolysis will lead to the events of T-segment binding and strand passage becoming directly coupled.

Several studies have indicated the necessity of binding a G segment and a T segment in order to achieve maximum stimulation (Maxwell and Gellert, 1984, 1986; Hammonds and Maxwell, 1997). Given that the overall DNA-dependent rate of the 52 kDa fragment is lower than the full-length enzyme this may reflect the lack of a bound G segment. However, the DNA stimulation is still high, so it is possible that the 52 kDa fragment is making contacts that mimic a conformation in which the G segment is bound in the full-length enzyme leading to near maximal stimulation. The observation that the 52 kDa fragment is stimulated to the same degree by both relaxed and supercoiled DNA may indicate that the preference in the full-length enzyme for supercoiled DNA is a product of binding of the G segment. It clear that an area of immediate interest will be discerning the exact nature of the protein-DNA interactions within this domain. In the

context of the existence of the DNA-dependent rate, the role of the intrinsic rate must be considered. If the 52 kDa protein is acting as a DNA-stimulated, ATP-operated clamp and in the absence of DNA were to bind ATP then the clamp would close and there for be inaccessible to DNA. To prevent the enzyme becoming trapped in this conformation a slow intrinsic rate may allow the enzyme to re-cycle, allowing it to once more be accessible to DNA. It may be possible to suggest modifications to the current model of eukaryotic topo II in which the ATP operated clamp is also DNA sensitive. In the presence of DNA the ATP is hydrolysed rapidly leading to a greater coupling efficient ATP use to strand passage. The relatively weak interactions between the 52 kDa fragment and DNA shown by the calculated K_d of 1.4 μM may be a reflection on the role of this domain in the passaging event. The clamp would only transiently bind DNA before it is passed through the G segment.

FUTURE WORK

The production of the 52 kDa fragment of human topoisomerase II α from the TOPO/HIS clone proved to be very problematic to work with due mainly to the insolubility of the resulting protein. This may be due to a poorly defined C-terminal domain boundary. To improve the yield and solubility of the protein the fragment should be re-cloned. A series of constructs that terminate around the C-terminal boundary may result in a protein that is more representative of the whole domain and so perhaps more soluble.

Nucleotide binding studies in the presence and absence of DNA may provide valuable insights into the nucleotide binding characteristics of the 52 kDa fragment. Current models (Lindsley and Wang, 1993; Tamura *et al*, 1992) would suggest that the binding of nucleotide would be cooperative. Limited proteolysis of the C-terminal

domain in the presence and absence of nucleotide might provide information on any conformational changes that may take place upon binding of the nucleotide to the enzyme.

Interactions between the protein and the DNA require further investigations. Initial studies should examine the minimum length of DNA that is required to stimulate the ATPase activity of the enzyme. Such a study would allow a more accurate assessment of K_d and provide an insight into the binding of DNA to the clamp. Possible limited proteolysis on the enzyme in the presence of DNA may provide some insights into any conformational changes in the presence of DNA.

The mutation of the phosphorylation site at Ser 29 in the 52 kDa fragment did not demonstrate any obvious role for this site in regulating the ATPase activity of the enzymes. It would be interesting to make these mutations in the full length enzyme, using a yeast expression system to look for the effect of mutation at Ser 29 in the full length enzyme.

REFERENCES

Alghisi, G.-C., Roberts, E., Cardenas, M. E. & Gasser, S. M. (1994). The regulation of DNA topoisomerase II by casein kinase II. *Cell. Mol. Biol. Res.* **40**, 563-571.

Ali, J. A., Jackson, A. P., Howells, A. J. & Maxwell, A. (1993). The 43-kDa N-terminal fragment of the gyrase B protein hydrolyses ATP and binds coumarin drugs. *Biochemistry* **32**, 2717-2724.

Ali, J. A., Orphanides, G. & Maxwell, A. (1995). Nucleotide binding to the 43-kilodalton N-terminal fragment of the DNA gyrase B protein. *Biochemistry* **34**, 9801-9808.

Baldi, M. I., Benedetti, P., Mattoccia, E. & Tocchini-Valentini, G. P. (1980). In vitro catenation and decatenation of DNA and a novel eucaryotic ATP-dependent Topoisomerase. *Cell* **20**, 461-467.

Bates, A. D., and A. Maxwell. 1993. DNA topology. *In* In focus. D. Rickwood, editor. IRL Press, Oxford. 114.

Benedetti, P., A. Silvestri, P. Fiorani, and J. C. Wang. 1997. Study of yeast DNA topoisomerase II and its truncation derivatives by transmission electron microscopy. *J. Biol. Chem.* **272**:12132-12137.

Berger, J. M., Gamblin, S. J., Harrison, S. C. & Wang, J. C. (1996). Structure at 2.7 Å resolution of a 92K yeast DNA topoisomerase II fragment. *Nature* **379**, 225-232.

Bradford, M. M. (1976). A rapid and sensitive method for the quantitation of microgram quantities of protein utilizing the principle of protein-dye binding. *Anal. Biochem.* **72**, 248-254.

Burden, D. A. & Sullivan, D. M. (1994). Phosphorylation of the a and b isoforms of the DNA topoisomerase II is qualitatively different in interphase and mitosis in chinese hamster ovary cells. *Biochemistry* **33**, 14651-14655.

Cardenas, M. E., Dang, Q., Glover, C. V. C. & Gasser, S. M. (1992). Casein kinase II phosphorylates the eukaryote-specific C-terminal domain of topoisomerase II *in vivo*. *EMBO J.* **11**, 1785-1796.

Chen, A. Y. & Liu, L. F. (1994). DNA topoisomerases: Essential enzymes and lethal targets. *Annu. Rev. Pharmacol. Toxicol.* **34**, 191-218.

Chen, M. & Beck, W. T. (1995). Differences in inhibition of chromosome separation and G2 Arrest by DNA topoisomerase II inhibitors merbarone and VM-26. *Cancer. Res* **55**, 1509-1516.

Corbett, A. H., DeVore, R. F. & Osheroff, N. (1992). Effect of casein kinase II-mediated phosphorylation on the catalytic cycle of topoisomerase II. *J. Biol. Chem.* **267**, 20513-20518.

Corbett, A. H., Fernald, A. W. & Osheroff, N. (1993a). Protein kinase C modulates the catalytic activity of topoisomerase II by enhancing the rate of ATP hydrolysis: evidence for a common mechanism of regulation by phosphorylation. *Biochemistry* **32**, 2090-2097.

Corbett, A. H., Hong, D. & Osheroff, N. (1993b). Exploiting mechanistic differences between drug classes to define functional drug interaction domains on topoisomerase II. *J. Biol. Chem.* **268**, 14394-14398.

Corbett, A. H. & Osheroff, N. (1993). When good enzymes go bad: conversion of topoisomerase II to a cellular toxin by antineoplastic drugs. *Chem. Res. Toxicol.* **6**, 585-597.

Corbett, A. H., Zechiedrich, E. L., Lloyd, R. S. & Osheroff, N. (1991). Inhibition of eukaryotic topoisomerase II by ultraviolet-induced cyclobutane pyrimidine dimers. *J. Biol. Chem.* **266**, 19666-19671.

Corbett, A. H., Zechiedrich, E. L. & Osheroff, N. (1992b). A role for the passage helix in the DNA cleavage reaction of eukaryotic topoisomerase II. *J. Biol. Chem.* **267**, 683-686.

DeVore, R. F., Corbett, A. H. & Osheroff, N. (1992). Phosphorylation of topoisomerase II by casein kinase II and protein kinase C: effects on enzyme-mediated DNA cleavage/religation and sensitivity to the antineoplastic drugs etoposide and 4 β -(9-acridinylamino)methane-sulfon-*m*-anisidide. *Cancer Res.* **52**, 2156-2161.

Drake, F., Hofmann, G., Bartus, H., Mattern, M., Crooke, S. & Miracelli, C. (1989). Biochemical and pharmacological properties of p170 and p180 forms of topoisomerase II. *Biochemistry* **28**, 8154-8160.

Dulbecco, R. & Vogt, M. (1963). Evidence for the ring structure of polyoma virus DNA. *Proc. Natl. Acad. Sci. USA.* **50**, 730-739.

Fisher, L. M., Mizuuchi, K., O'Dea, M. H., Ohmori, H. & Gellert, M. (1981). Site-specific interaction of DNA gyrase with DNA. *Proc. Natl. Acad. Sci. USA* **78**, 4165-4169.

Freudenreich, C. H. & Kreuzer, K. N. (1993). Mutational analysis of a type II topoisomerase cleavage site: distinct requirements for enzyme and inhibitors. *EMBO J.* **12**, 2085-2097.

Freudenreich, C. H. & Kreuzer, K. N. (1994). Localization of an aminoacridine antitumor agent in a type II topoisomerase-DNA complex. *Proc. Natl. Acad. Sci. USA* **91**, 11007-11011.

Froelich-Ammon, S. J. & Osheroff, N. (1995). Topoisomerase poisons: harnessing the dark side of enzyme mechanism. *J. Biol. Chem.* **270**, 21429-21432.

Gellert, M., Mizuuchi, K., O'Dea, M. H., Itoh, T. & Tomizawa, J. (1977). Nalidixic acid resistance: a second genetic character involved in DNA gyrase activity. *Proc. Natl. Acad. Sci. USA* **74**, 4772-4776.

Gellert, M., Mizuuchi, K., O'Dea, M. H. & Nash, H. A. (1976). DNA gyrase: an enzyme that introduces superhelical turns into DNA. *Proc. Natl. Acad. Sci. USA* **73**, 3872-3876.

Goto, T. & Wang, J. C. (1984). Yeast DNA Topoisomerase II Is Encoded by a Single-Copy, Essential Gene. *Cell* **36**, 1073-1080.

Gottlieb, M. & Chavko, M. (1987). *Analytical Biochemistry* **165**, 33-37.

Hager, A. D. & Burgess, R. R. (1980). Elution of protein from sodium dodecyl sulfate polyacrylamide gels. Removal of sodium dodecylsulfate, and renaturation of enzymatic

activity: results with sigma subunit of E.coli RNA polymerase, wheat germ DNA topoisomerase and other enzymes. *Analytical Biochemistry* **109**, 76-86.

Hammonds, T. R. & Maxwell, A. (1997). The DNA dependence of the ATPase activity of human DNA topoisomerase II α . *J. Biol. Chem.* **272**, 32696-32703.

Harkins, T. T., Lewis, T. J. & Lindsley, J. E. (1998). Pre-steady state analysis of ATP hydrolysis by *Saccharomyces cerevisiae* DNA topoisomerase II. 2. Kinetic mechanism for the sequential hydrolysis of two ATP. *Biochemistry* **37**, 7299-7312.

Harkins, T. T. & Lindsley, J. E. (1998). Pre-steady state analysis of ATP hydrolysis by *Saccharomyces cerevisiae* DNA topoisomerase II. 1. A DNA-dependent burst in ATP hydrolysis. *Biochemistry* **37**, 7292-7298.

Howard, M. T., Neece, S. H., Matson, S. W. & Kreuzer, K. N. (1994). Disruption of a topoisomerase-DNA cleavage complex by a DNA helicase. *Proc. Natl. Acad. Sci. USA* **91**, 12031-12035.

Hsieh, T. & Brutlag, D. (1980). ATP-dependent DNA topoisomerase from *D. melanogaster* reversibly catenates duplex DNA rings. *Cell* **21**, 115-125.

Isaacs, R. J., Davies, S. L., Wells, N. J. & Harris, A. L. (1995). Topoisomerase II α and II β as therapy targets in breast cancer. *Anti-cancer drugs* **6**, 195-211.

Jackson, A. P. & Maxwell, A. (1993). Identifying the catalytic residue of the ATPase reaction of DNA gyrase. *Proc. Natl. Acad. Sci. USA* **90**, 11232-11236.

Jenkins, J. R., Ayton, P., Jones, T., Davies, S. L., Simmons, D. L., Harris, A. L., Sheer, D. & Hickson, I. D. (1992). Isolation of cDNA clones encoding the β isozyme of human DNA topoisomerase II and localisation of the gene to chromosome 3p24. *Nucleic Acids Res.* **20**, 5587-5592.

Kavenoff, R., Klotz, L. C. & Zimm, B. H. (1974). On the nature of chromosome-sized DNA molecules. *Cold Spring Harbor Symp. Quant. Biol.* **38**, 1-8.

Kreuzer, K. N. & Alberts, B. M. (1984). Site-specific recognition of bacteriophage T4 DNA by T4 Type II DNA topoisomerase and *Escherichia coli* DNA gyrase. *J. Biol. Chem.* **259**, 5339-5346.

Li, W. & J.C., Wang. (1997). Footprinting of the yeast DNA topoisomerase II lysyl side chains involved in substrate binding and interdomainal interactions. *J. Biol. Chem.* **272**, 31190-31195.

Lindsley, J. E. & Wang, J. C. (1991). Proteolysis patterns of epitopically labeled yeast DNA topoisomerase II suggest an allosteric transition in the enzyme induced by ATP binding. *Proc. Natl. Acad. Sci. USA* **88**, 10485-10489.

Lindsley, J. E. & Wang, J. C. (1993). On the coupling between ATP usage and DNA transport by yeast DNA topoisomerase II. *J. Biol. Chem.* **268**, 8096-8104.

Liu, L. F. & Alberts, B. M. (1979). T4 DNA topoisomerase : A new ATP-dependent enzyme essential for initiation of T4 bacteriophage DNA replication. *Nature* **281**, 456-461.

Liu, L. F., Rowe, T. C., Yang, L., Tewey, K. M. & Chen, G. L. (1983). Cleavage of DNA by mammalian DNA topoisomerase II. *J. Biol. Chem.* **258**, 15365-15370.

Lyubchenko, Y. & Shlyakhtenko, L. (1988). Early melting of supercoiled DNA. *Nucleic Acids Research* **8**, 3269-3281.

Maxwell, A. & Gellert, M. (1984). The DNA dependence of the ATPase activity of DNA gyrase. *J. Biol. Chem.* **259**, 14472-14480.

Maxwell, A. & Gellert, M. (1986). Mechanistic aspects of DNA topoisomerases. *Adv. Prot. Chem.* **38**, 69-107.

Meselson, M. (1972). Formation of hybrid DNA by rotary diffusion during genetic recombination. *J. Mol. Biol.* **71**, 795-798.

Meselson, M. & Stahl, F. W. (1958). The replication of DNA in *E. coli*. *Proc. Natl. Acad. Sci. USA.* **77**, 1847-1851.

Miller, K. G., Liu, L. F. & Englund, P. T. (1981). A homogeneous type II DNA topoisomerase from HeLa cell nuclei. *J. Biol. Chem.* **256**, 9334-9339.

Mizuuchi, K., Fisher, M., O'Dea, M. & Gellert, M. (1980). DNA gyrase action involves the introduction of transient double-strand breaks into DNA. *Proc. Natl. Acad. Sci USA* **77**, 1847-1851.

Moffatt, B. A. & Studier, F. W. (1987). T7 lysozyme inhibits transcription by T7 RNA polymerase. *Cell* **49**, 221-227.

Morais Cabral, J. H., Jackson, A. P., Smith, C. V., Shikotra, N., Maxwell, A. & Liddington, R. C. (1997). Structure of the DNA breakage-reunion domain of DNA gyrase. *Nature* **388**, 903-906.

Morrison, A. & Cozzarelli, N. R. (1979). Site-specific cleavage of DNA by *E. coli* DNA gyrase. *Cell* **17**, 175-184.

Negri, C., Scovassi, A. I., Braghetti, A., Guano, F. & Astaldi Ricotti, G. C. B. (1993).

DNA topoisomerase II b: stability and distribution in different animal cells in comparison to DNA topoisomerase I and II a. *Exp. Cell Res.* **206**, 128-133.

Nelson, E. M., Tewey, K. M. & Liu, L. F. (1984). Mechanism of antitumor drug action: poisoning of mammalian DNA topoisomerase II on DNA by 4'-(9-acridinylamino)-methanesulfon-*m*-anisidide. *Proc. Natl. Acad. Sci. USA* **81**, 1361-1365.

Osheroff, N. (1989). Effect of Antineoplastic Agents on the DNA Cleavage/Religation Reaction of Eukaryotic Topoisomerase II: Inhibition of DNA Religation by Etoposide. *Biochemistry* **28**, 6157-6160.

Osheroff, N. & Zechiedrich, E. (1986). Calcium-Promoted DNA Cleavage by Eukaryotic Topoisomerase II: Trapping the Covalent Enzyme-DNA Complex in an Active Form. *Biochemistry* **26**, 4303-4309.

Peebles, C. L., Higgins, N. P., Kreuzer, K. N., Morrison, A., Brown, P. O., Sugino, A. & Cozzarelli, N. R. (1978). Structure and activities of *Escherichia coli* DNA gyrase. *Cold Spring Harbor Symp. Quant. Biol.* **43**, 41-52.

Robinson, M. & Osheroff, N. (1989). Stabilization of the Topoisomerase II-DNA Cleavage Complex by Antineoplastic Drugs: Inhibition of Enzyme-Mediated DNA

Religation by 4'-(9-Acridinylamino)methanesulfon-m-anisidide. *American Chemical Society* **29**, 2511-2515.

Robinson, M. & Osheroff, N. (1991). Effects of Antineoplastic Drugs on the Post-Strand-Passage DNA Cleavage/Religation Equilibrium of Topoisomerase II. *Biochemistry* **30**, 1807-1813.

Robinson, M. J., Corbett, A. H. & Osheroff, N. (1993). Effects of topoisomerase II-targeted drugs on enzyme-mediated DNA cleavage and ATP hydrolysis: evidence for distinct drug interaction domains on topoisomerase II. *Biochemistry* **32**, 3638-3643.

Robinson, M. J., Martin, B. A., Gootz, T. D., McGuirk, P. R., Moynihan, M., Sutcliffe, J. A. & Osheroff, N. (1991). Effects of quinolone derivatives on eukaryotic topoisomerase II. A novel mechanism for enhancement of enzyme-mediated DNA cleavage. *J. Biol. Chem.* **266**, 14585-14592.

Roca, J., Berger, J. M., Harrison, S. C. & Wang, J. C. (1996). DNA transport by a type II topoisomerase: direct evidence for a two-gate mechanism. *Proc. Natl Acad. Sci. USA* **93**, 4057-4062.

Roca, J., Ishida, R., Berger, J. M., Andoh, T. & Wang, J. C. (1994). Antitumour bisdioxopiperazines inhibit yeast DNA topoisomerase II by trapping the enzyme in the form of a closed protein clamp. *Proc. Natl. Acad. Sci. USA* **91**, 1781-1785.

Roca, J. & Wang, J. C. (1992). The capture of a DNA double helix by an ATP-dependent protein clamp: a key step in DNA transport by type II DNA topoisomerases. *Cell* **71**, 833-840.

Roca, J. & Wang, J. C. (1994). DNA transport by a type II DNA topoisomerase: evidence in favor of a two-gate mechanism. *Cell* **77**, 609-616.

Roca, J. & Wang, J. C. (1996). The probabilities of supercoil removal and decatenation by yeast topoisomerase II. *Genes to Cells* **1**, 17-27.

Rodnina, M. V., Savelsbergh, A., Katunin, V. I. & Wintermeyer, W. (1997). Hydrolysis of GTP by elongation factor G drives tRNA movement on the ribosome. *Nature* **385**, 37-41.

Sambrook, J., Fritsch, E. F. & Maniatis, T. (1989). *Molecular cloning: a laboratory manual*, Cold Spring Harbor Laboratory Press, Cold Spring Harbor.

Sander, M. & Hsieh, T. (1983). Double Strand DNA Cleavage by Type II DNA Topoisomerase from *Drosophila melanogaster*. *Biological Chemistry* **258**, 84221-8428.

Sawadogo, M. & Van Dyke, M. W. (1991). A rapid method for the purification of deprotected oligodeoxynucleotides. *Nucleic Acids Res.* **19**, 674.

Schultz, P., S. Olland, P. Oudet, and R. Hancock. 1996. Structure and conformational changes of DNA topoisomerase II visualized by electron microscopy. *Proc. Natl. Acad. Sci. USA*. 93:5936-5940

Shiozaki, K. & Yanagida, M. 1991. A functional 125-kDa core polypeptide of fission yeast DNA topoisomerase II. *Mol. Cell. Biol.* 11, 6093-6102.

Smith, C. V. (1998). Investigating the mechanism and energy coupling of DNA gyrase. *Thesis*, Department of Biochemistry, University of Leicester.

Sorensen, B. S., Sinding, J., Anderson, A. H., Alsner, J., Jensen, P. B. & Wetergaard, O. (1992). Mode of action of topoisomerase II-targeting agents at a specific DNA sequence: Uncoupling the DNA binding, cleavage and religation events. *J. Mol. Biol.* 223, 778-786.

Stetler, G. L., King, G. J. & Huang, W. M. (1979). T4 DNA-delay proteins, required for specific DNA replication, form a complex that has ATP-dependent DNA topoisomerase activity. *Proc. Natl. Acad. Sci. USA* 76, 3737-3741.

Sugino, A., Peebles, C. L., Kruezer, K. N. & Cozzarelli, N. R. (1977). Mechanism of action of nalidixic acid: purification of *Escherichia coli* *nalA* gene product and its relationship to DNA gyrase and a novel nicking-closing enzyme. *Proc. Natl. Acad. Sci. USA* 74, 4767-4771.

Sugino, A., Higgins, N. P., Brown, P. O., Peebles, C. L. & Cozzarelli, N. R. (1978).

Energy coupling in DNA gyrase and the mechanism of action of novobiocin. *Proc. Natl. Acad. Sci. USA* **75**, 4838-4842.

Sugino, A., Higgins, N. P. & Cozzarelli, N. R. (1980). DNA gyrase subunit stoichiometry and the covalent attachment of subunit A to DNA during DNA cleavage. *Nucleic Acids Res.* **8**, 3865-3874.

Szabo, A., Stolz, L. & Granzow, R. (1995). Surface plasmon resonance and its use in biomolecular interaction analysis (BIA). *Curr. Op. Struct. Biol.* **5**, 699-705.

Tamura, J. & Gellert, M. (1990). Characterization of the ATP binding site on *Escherichia coli* DNA gyrase. *J. Biol. Chem.* **265**, 21342-21349.

Tamura, J. K., Bates, A. D. & Gellert, M. (1992). Slow interaction of 5'-adenylyl- β,γ -imidodiphosphate with *Escherichia coli* DNA gyrase. *J. Biol. Chem.* **267**, 9214-9222.

Tan, K. B., Dorman, T. E., Falls, K. M., Chung, T. D. Y., Mirabelli, C. K., Crooke, S. T. & Mao, J. (1992). Topoisomerase II α and Topoisomerase II β genes: Characterization and mapping to human chromosomes 17 and 3, respectively. *Cancer Res.* **52**, 231-234.

Tingey, A. P. & Maxwell, A. (1996). Probing the role of the ATP-operated clamp in the strand-passage reaction of DNA gyrase. *Nucleic Acids Res.* **24**, 4868-4873.

Tsai-Pflugelder, M., Liu, L. F., Liu, A. A., Tewey, K. M., Whang-Peng, J., Knutsen, T., Huebner, K., Croce, C. M. & Wang, J. C. (1988). Cloning and sequencing of cDNA encoding human DNA topoisomerase II and localization of the gene to chromosome region 17q21-22. *Proc. Natl. Acad. Sci. USA* **85**, 7177-7181.

Tse, Y. C., Kirkegaard, K. & Wang, J. C. (1980). Covalent bonds between protein and DNA. *J. Biol. Chem.* **255**, 5560-5565.

Wang, J. C. (1971). Interaction between DNA and an *Escherichia coli* protein w. *J. Mol. Biol* **55**, 523-533.

Wang, J. (1979). Helical repeat of DNA in solution. *Proc. Natl. Acad. Sci. USA* **76**, 200-203.

Wang, J. C. (1996). DNA topoisomerases. *Annu. Rev. Biochem.* **65**, 635-692.

Wang, J. C. (1998). Moving one DNA double helix through another by a type II DNA topoisomerase: The story of a simple molecular machine. *Quart. Rev. Biophys.* **In press.**

Wang, J. C., Gumpert, R. I., Javaherian, K., Kirkegaard, K., Klevan, L., Kotewicz, M. L. & Tse, Y.-C. (1980). DNA topoisomerases. In *Mechanistic studies of DNA replication and genetic recombination* (Alberts, B. & Fox, C. F., eds.), pp. 769-784. Academic Press, New York.

Wang, J. C. & Liu, L. F. (1979). DNA Topoisomerases: Enzymes That Catalyze the Concerted Breaking and Rejoining of DNA Backbone Bonds. *Molecular Genetics, Part III Chapter II*, 65-88.

Watson, J. D. & Crick, F. H. C. (1953). Genetic implications of the structure of deoxyribonucleic acid. *Nature* **171**, 964-967.

Watt, P. M. & Hickson, I. D. (1994). Structure and function of type II DNA topoisomerases. *Biochem. J.* **303**, 681-695.

Weil, R. & Vinograd, J. (1963). The cyclic coil and cyclic forms of polyoma viral DNA. *Proc. Natl. Acad. Sci. USA.* **50**, 730-739.

Wells, N. J., Addison, C. M., Fry, A. M., Ganapathi, R. & Hickson, I. D. (1994). Serine 1524 is a major site of phosphorylation on human topoisomerase II α protein *in vivo* and is a substrate for casein kinase II *in vitro*. *J. Biol. Chem.* **269**, 29746-29751.

Wells, N. J., Fry, A. M., Guano, F., Norbury, C. & Hickson, I. D. (1995). Cell cycle phase-specific phosphorylation of human topoisomerase II α . *J. Biol. Chem.* **270**, 28357-28363.

Wells, N. J. & Hickson, I. D. (1995). Human topoisomerase II α is phosphorylated in a cell-cycle phase-dependent manner by a proline-directed kinase. *Eur. J. Biochem.* **231**, 491-497.

Wigley, D. B., Davies, G. J., Dodson, E. J., Maxwell, A. & Dodson, G. (1991). Crystal structure of an N-terminal fragment of the DNA gyrase B protein. *Nature* **351**, 624-629.

Willmott, C. J. R., Critchlow, S. E., Eperon, I. C. & Maxwell, A. (1994). The complex of DNA gyrase and quinolone drugs with DNA forms a barrier to transcription by RNA polymerase. *J. Mol. Biol.* **242**, 351-363.

Wilson, W. R., Baguley, B. C., Wakelin, L. P. G. & Waring, M. (1981). Interactions of the antitumor drug 4'-(9-acridinylamino)-methanesulfon-*m*-anisidide and related acridines with nucleic acids. *Mol. Pharmacol* **20**, 404-414.